Disease Effects on Antigen Presentation
by Class II Major Histocompatibility Molecules

by

Lawrence Lem

DISSERTATION

Submitted in partial satisfaction of the requirements for the degree of

DOCTOR OF PHILOSOPHY

in

Microbiology and Immunology

in the

GRADUATE DIVISION

of the

UNIVERSITY OF CALIFORNIA SAN FRANCISCO

Date **University Librarian**

Degree Conferred: .....

Dedication

This dissertation is dedicated to the One who knows all my faults and mistakes and still loves me

ACKNOWLEDGMENTS

Work is rarely accomplished in isolation and this work is no different. It is a tribute to all who graciously supported me through thick and thin. Many have been a part of my experience at UCSF and I cannot mention everyone, but I would like to specifically thank:

My parents for encouraging me to pursue higher education and do my best

My wonderful friends David and Linda Hau, who gave me a home away from home during my studies here

My brothers and sisters in Young Adult Fellowship, who are too numerous to name, for their patience and loving support during all my long days in lab and for constantly reminding me about life outside of lab.

My sister Anita and Brother in law, David, who have been loving and encouraging.

My sister, Karen, who took the time to remind me to have fun.

My friend, Denise, who listened and sympathized with me in all my growing

Members of the Hooper Foundation:

Shaival 'TV Guide' Dave': for the lighthearted times in the Skybar and exciting pool

Malcolm 'Classic' Lowry: For teaching me about 'classic' jazz and late night dinners

Christine 'Cool' Burke: for reintroducing me to soccer for the 'first time' and the cool ski trips

Tim Tian: for the scientific advice and fun tennis games

Rong Wang: for the great times learning Chinese and the chance to talk about culture

Kent 'Joker' Nybakken: for always keeping me on guard for new nicknames and honing my wits

To the Brodsky lab members, current and former:

Andy Wilde: for the constant reminders to consider the cell biological aspects of my work

Barrie Greene: for her witty humor to keep me laughing when experiments failed

Shu-Hui Liu: for her patient instruction and alternative perspectives on all my confusing data

Bill Mallet: for the showing me what it meant to persevere with experiments

Steve Morris: For the reminders that I speak American, not English

Betsy Bennett: (my lab sister) for all the laughs and good times we had in between experiments talking about everything under the sun

Jean Chen: For helping me hone my consulting skills

Diane Wakeham: For all the deep conversations about life, love and lab

Joel Ybe: For introducing me to the concepts of protein structure and crystalization

Dave "Weatherman" Riethof: For bringing your unique perspectives to lab and your minute by minute weather forecasts

Debbie Williams-Herman, Alejandra Solache-Diaz, Diana Slowiejko, Tina Tran, Lin Chen: For patiently listening to my lab meetings

My advisor, Frances Brodsky, for giving me a place to 'park my pipetmen' for six years and the opportunity to open up a new area of research in the lab as well as the opportunity to finish my master's thesis during my work at UCSF

SCIENTIFIC CONTRIBUTORS

A number of publications resulted from the dissertation work described here, two of which are reprinted here. These publications also involved the work of some co-authors and collaborators. The publications are listed below with the contributions of the various co-authors:

Brodsky, F.M., **Lem, L.**, Solache, A., Bennett, E.M. (1999). Human pathogen subversion of antigen presentation. *Immunological Reviews.* 168:199-215.

L. Lem contributed Figures 3-6 and editorial work for the sections on class II MHC.

Lem, L., Riethof, D.A., Scidmore-Carlson, M., Griffiths, G., Hackstadt, T., Brodsky, F.M. (1999). Enhanced interaction of HLA-DM with HLA-DR in enlarged vacuoles of hereditary and infectious lysosomal diseases. *Journal of Immunology.* 162:523-532.

This publication is reprinted as Chapter 2. All of the data published here are the work of L. Lem. D. Riethof performed experiments not published in the manuscript while M. Scidmore-Carlson, G. Griffiths and T. Hackstadt provided reagents and experimental guidance.

Wilde, A., Beattie, E.C., **Lem, L.**, Riethof, D.A., Liu, S.H., Mobley, W.C., Soriano, P., Brodsky, F.M.. (1999). EGF receptor signaling stimulates src kinase phosphorylation of clathrin influencing clathrin redistribution and EGF uptake. *Cell.* 96:677-687.

This article is reprinted in the appendix. L. Lem performed the microscopy in Figures 1,2, 4 and 7.

Brodsky, F.M., **Lem, L.**, Bresnahan, P.A. (1996). Antigen processing and presentation. *Tissue Antigens.* 47:464-471.

L. Lem provided editorial assistance and the figures on class II MHC.

University of California
San Francisco
UCSF
The George Williams Hooper Foundation
and the Karl Friedrich Laboratories

March 30, 2000

G.W. Hooper Foundation
513 Parnassus Avenue
Campus Box 0552
Health Science West 1691
San Francisco, CA 94143-0552
fax: 415/476-6185

Cell
1050 Massachusetts Ave.
Cambridge, MA 02138

To whom it may concern:

I am writing to request permission to reprint the following paper published in Cell as a part of my Ph.D thesis at the university of California, San Francisco.

> Wilde, A., Beattie, E.C., Lem, L., Riethof, D.A., Liu, S.H., Mobley, W.C., Soriano, P., Brodsky, F.M.. (1999). EGF receptor signaling stimulates src kinase phosphorylation of clathrin influencing clathrin redistribution and EGF uptake. *Cell*. 96:677-687.

The thesis will be microfilmed by University Microfilms International and they request permission to supply single copies on demand.

Please respond by FAX to (415) 476-6185. Thank you in advance.

Sincerely,

Lawrence Lem

Lawrence Lem
Phone: (415) 476-6405
Email: lawrence_lem@hotmail.com

"PERMISSION GRANTED SUBJECT TO CITATION OF THE ORIGINAL MANUSCRIPT AND NOTATION THAT COPYRIGHT [illegible] RIGHTS. (OUR PERMISSION IS CONTINGENT ON PERMISSION OF THE AUTHOR.)"

The Journal of Immunology
9650 Rockville Pike
Bethesda, MD 20814-3994
Phone: (301) 530-7197 FAX: (301) 571-1813

December 21, 1999

Lawrence Lem
University of California
San Francisco, CA 94143-0552

Dear Dr. Lem:

The Journal of Immunology grants permission to reproduce text and figures from the manuscript found in Volume 162, p. 523-532, in 1999, in your doctoral thesis, contingent upon the following conditions:

1. That you give proper credit to the authors and to *The Journal of Immunology* , including in your citation the volume, date and page numbers.

2. That you include the statement, *Copyright 1999. The American Association of Immunologists.*

Please understand that permission is granted for one-time use only. Permission must be requested separately for future editions, revisions, translations, derivative works and promotional pieces. Permission is not granted for any type of electronic reproduction or distribution.

Thank you for your interest in *The Journal of Immunology*.

Cordially,

C M Burke

Cheryl M. Burke
Production Coordinator

ABSTRACT

Disease Effects on Antigen Presentation by Class II Major Histocompatibility Molecules

Lawrence Lem

Class II major histocompatibility (MHC) molecules initiate immune responses to extracellular antigens by binding antigen-derived peptides and displaying them to CD4 T cells at the cell surface. This process involves the degradation of antigens into peptides and the peptide loading of class II molecules in endocytic compartments. In this thesis research, I studied three diseases affecting the endocytic pathway as probes to dissect the process of class II antigen presentation.

Class II molecules are loaded with peptide in membrane compartments similar to late endosomes or lysosomes. I examined cells with either a genetic or infectious lysosomal disease to determine their effects on class II molecules. The genetic immunodeficiency, the Chediak-Higashi syndrome (CHS), and an infection with the obligate intracellular pathogen *Coxiella burnetii* both result in cells with enlarged lysosomes. Class II and its associated molecules localized to these enlarged lysosomes/bacterial vacuoles, but their protein levels and surface expression were not affected in either disease. However, in CHS B lymphoblasts, class II molecules were found to be more frequently associated with DM molecules, a class II-like molecule necessary for peptide loading, resulting in decreased levels of class II molecules with bound invariant chain peptides. This increased DM/class II association is the likely molecular mechanism for the altered peptide repertoire seen in CHS B cells. An increase in class II/DM complexes was also detected in *Coxiella*-infected cells expressing class II molecules. This finding may partially account for the persistence of chronic *Coxiella* infections.

Chlamydia trachomatis is an obligate intracellular bacteria that alters host membrane trafficking despite occupying an isolated vacuole containing no known host proteins. Decreased levels of class II, DM and invariant chain were observed in *Chlamydia*-infected cells. The decreased levels of invariant chain were due to proteolysis by a *Chlamydia*-encoded protease that was active *in vitro* and could be inhibited by LLnL. This protease may be responsible for the absence of host proteins on the inclusion membrane and may also prevent presentation of chlamydial antigens on class II molecules. Further work must be done to demonstrate its *in vivo* role in *Chlamydia* pathogenesis.

TABLE OF CONTENTS

LIST OF FIGURES

Chapter 1

Chapter 2

Chapter 3

Chapter 5

ABBREVIATIONS

β_2m	β_2-microglobululin
CHS	Chediak-Higashi syndrome
CLIP	class II associated invariant chain peptide
EB	*Chlamydia* elementary body
ECL	enhanced chemiluminescence
EDTA	ethylenediamine tetraacetic acid
ER	Endoplasmic reticulum
FCS	fetal calf serum
HBSS	Hank's BSS
IFN-γ	interferon-gamma
kD	kilodalton
mAb	monoclonal antibody
MHC	major histocompatibility complex
NP-40	Non-idet P-40
PAGE	polyacrylamide gel electrophoresis
PBS	phosphate buffered saline
RB	*Chlamydia* reticulate body
SDS	sodium dodecyl sulfate
TGN	trans-Golgi network

Chapter 1

Introduction

In the natural world, a constant competition occurs between the host and its pathogens. Each infection challenges the host to stave off the parasitic invasion of microbes. While the host boasts a wide array of defense mechanisms ranging from entry barriers to targeted elimination of pathogens, microbes counter with a set of their own formidable tools for invasion and establishment of infection. Each tool is specialized to create a particular niche for the microbe that possesses it. These tools serve both to adapt the microbes to an intracellular environment as well as to protect it from host defenses.

Extracellular bacteria and intracellular bacteria pose differing sorts of challenges for host immune systems. Pathogenic extracellular bacteria strive to avoid the humoral immune system or complement lysis by altering their outer coats, all to prevent their uptake into and subsequent degradation by phagocytic cells (Nahn et al., 1999). On the other hand, intracellular bacteria are easily phagocytosed and some bacteria even have mechanisms to encourage their own uptake (Kaufmann, 1999). Their protection from the immune system lies in their ability to modify or escape the degradative compartments of the phagocyte.

As a group, the intracellular pathogens are of great medical significance as a list of just four species, *Mycobacterium tuberculosis*, *Mycobacterium leprae*, *Salmonella enterica*, and *Chlamydia trachomatis*, present a patient caseload of over 600 million individuals worldwide (Kaufmann, 1999). This thesis will describe an investigation into two intracellular pathogens, *Coxiella burnetii* and *Chlamydia trachomatis*, as well as a genetic disease, Chediak-Higashi syndrome (CHS) that results in intracellular compartment changes similar to those caused by *Coxiella*. The work centers on how these pathogens and the disease alter the normal cellular mechanism for initiating antigen specific immune responses to phagocytosed antigens, the class II major histocompatibility (MHC) antigen presentation system, and how the alterations allow for evasion of the host immune system by the bacteria.

CLASS I MHC MOLECULES

Host cells may carry two systems for alerting T cells to the presence of intracellular pathogens. The class I major histocompatibility molecule is expressed in all nucleated cells and serves primarily to detect cytosolic pathogens, such as viruses or bacteria residing in the cytoplasm. Antigens in the cytoplasm are degraded primarily by the 26S proteasome and the resultant peptides are transported into the endoplasmic reticulum (ER), by the transporter associated with antigen processing, TAP. These peptides are bound by a heterodimer of β_2-microglobulin (β_2m) and class I heavy chain and transported through the Golgi and trans-Golgi network (TGN) to the cell surface. There, the peptide-class I complexes are bound and recognized by cytolytic CD8 T cells that destroy the infected cell (for a review, see (Brodsky et al., 1999)).

CLASS II MHC MOLECULES

Structure and expression pattern

In contrast to class I molecules, class II MHC molecules primarily present extracellularly-derived antigens that are internalized by means of a membrane-bound compartment. The human class II MHC complex is located on chromosome 6 and consists of three loci designated human leukocyte antigen (HLA)-DR, DP and DQ, each encoding a minimum of one α and one β chain gene. Class II MHC molecules are non-covalently linked heterodimers consisting of one α and one β chain (Kaufman et al., 1984). Nascent α and β chains originating from the same locus associate almost exclusively with their paired gene product, with DR$\alpha\beta$ dimers being the most abundant of the three. Both chains are type I integral membrane proteins and have two immunoglobulin domains named α1, α2, β1 and β2. The N-terminal α1 and β1 domains combine to form a β-sheet platform flanked by two α-helices (Figure 1-1)(Ghosh et al., 1995). These α-helices form a groove that is capable of binding antigenic peptides of varying lengths. Constitutive expression of class II molecules and its related loading machinery are limited to a subset of cells

specialized for antigen presentation, namely B cells, dendritic cells and macrophages. However, some nonexpressing cell types may be induced to express all the components of the class II MHC system by stimulation with interferon-γ (IFN-γ). The studies presented here take advantage of this fact in the experimental design discussed later.

αβ heterodimer formation occurs in the ER after their synthesis and is followed shortly by their association with a third protein called the invariant chain. Three αβ heterodimers bind trimers of invariant chain to form a large nonameric complex which will traffic into the Golgi complex (Roche et al., 1991). An excess of invariant chain is always present in the ER, virtually ensuring that every class II heterodimer will be bound by invariant chain (Marks et al., 1990).

Invariant chain function

This association with invariant chain serves several major functions for class II molecules. First of all, the invariant chain binds to class II molecules in the peptide binding groove, thus precluding the binding of various peptides residing in the ER. By preventing possibly tight binding of ER peptides to the αβ heterodimers, the invariant chain effectively

---

Figure 1-1. Structure of a human class II major histocompatibility molecule (HLA-DR3).

(A) Crystal structure of a human class II MHC molecule (HLA-DR3) showing the α1 (dark blue), α2 (blue), β1 (green), β2 (yellow) domains and a peptide (red) in the peptide binding groove formed by the α1 and β1 domains. The structure shown does not include the transmembrane regions of the proteins. The portions of the structure that are most distal to the membrane are the α1 and β1 domains.

(B) T cell receptor (top down) view of the peptide binding groove formed by the α1 and β1 domains with a bound invariant chain peptide, CLIP. These figures were created using PDB ID: 1A6A, Molescript and Raster 3D (Kraulis, 1991; Merritt and Murphy, 1994).

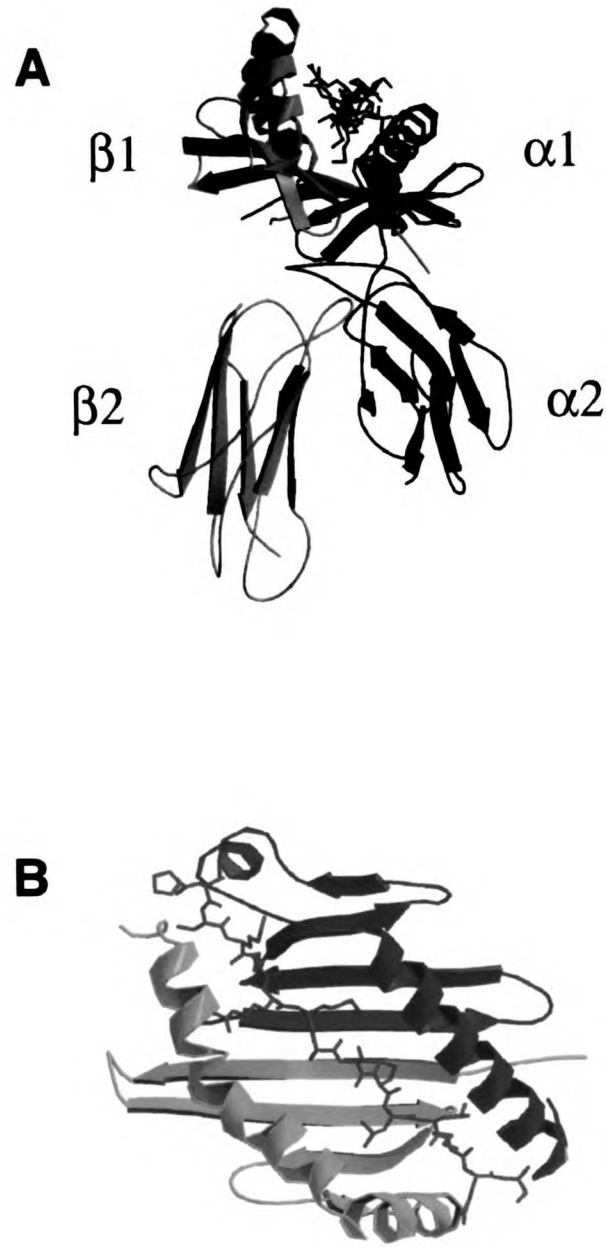

Figure 1-1

reserves class II molecules for the extracellularly derived peptides that it will encounter later in its journey to the cell surface (Busch et al., 1996; Roche and Cresswell, 1990). Crystal structures confirm that a portion of invariant chain binds in the peptide binding groove (Ghosh et al., 1995) rather than outside the site. Its occupancy of the peptide binding groove also serves to confer stability to the heterodimer until an antigenic peptide binds. This function is essential to class II molecules because of the inherent instability of the heterodimer without a peptide. However, once a peptide is fixed in the binding groove the heterotrimer becomes fairly stable. The portion of invariant chain serving as a surrogate peptide, termed CLIP, for class II-associated invariant chain peptide, confers less stability than most antigenic peptides but enough to allow the heterodimer to remain intact during its transport (Sadegh-Nasseri et al., 1994; Zhong et al., 1996). The lower affinity of CLIP allows for its removal later in the loading process. The extraordinary stability of the peptide/class II complex serves as the basis for an assay measuring the amount of complexes in a detergent lysate. αβ-peptide complexes immersed in SDS sample buffer remain stable until they are boiled and can be quantified on SDS-PAGE (Pious et al., 1985).

The invariant chain also directs the trafficking of class II heterodimers. As a type II integral membrane protein, the invariant chain contains an N-terminal tail in the cytoplasm with its lumenal domain binding class II molecules. The cytoplasmic tail contains a di-leucine localization signal that directs invariant chain-bound class II molecules into the endocytic pathway (Bakke and Dobberstein, 1990) as shown by endocytic targeting of various receptor/invariant chain tail chimeras but not chimera with truncated tails (Odorizzi et al., 1994; Pieters et al., 1993). This endocytic targeting function is enhanced by the multimerization of the invariant chain targeting sequences. Class II-associated trimers composed of two N-terminally truncated invariant chains and a single intact invariant chain were targeted to the cell surface in transfected cells whereas trimers of intact invariant chain traveled predominantly to an endosomal compartment (Arneson and Miller, 1995). Once

the complexes are in the endocytic compartment, the targeting signal becomes a hindrance to further trafficking by class II molecules. To allow further trafficking of class II molecules, the invariant chain must be proteolytically removed from class II molecules for the dimers to travel to the cell surface (Brachet et al., 1997).

The class II/invariant chain complexes accumulate in what once were thought to be compartments specialized for loading antigenic peptides onto class II molecules. Studies from a number of groups identified compartments that were similar but not identical in their distinguishing membrane protein markers. Depending on the method of analysis and the cell type, the class II loading compartment has been characterized as a specialized compartment with either late endosomal or lysosomal traits. Class II-containing compartments from B cells co-sediment on a Percoll gradient with the lysosomal markers LAMP-1 and rab7 and endocytic tracers after an hour chase period (Qiu et al., 1994). Murine macrophages also contain compartments with large amounts of class II co-localizing with lysosomal markers like β-hexosaminidase, LAMP-1 and cathepsin D (Harding and Geuze, 1993). Finer isolation techniques using both density and an electric current have provided an even purer population of these compartments for study. Such studies demonstrate that class II/invariant chain complexes are present in compartments called MIIC, for MHC class II compartment, that contain LAMP-1 and proteases and receive endocytosed material, as expected. However, these compartments are not traditional lysosomes as they only partially overlap the lysosomal marker distribution and contain a differing protein composition than other lysosomes (Tulp et al., 1994). These compartments are multi-vesicular compartments, having vesicles contained within other larger membrane vesicles. Another group, using murine B cells, has characterized the class II loading compartment as a multi-lamellar compartment, one that contains stacks of membrane sheets within a membrane bound compartment. These compartments, called CIIV for class II-containing vesicles, partially overlapped with late endosomal compartments and unlike the MIIC, contained some transferrin receptors, an early

endosome marker (Amigorena et al., 1994). Interestingly, CIIV contain little invariant chain, indicating the removal of invariant chain from class II molecules just prior to arrival in CIIV or shortly thereafter. Other groups have also identified class II loading compartments from B cells and shown that the compartments contain lysosomal markers but are distinct from both endosomes and lysosomes though they may contain markers characteristic of both (Riberdy et al., 1994; West et al., 1994).

Class II Loading Compartments

More recent work has characterized the class II loading compartment as a nonspecialized endocytic compartment that antigen presenting cells use for peptide loading. Detailed electron microscopy of B cells allowed for a rough classification of endocytic compartments into six subtypes (Kleijmeer et al., 1997). These studies indicate that class II molecules are spread throughout the endocytic pathway, with concentrations occurring in two distinctive compartments. A large percentage of the molecules are found in an 'early MIIC', a multi-vesicular late endosomal compartment, not accessible by transferrin receptor, and a 'late MIIC', which contained both internal membrane sheets and vesicles (Kleijmeer et al., 1997) and received endocytic tracers later than the 'early MIIC'. The fact that endocytic tracers co-localize with class II molecules and/or DM molecules throughout the latter half of the endocytic pathway argues that the morphological subtypes represent compartments that are not unique to antigen presenting cells, but instead are part of the normal trafficking pathway traveled by internalized material. Supporting this idea of a nonspecialized loading compartment is the fact that HLA-DM can be found in a number of endocytic compartments, some of which do not contain class II molecules, rather than being localized to a unique compartment (Pierre et al., 1996). Moreover, the multi-lamellar or multi-vesicular morphology thought to be unique to the loading compartment is also found in lysosomes of cells that do not express class II molecules (Dunn, 1994; Holtzman, 1989). In fact, the apparent induction of class II compartments by transfection of class II

and related genes in epithelial cells (Calafat et al., 1994) has been suggested to be a result of overexpression of degradation-resistant class II molecules accumulating in lysosomes (Pierre et al., 1996). It appears then that the concept of a singular class II loading compartment is somewhat misleading since class II molecules are found in a number of compartments, none of which are uniquely specialized for peptide loading. However, for the sake of ease, the compartments in which class II molecules briefly reside and are loaded with peptide shall be referred to hereafter as class II loading compartments (CLC).

Class II/invariant complexes may travel two routes to ultimately reach the late endosomal compartments or CLC. The majority of class II/invariant chain complexes travel directly to the endocytic pathway, though their entry point has been debated. In some cell lines, pulse/chase and subcellular fractionation experiments show that the vast majority of class II complexes travel directly from the TGN to late endosomes (Amigorena et al., 1994; Benaroch et al., 1995; Tulp et al., 1994). Class II/invariant chain complexes have also been detected by pulse/chase experiments in early endosomes (Gorvel et al., 1995), particularly of complexes containing the p33 invariant chain isoform (Warmerdam et al., 1996). Electron microscopy confirms the presence of both HLA-DR and invariant chain in early endosomes (Guagliardi et al., 1990). Newly synthesized class II/invariant chain complexes quickly appear in early endosomes containing transferrin receptor (Castellino and Germain, 1995) suggesting that the complexes first travel to early endosomes and then into CLC where peptide loading occurs. Examination of the entire endocytic pathway for class II/invariant chain complexes indicates that a transitional compartment upstream of late endosomes but containing little or no transferrin receptor is where a large amount of complexes seem to enter the endocytic pathway (Kleijmeer et al., 1997). While the details of these studies may differ, it is clear that in most cells, class II/invariant chain complexes travel to an early endosome-like compartment where invariant chain removal begins.

A minor proportion of the complexes utilize a second route comprised of trafficking from the TGN to the cell surface followed by a rapid internalization into the endocytic pathway. Several studies have demonstrated the existence of this pathway. Golgi-enzyme labeled class II complexes can also be detected at the cell surface shortly after pulse-labeling, indicating their arrival shortly after leaving the TGN (Warmerdam et al., 1996). Invariant chain tail chimeras can also be detected at the surface in small amounts (Pieters et al., 1993). Prolonged treatments with the vacuolar-H+ ATPase inhibitor concanamycin B also results in a slow accumulation of class II/invariant chain complexes at the cell surface (Benaroch et al., 1995). In addition, use of dominant negative clathrin protein to prevent endocytosis from the cell surface results in accumulation of αβ-invariant chain complexes at the cell surface (Liu et al., 1998).

Once the class II/invariant chain complexes reach the endocytic pathway, the process of peptide loading begins with the removal of the chaperoning invariant chain through proteolysis. A number of different proteases present in the endocytic pathway have been shown to be capable of invariant chain degradation through in vitro digestion experiments or use of protease inhibitors (Cresswell, 1996; Mizuochi et al., 1994; Reyes et al., 1992). Cathepsins B and D have even been used to generate CLIP/class II complexes in vitro (Avva and Cresswell, 1994). However, the cysteine proteases (cathepsin B, D and H) implicated in these studies were shown to not be essential for invariant chain degradation in B cells or dendritic cells in vivo by more recent data using highly purified enzymes or very specific protease inhibitors. These experiments confirm the results from cathepsin B and D knockout mice, both of which show no defect in class II antigen presentation (Deussing et al., 1998). Instead, the protease responsible for the complete degradation of invariant chain is cathepsin S, a cysteine protease highly expressed in professional antigen presenting cells, like B cells and dendritic cells (Riese et al., 1996). Specific inhibition of cathepsin S in vivo resulted in class II molecules complexed with a 13 kD invariant chain fragment. Subjecting intact invariant chain/class II complexes to

cathepsin S in vitro resulted in the generation of CLIP/class II complexes, indicating that cathepsin S alone was sufficient to degrade invariant chain down to CLIP (Riese et al., 1996). In vivo studies in cathepsin S null mice also demonstrated a marked impairment of invariant chain degradation and subsequent class II antigen presentation (Nakagawa et al., 1999). While professional antigen presenting cells such as B cells and dendritic cells clearly require cathepsin S to remove invariant chain, thymic epithelial cells responsible for positive selection of CD4 T cells instead require cathepsin L, a similar cysteine protease (Nakagawa et al., 1998). The end result of these proteases' activities is that invariant chain is pared down to a peptide, leaving a class II/CLIP complex.

HLA-DM: Peptide Loading Enzyme

In order for peptide loading to occur, CLIP must first be removed from the peptide binding groove of the class II molecules. This function is performed by the class II-like molecule, HLA-DM or its murine equivalent, H2-M. This molecule is an αβ heterodimer that is localized to late endocytic compartments where peptide loading occurs (Lindstedt et al., 1995; Sanderson et al., 1994). HLA-DM associates with class II/invariant chain complexes after both molecules leave the Golgi and arrive at CLC (Denzin et al., 1996). The invariant chain must first be partially degraded for the interaction of HLA-DM and HLA-DR to occur since αβ dimers complexed with full length invariant chain does not bind to DM molecules. However, DM readily associates with class II complexed with invariant chain fragments as well as with DR/CLIP complexes (Denzin et al., 1996; Sanderson et al., 1996). During this association in the acidic CLC, DM molecules enzymatically catalyze the dissociation of CLIP peptides and larger invariant chain fragments from class II molecules (Denzin and Cresswell, 1995; Sherman et al., 1995; Sloan et al., 1995). DM then acts as a stabilizing chaperone for empty class II molecules until antigenic peptides are loaded (Denzin et al., 1996; Kropshofer et al., 1997). Evidence also suggests that DM facilitates the binding of antigenic peptides in an enzymatically-

catalyzed manner (Vogt et al., 1996). Since DM can also remove peptides other than CLIP from the peptide binding groove, this function allows DM molecules to act as a peptide editor that alters the peptide repertoire displayed by class II molecules (Kropshofer et al., 1996). Without the chaperone/CLIP removal activity of DM, class II-peptide loading is severely impaired and the majority of αβ dimers retain CLIP (Fling et al., 1994; Morris et al., 1994; Sette et al., 1992). Mice deficient in H2-M show similar defects in class II loading (Fung-Leung et al., 1996; Martin et al., 1996; Miyazaki et al., 1996).

The antigenic peptides that DM loads onto class II molecules are generated by the proteolytic degradation of endocytosed antigens. Lysosomal proteases such as cathepsin B and D are thought to be important in the generation of these peptides (Rodriguez and Diment, 1992) and inhibition of these proteases can shift the resulting immune responses (Maekawa et al., 1998).

Peptide-loaded class II molecules then travel to the surface through a pathway that is not well characterized. There is evidence that class II compartments can travel to the surface and deliver loaded class II to the plasma membrane (Wubbolts et al., 1996). The loaded class II molecules travel directly to the surface and do not intersect the early endocytic pathway. In B cells, CLC can also be released as vesicles containing class II/peptide complexes to the extracellular medium (Raposo et al., 1996). Whatever route the class II/peptide complexes take to the surface, there they perform their job of stimulating CD4 T cells to elicit a cellular immune response. Figure 1-2 summarizes the major features of the class II MHC loading pathway.

EXPERIMENTAL SYSTEMS

The process of loading a class II molecule is a complex one, involving a complicated trafficking pathway and a variety of accessory molecules. Because of its complexity, it presents a plethora of points which a pathogen might disrupt to prevent antigen presentation on class II molecules. This study describes two such mechanisms.

The first, disruption of lysosomal trafficking, is utilized by *Coxiella burnetii* and accomplished by a genetic mutation in the heritable immunodeficiency Chediak-Higashi syndrome (CHS). The second mechanism is the *Chlamydia*-catalyzed degradation of invariant chain resulting in disruption of class II trafficking and loading. These infectious diseases and inherited immunodeficiency are introduced below.

The Chediak-Higashi Syndrome

The Chediak-Higashi syndrome (CHS) is a rare, inherited immunodeficiency that results in frequent bacteria infections resulting in pus formation and intermittent bouts of fever (Barak and Nir, 1987). Infections typically occur on the skin, in the lungs or in the upper respiratory tract. Case studies show that infections are manageable with antibiotic therapy but nevertheless are severe and debilitating (Blume and Wolff, 1972). Patients presenting with CHS also display a partial albinism in the skin, hair and eyes such that the hair contains a silvery tint and the skin is sensitive to sunburn (Blume and Wolff, 1972). Animal models of CHS, such the Aleutian Blue mink, the *beige* mouse and blue and silver

---

Figure 1-2. The Class II MHC trafficking pathway.
Newly synthesized class II MHC αβ dimers bind homotrimers of invariant chain in the ER and travel to the trans-Golgi network (TGN) where the proteins are glycosylated. From there, the majority of class II/invariant chain complexes travel to an early endosomal compartment and then down into increasingly acidic compartments where the invariant chain is proteolytically degraded and the residual CLIP is exchanged for an antigenic peptide by HLA-DM. A minor proportion of complexes travel first to the cell surface before entering the endocytic pathway and progressing to late endosomes/loading compartments. Ultimately, peptide-loaded class II molecules are trafficked to the surface where they present the antigenic peptides to helper T cells.

Class II assembly pathway

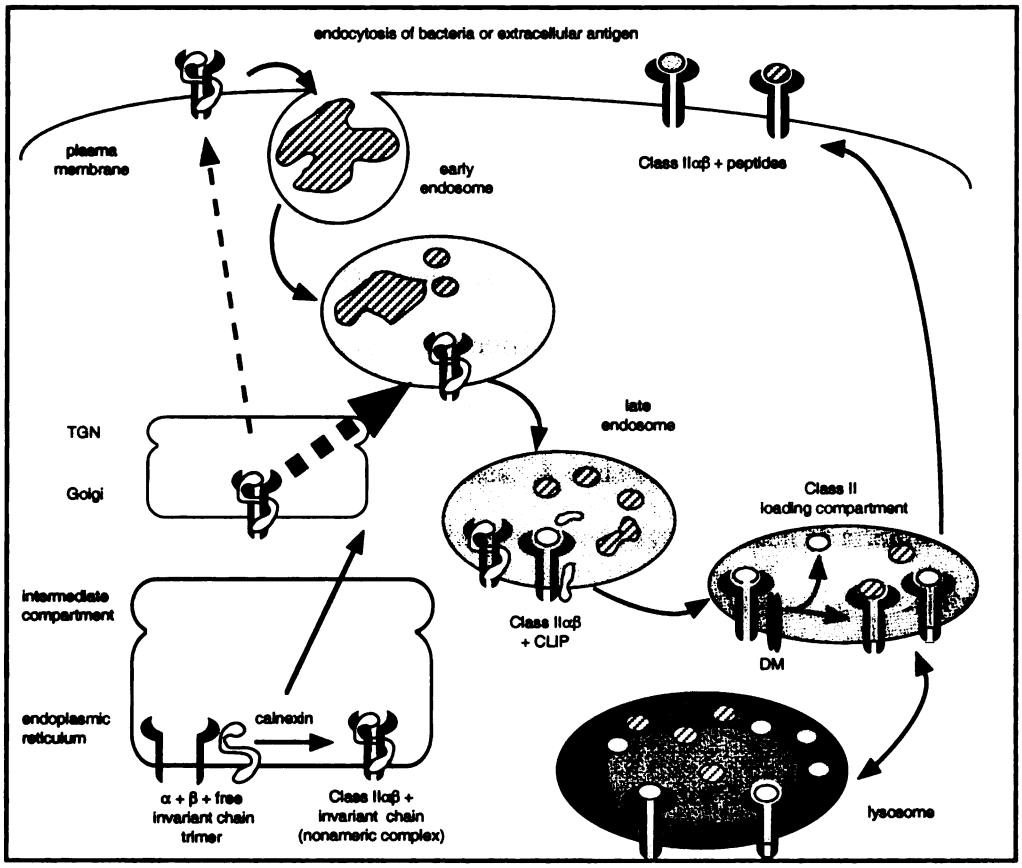

Figure 1-2

foxes, all display this notable alteration in their fur coloration (Penner and Prieur, 1987). Neurological abnormalities are also common, including clumsiness, muscle weakness, and paresthesias, among others (Barak and Nir, 1987). Most CHS patients eventually enter a phase of disease called the accelerated phase in which they are often beset with fever, jaundice, hepatosplenomegaly, lymphadenopathy, frequent bleeding and diffuse mononuclear infiltration in tissues. The pathology of the accelerated phase is not known and usually results in death by infection or hemorrhaging (Barak and Nir, 1987).

At a cellular level, CHS cells display the unusual phenotype of containing enlarged granules which have been identified as lysosomes. A wide variety of cell types contain the enlarged lysosomes, particularly cells of the hematopoietic system, such as granulocytes, monocytes, lymphocytes and platelets. The lysosomal granules have also been located in neurons, fibroblasts, melanocytes, pneumocytes and hepatocytes, indicating that the defect is nearly ubiquitous (Barak and Nir, 1987).

The CHS immunodeficiency results from a dysfunction of several of the neutrophils and natural killer (NK) cells. CHS neutrophils phagocytose bacteria normally but do not release their granule material into the phagosome (Root et al., 1972). CHS patients have normal NK cell counts but no detectable lytic function (Barak and Nir, 1987). Cytotoxic T lymphocytes also are impaired in their granule release and thus have decreased ability to kill target cells (Baetz et al., 1995).

The enlarged CHS lysosomes have been characterized and seem to be similar in content and function to wild-type lysosomes. CHS granules in cytotoxic T cells contain cathepsin D and granzyme A and lack the mannose-6-phosphate receptor just as wild-type granules do (Baetz et al., 1995). Characterization of CHS fibroblasts and the murine immunodeficient equivalent, *beige* fibroblasts, also demonstrated the presence of normal lysosomal markers, such as LAMP-1, cathepsin D and lysosomal glycoprotein [Burkhardt, 1993 #865]. Protein degradation also occurred at normal rates in the CHS and *beige* fibroblasts (Burkhardt et al., 1993). Comparisons of the total volume of lysosomes within

cells also indicated that, per cell, CHS cells do not have more volume of lysosomal compartments than wild-type cells. The differences seem to be that the lysosomes are distributed between numerous smaller vesicles in wild-type cells and aggregated into several gigantic structures in CHS cells (Burkhardt et al., 1993).

The genetic mutation for CHS was recently identified and confirmed to be homologous to the murine *beige* defect (Barbosa et al., 1996; Nagle et al., 1996; Perou et al., 1996). Sequencing of patient DNA has confirmed the presence of mutations in that gene in affected humans (Barbosa et al., 1997; Karim et al., 1997). Genetic rescue of *beige* fibroblasts by transfection with the wild-type gene decreases the size of lysosomes with an accompanied increase in their number (Perou et al., 1997). The gene is located on human chromosome 1 and mouse chromosome 13 and encodes for a very large gene product, with a predicted amino acid sequence of 3801 residues (Nagle et al., 1996). The protein bears faint homology resemblance to a trafficking protein in yeast, VPS 15, but not to any known mammalian proteins. The CHS protein seems to be cytosolic with no membrane association (Perou et al., 1997). Its exact function remains unknown but it is believed to regulate lysosome fission based on the genetic rescue data (Perou et al., 1997).

The CHS system represents an ideal model system in which to investigate class II trafficking and peptide loading. Since class II molecules traffic extensively in the late stages of the endocytic pathway, including late endosomes and lysosomes, it is likely that altered trafficking would affect the movement of class II molecules either into or out of the loading compartments. It is also likely that the mutation would affect the morphology of the loading compartments. Chapter 2 discusses our characterization of the class II maturation defects identified in B lymphoblasts from CHS patients.

Coxiella burnetii

Coxiella burnetii is an obligate intracellular rickettsia that is usually acquired through inhalation of infectious particles. The particles are highly infectious and resistant

to rather harsh environmental conditions, such as desiccation, heat and low pH, contributing to its ability to survive in soil for an extended period of time or be dispersed over long distances by the wind (Stein and Raoult, 1995). *Coxiella* are considered to be highly infectious since estimates are that inhalation of one bacterium is a sufficient inoculation dose (Stein and Raoult, 1995). Once inside the cells of the respiratory tract, the *Coxiella* proliferate and then disseminate to the liver or heart valve. Acute Q fever arises after an incubation period ranging from 2 to 6 weeks. Patients generally show the signs of an atypical flu or pneumonia, displayed in high fevers, chills, headaches and sometimes chest pains, hepatosplenomegaly and coughing. Liver involvement also is shown by the elevation of liver enzymes and jaundice (Reimer, 1993). Most cases of Q fever resolve themselves after 1 to 2 weeks although immunity does not always last since relapses are known to occur (Raoult and Marrie, 1995). Some cases progress to chronic infections from 1 to 20 years post exposure (Reimer, 1993) in which the organism most often infects previously defective heart valves causing endocarditis (Raoult and Marrie, 1995). These symptoms are severe and often fatal as a result of cardiac or valvular failure (Stein and Raoult, 1995).

The existence of chronic infections indicate a priori that *Coxiella* are able to evade the host immune response directed against it. The long incubation times also argue that *Coxiella* somehow remain shielded from the host immune system. Part of this evasion could be attributed to *Coxiella*'s ability to survive in the harsh environment of the host lysosome. Because *Coxiella* thrive in the lysosome, it is likely that they are able to resist the degradative enzymes present in the endocytic pathway and thus are inherently resistant to antigen presentation on class II MHC. Despite its specialization for the lysosome, some antigens are certainly presented since a primary diagnostic approach is identification of anti-*Coxiella* antibodies in the serum (Reimer, 1993). More specific studies are necessary to determine the action of the host immune system in *Coxiella* infections.

On a cellular level, *Coxiella* are passive entrants into the host cell, relying upon host mechanisms for its uptake. Once inside the cell, *Coxiella* travel down the endocytic pathway to the acidic lysosomes where they propagate. As mentioned previously, *Coxiella* thrive in the acidic lysosomes and even depend on the acidic environment for its metabolism (Hackstadt and Williams, 1983). *Coxiella* do not alter the acidity of the lysosome during infections since pH remains acidic during prolonged infections (Maurin et al., 1992) as indicated by the presence of the vacuolar proton pump in *Coxiella* vacuoles (Heinzen et al., 1996). Lysosomes containing *Coxiella* continue to function normally as indicated by fusion with other lysosomes containing endocytosed yeast or other particles (Heinzen et al., 1996; Veras et al., 1994). Such fusion was slowed in *Leishmania* vacuoles. Moreover, superinfection of *Coxiella*-infected cells with *Leishmania amazonensis* resulted in cohabitation of the same lysosomes (Veras et al., 1995).

Closer examination of the *Coxiella* compartment indicates that it contains all the markers of a lysosome. Besides the presence of the vacuolar proton pump, the soluble lysosomal enzymes acid phosphatase and cathepsin D colocalized to *Coxiella* vacuoles (Heinzen et al., 1996). The lysosomal membrane proteins LAMP-1 and LAMP-2 also defined the compartment as a lysosome. Its acidity was also confirmed by the staining of the acidotropic dye acridine orange. In contrast, the late endosomal marker, mannose-6-phosphate receptor was not present, leaving no doubt as to the character of the *Coxiella* vacuole.

An interesting explanation for *Coxiella*'s persistence in the infected host was the possibility that the bacteria might be interfering with the class II antigen presentation pathway. Since class II MHC molecules traffic into late endosomal compartments and are often found in compartments with the density of lysosomes (Qiu et al., 1994; Tulp et al., 1994), *Coxiella* might possibly alter the loading and trafficking of class II molecules. The *Coxiella* vacuole slowly enlarges during the infection cycle and forms an enlarged lysosome. If *Coxiella* induce fusion of its vacuole with host lysosomes, they would likely

alter the distribution of class II molecules in the same manner. In addition, class II molecules have been shown to accumulate in the vacuole of *Leishmania amazonensis* (De Souza Leao et al., 1995). As *Leishmania* and *Coxiella* both reside in the same compartment during a co-infection, it was likely that class II molecules would reside in *Coxiella* vacuoles.

Using a combination of immunofluorescent microscopy and biochemical experiments, this project attempts to determine if and how *Coxiella* infection affects the trafficking and loading of class II molecules. The biochemical infection experiments for both *Coxiella* and *Chlamydia* were done in an IFN-γ induced HeLa system. HeLa are readily infectable by both bacteria and the system has been previously characterized by others. Moreover, IFN-γ induction results in upregulation of class II, invariant chain and DM. The presence of these molecules is sufficient to reconstitute class II antigen presentation (Calafat et al., 1994; Karlsson et al., 1994) and for the purposes of this work, presents a suitable model for both infection and class II trafficking. The work detailed in Chapter 2 chronicles our understanding of how *Coxiella* does, in fact, alter intracellular distribution of class II MHC and its related molecules, and antigen presentation. Comparisons to the effects of the physiologically similar lysosomal defect seen in CHS cells demonstrate a common effect on class II antigen presentation.

Chlamydia trachomatis

Chlamydia trachomatis is an obligate intracellular bacteria that infects humans through two primary routes, the epithelium of the eye and the genital tract. As a prominent human pathogen worldwide, *Chlamydia trachomatis* is the leading cause of infectious blindness in developing nations. In developed nations, it is the most common form of sexually transmitted disease. Both forms of *Chlamydia* infection are costly, by economic and personal health standards. Infections cause considerable damage to their human hosts since genital tract infections in women often result in pelvic inflammatory disease with

subsequent ectopic pregnancies or tubal infertility (Ward, 1995). Evidence suggests that *Chlamydia* may also cause male infertility (Greendale et al., 1993). Ocular infections range upwards of 300 million cases worldwide with approximately 9 million resulting in blindness. The risk of complications from *Chlamydia* infections are compounded with recurrent infections which can become chronic if left untreated. Lack of treatment is in fact a common problem, particularly in the case of the sexually transmitted disease which can often present as an asymptomatic 'silent' infection (Ward, 1995).

The possibility of asymptomatic infections implies that *Chlamydia* evades or disables the immune response. Characterization of the host immune response to *Chlamydia* has been the subject of many investigations, whose eventual goal has often been the production of a chlamydial vaccine. Which components of the immune system are necessary for elimination of *Chlamydia* from the host? For a number of years, it has been controversial as to whether CD8 or CD4 T cells were more important for immunity to *Chlamydia* infection. The literature contains reports both asserting and denying the need for CD8 T cells in *Chlamydia* immunity. Cytotoxic T cells are certainly able to lyse *Chlamydia*-infected cells despite the seclusion of bacterial antigens in a membrane bound vacuole (Rasmussen et al., 1996). Transfer of a *Chlamydia*-specific CD8 T cell clone into nude mice confers immunity and results in clearance of the bacteria (Igietseme et al., 1994) suggesting that CD8 cells are both necessary and sufficient for immunity. Moreover, in β_2m null mice which express no class I molecules and have very few functional CD8 T cells, bacteria levels were double that of wild type mice early in the infection, but eventually cleared. Higher doses of bacteria also resulted in a higher mortality rate (Magee et al., 1995). However, antibody depletion of CD8 T cells in mice results in only slightly higher mortality rates after *Chlamydia trachomatis* pulmonary infections (Magee et al., 1995). The effects of CD8 T cells may lie not in their lytic activity but their ability to produce IFN-γ. Transfer of *Chlamydia* specific CD8 cells from IFN-γ null mice into wild type mice does not confer protection while wild type CTL do (Lampe et al., 1998). These studies conflict

with the findings of Morrison, et al. (Morrison et al., 1995) who showed that genital *C. trachomatis* infections of class I-deficient mice were cleared with normal kinetics. Also, mice deficient in the lytic proteins used by CD8 or CD4 cytotoxic T cells produced a fairly normal cytokine and antibody response and more importantly, cleared the bacteria with kinetics similar to control mice (Perry et al., 1999). While it is difficult to compare the results of experiments done using different *Chlamydia* strains and infection routes, the evidence argue that CD8 T cells do participate in immunity to *Chlamydia* though their contribution seems to be more necessary under higher bacterial burden.

The evidence for a prominent role for CD4 T cells in *Chlamydia* immunity is less controversial. Most all models indicate that CD4 T cells are required for efficient clearance of *Chlamydia*. Antibody depletion of CD4 T cells results in higher mortality rates than in control mice (Magee et al., 1995). Adoptive transfer of bulk activated CD4 T cells from mice following resolution of a *Chlamydia* infection will confer immunity to naive animals challenged after the transfer (Su and Caldwell, 1995). Transfer of resting CD4 cells also confers immunity, suggesting an important role for CD4 helper cells in the host response to *Chlamydia* infections.

Studies with IFN-γ knockout mice suggest that part of the requirement for CD4 helper cells is due to their production of IFN-γ from Th1 type helper cells. Interleukin-12 (IL-12) p40 is required for the development of Th1 helper cells and lack of IL-12 prevents dendritic cells from stimulating a protective response (Lu and Zhong, 1999). IFN-γ is known to inhibit growth of *C. trachomatis* (Rothermel et al., 1983) by inducing the catabolism of cellular tryptophan stores (Byrne et al., 1986).

The necessity of CD4 T cells argues for the necessity of an adequate class II-mediated antigen presentation of *Chlamydia* antigens in order to produce immunity. In addition, the necessity for a strong IFN-γ response also highlights the significance of Th1 CD4 T cells in particular. How can *Chlamydia* prevent the stimulation of helper T cells?

The answers lie in a cellular model of infection where the interaction of the bacteria with its host cell can be more closely examined.

Like *Coxiella*, *Chlamydia* has two developmental forms during its life cycle (Figure 1-3). The inert, extracellular elementary body (EB) is metabolically inactive and nonreplicating but initiates all *Chlamydia* infections. EB's attach to a host cell through high mannose oligosaccharides (Campbell et al., 1998) on an unknown receptor or receptors. When the 300 nm, electron dense EB's enter the cell, they are taken up into a membrane-bound compartment called the vacuole or inclusion. During the first few hours within the cell, the EB's begin to synthesize proteins and rearrange their DNA. During this time, the EB's differentiate into a larger 1 μm form called the reticulate body or RB. The RB form is metabolically active and replicates by binary fission within the confines of the vacuole but is nonviable when released from the cell. As the infection progresses, the RB's can be found lining the inclusion membrane while EB's seem to dance within the inclusion lumenal space. The RB's continue to divide until the vacuole nearly fills all the host cell cytoplasm. 24 to 72 hours post infection (hpi), the RB's begin differentiating back to EB's which are released when the cell lyses, presumably under the weight of the enormous vacuole. The EB's then attach to other host cells, beginning another round of infection.

Figure 1-3. The *Chlamydia* life cycle.

Infectious, small dense, elementary bodies (EB's) attach to an epithelial cell, are endocytosed into a membrane bound vacuole. Within hours, the EB's synthesize protein, aggregate in a peri-nuclear region, fuse with other vacuoles and differentiate into larger, metabolically active reticulate bodies, RB's, which attach to the membrane of the expanding vacuole. The RB's replicate until the host cell can no longer support the bacteria, at which time, the RB's redifferentiate into EB's to be released on cell lysis. The freed EB's then establish a new infection cycle in another host cell.

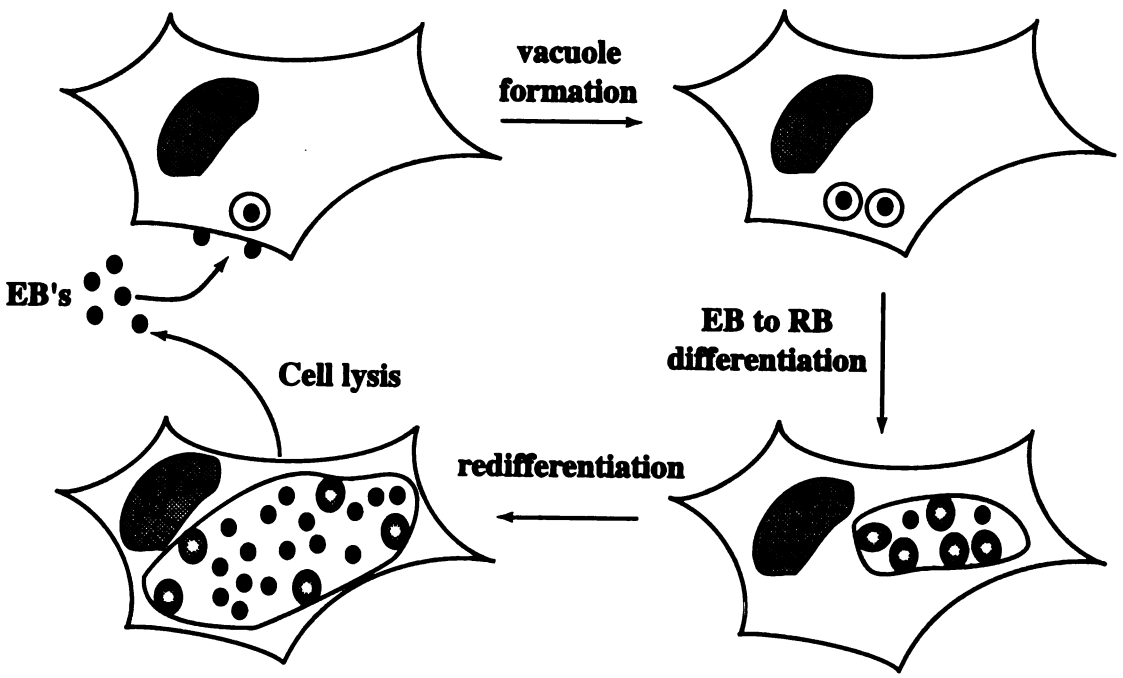
vacuole
formation
EB's
EB to RB
differentiation
Cell lysis
redifferentiation

Figure 1-3

In contrast to the *Coxiella* vacuole, the chlamydial inclusion does not fuse with lysosomes. Very early in the infection, the early endosome marker, transferrin receptor, has been detected in close association with *Chlamydia* vacuoles (van Ooij et al., 1997). The late endosome marker mannose-6-phosphate receptor has also been detected very close to the early inclusions (van Ooij et al., 1997). Because the vacuoles are extremely small at that early time, it is not clear whether the transferrin receptor or mannose-6-phosphate receptor staining vesicles were present on the bacterial vacuoles or merely in close proximity to the nascent inclusions. However, during later stages of infection no lysosomal or other host proteins, soluble or membrane, have been detected on *Chlamydia* vacuoles (Heinzen et al., 1996; Taraska et al., 1996). Unlike endosomes that fuse with lysosomes, the vacuoles showed no signs of acidification, remaining above pH 6 as shown by the absence of staining by acidotropic dyes (Heinzen et al., 1996; Schramm et al., 1996).

These characterizations provide the impression that *Chlamydia* inclusions are isolated chambers in which the bacteria can safely multiply. However, there is mounting evidence that *Chlamydia* do interact with host trafficking for its own use while still allowing the cell to continue most metabolic activities. While no host proteins have been detected on the inclusion membrane, TGN38, a trans-Golgi network (TGN) marker, has been found to redistribute to an area around the inclusion (van Ooij et al., 1997). As seen later in this work, the lysosomal marker CD63 also redistributes in a perivacuolar pattern (Fig. 3-1). In addition, host membrane in the form of sphingomyelin is redirected to the inclusion from the TGN and incorporated into the growing bacteria (Hackstadt et al., 1995). Clearly, a dynamic relationship exists between the growing inclusion and host membrane compartments.

How might *Chlamydia* redirect host membrane trafficking from within the vacuole? A likely mechanism involves a putative type III secretion system recently discovered in the *Chlamydia* genome (Hsia et al., 1997). Type III secretion systems are found in pathogenic

bacteria as part of a cluster of virulence genes (Galan and Collmer, 1999). The apparatus, similar in structure to bacteria flagellar assembly complexes, allows the bacteria to secrete proteins across its cell wall, and through a host plasma membrane into the cytoplasm. Such a mechanism could exist in *Chlamydia* except that secretion would occur from the vacuole lumen into the cytosol rather than from outside the cell into the cytosol.

Other mechanisms *Chlamydia* uses for redirecting host membrane trafficking to and from the inclusion include the insertion of its own proteins into the inclusion membrane (Scidmore-Carlson et al., 1999). IncA is one such inclusion membrane protein (Bannantine et al., 1998) whose function was determined with the use of serendipitously occurring natural mutants in inclusion fusogenicity. Normally, multiple vacuoles in the same cell will congregate in the perinuclear region and fuse during the course of infection. However, these variants did not fuse and antibody staining correlated this defect to the lack of IncA on the inclusion membrane. Gene sequencing in two variants confirmed the presence of mutations in the IncA gene leading to two amino acid changes (Suchland et al., 2000).

All of these mechanisms could be used for the disruption of class II trafficking and loading. Our foray into *Chlamydia* effects of class II molecules was actually serendipitous. Its apparent isolation from the rest of the endocytic pathway made it, or so it was thought, an ideal control for the class II/*Coxiella* studies. As it turned out, *Chlamydia* have at least two systems for altering class II antigen presentation. *Chlamydia* are able to prevent the induction of class II and DM transcription by interferon-γ through the degradation of USF-1. IFN-γ induction of class II normally occurs through upregulation of USF-1, which upregulates CIITA, the transcription factor that directly activates the class II genes. *Chlamydia*-infected cells degrade USF-1 through a proteasome like protease thereby inhibiting class II expression (Zhong et al., 1999). The second mechanism of preventing class II expression is a targeted degradation of invariant chain that may prevent class II trafficking and destabilize the heterodimer. While viral disruption of class I trafficking and

its subsequent degradation has been well documented, such a mechanism is unprecedented for class II molecules. Chapter 3 describes this second mechanism and its implications for the field of immunity to intracellular bacteria.

AIMS AND ORGANIZATION OF THIS THESIS

The overall goal of this thesis was to identify genetic or bacteria-induced disruptions in the class II MHC trafficking pathway that possibly would lead to immunodeficiencies in humans. To accomplish this task, I used microscopy and biochemical approaches to study the subcellular events preventing antigen presentation by class II molecules.

Aim 1: To determine if and how the enlarged lysosomes in Chediak-Higashi B lymphoblasts disrupt class II trafficking and loading. (Chapter 2)

Aim 2: To determine if the growing, lysosome-like, *Coxiella* vacuole alters the distribution and loading of class II molecules. Chapter 2)

Aim 3: To determine if and how the apparently isolated *Chlamydia* are able to affect the trafficking and loading of class II molecules. (Chapter 3)

Chapter 4 will present the broad implications of the results for antigen presentation and immunity to intracellular bacteria. This chapter also discusses questions remaining about the molecular mechanisms of evasion and suggests possible experiments to address them. Chapter 5 presents a detailed description of methods that were established in the lab during the course of this thesis or are unique to this project.

Chapter 2

Enhanced Interaction of HLA-DM with HLA-DR in Enlarged Vacuoles of Hereditary and Infectious Lysosomal Diseases

The text of this chapter was written by the author with editorial input from Dr. Frances Brodsky and others.

This work was done in collaboration with Marci Scidmore and Ted Hackstadt from the NIH Rocky Mountain Laboratories and Gillian M. Griffiths from Oxford. Dr. Hackstadt trained me to perform infections with *Coxiella* and *Chlamydia* and provided valuable feedback along with Dr. Scidmore-Carlson. Gillian Griffiths provided the Chediak-Higashi B lymphoblasts used in the paper and Dave Riethof, a technician in the lab, performed a number of experiments for which results were negative and are not displayed here. Data for all the figures in this paper was generated by this author. HLA-DR typing was generously performed by Drs. S.G. Marsh and A. Begovich.

ABSTRACT

Following biosynthesis, Class II MHC molecules are transported through a lysosome-like compartment where they acquire antigenic peptides for presention to T cells at the cell surface. This compartment is characterized by the presence of HLA-DM which catalyses the peptide loading process. Here we report that the morphology and function of the Class II loading compartment is affected in diseases with a phenotypic change in lysosome morphology. Swollen lysosomes are observed in cells from patients with the hereditary immunodeficiency Chediak-Higashi syndrome (CHS) and in cells infected with *Coxiella burnetii*, the rickettsial organism that causes Q fever. In both disease states, we observed that HLA-DR and HLA-DM accumulate in enlarged intracellular compartments, which label with the lysosomal marker LAMP-1. The distribution of Class I MHC molecules was not affected, localizing disease effects to the endocytic pathway. Thus cellular mechanisms controlling lysosome biogenesis also affect formation of the Class II loading compartment. Analysis of cell surface Class II molecules revealed that their steady state levels were not reduced on diseased cells. However in both disease states, enhanced interaction between HLA-DR and DM was detected. In the CHS cells, this correlated with more efficient removal of the CLIP peptide. These findings suggest a mechanism for perturbation of antigen presentation by Class II molecules and consequent immune deficiencies in both diseases.

INTRODUCTION

Class II molecules encoded by the major histocompatibility complex (MHC) bind antigenic peptides and display them on the cell surface for recognition by helper T cells, thereby initiating an antigen-specific immune response. Antigenic peptides are generated in the endocytic pathway by proteolysis of internalized, pathogen-derived proteins and are bound to Class II molecules in an intracellular vesicular compartment where newly synthesized Class II molecules accumulate. This so-called peptide loading compartment is part of the endocytic pathway and its vesicles have characteristics in common with lysosomes which include the lysosomal membrane protein LAMP-1 and the degradative enzymes cathepsin D and b-hexosaminidase. However, loading compartment vesicles do not co-fractionate with lysosomes during separation of intracellular organelles, indicating that they are distinct from lysosomes (Amigorena et al., 1994; Tulp et al., 1994). The exact nature of the Class II loading compartment and its biogenesis have yet to be fully defined. There is some debate as to whether it is a specialized compartment or part of the existing endocytic pathway, representing a pre-lysosomal compartment that has expanded in specialized cells due to accumulation of Class II molecules synthesized by these cells (Calafat et al., 1994; Karlsson et al., 1994; Kleijmeer et al., 1997). To learn more about the biogenesis and immunological role of the Class II loading compartment, we investigated whether its morphology and the distribution and function of Class II molecules are altered in disease states in which lysosome morphology is altered. We observed significant changes in the Class II pathway in cells from patients with Chediak Higashi syndrome (CHS) and in cells infected with *Coxiella burnetii*, which are both characterized by swollen lysosomes.

CHS is a rare autosomally-inherited immunodeficiency in which numerous cell types from affected patients have fewer and considerably larger lysosomes than usual. Lysosomal degradation occurs normally in CHS fibroblasts (Burkhardt et al., 1993), but in hematopoietic cells and melanocytes, secretion of lysosomes and lysosome-like organelles

is impaired (Baetz et al., 1995; Griffiths, 1996). Thus these patients are hypo-pigmented and have non-functional cytotoxic T cells and natural killer cells incapable of secreting lytic granules, as well as defects in enzyme secretion by macrophages and neutrophils (Barak and Nir, 1987). The mutations responsible for the CHS defect and the murine version in the *beige* mouse have all been mapped to the same gene (Barbosa et al., 1996; Nagle et al., 1996; Perou et al., 1996). The gene product has predicted sequence homology to the yeast protein VPS15, which is involved in protein trafficking to the yeast vacuole, a process thought to be analogous to lysosomal targeting. The *beige* gene produces a 400 kDa cytosolic protein that promotes lysosome fission when overexpressed (Perou et al., 1997). Mutations at various locations in the gene in both mouse and human result in swollen lysosomes characteristic of the disease. Enlarged lysosomes are also characteristic of cells infected with the rickettsiae *Coxiella burnetii* (Heinzen et al., 1996). *Coxiella* entry occurs by host cell phagocytosis after which bacteria-containing vacuoles fuse and acquire a characteristic lysosomal phenotype with low internal pH and typical lysosomal markers, becoming engorged with replicating organisms (Heinzen et al., 1996). Infection by this obligate intracellular bacteria often presents as an prolonged atypical pneumonia called Q fever. Despite an antibody response, infections may become chronic, resulting in relapse of symptoms years later (Raoult and Marrie, 1995). Thus both the genetic and infectious lysosomal diseases we examined are associated with an impaired immune response, as well as altered lysosome morphology.

Here we demonstrate that the HLA-DR human Class II molecules and the related HLA-DM molecules are localized to enlarged lysosome-like vacuoles in B lymphoblastoid cells from CHS patients and in *Coxiella*-infected cells. In both disease states, we can detect enhanced interaction between HLA-DR and DM by co-immunoprecipitation. Peptide loading of Class II molecules is dependent on HLA-DM, which is normally localized to the loading compartment and which functions by catalytic removal of the endogenous CLIP peptide from the Class II peptide binding site to allow peptide derived from exogenous

protein to bind (Denzin and Cresswell, 1995; Sherman et al., 1995; Weber et al., 1996). CLIP is a proteolytic remnant of the invariant chain, which is responsible for targeting Class II molecules to the endocytic pathway (Bakke and Dobberstein, 1990). In the CHS B cell lines, we observe that the peptide loading process is skewed towards more efficient removal of CLIP from HLA-DR molecules. While this manuscript was under revision, Faigle et al. (Faigle et al., 1998) reported that CHS B cells have an altered peptide repertoire and exhibit delayed antigen presentation to T cells. These properties, as well as reduced CLIP association, can be explained by the mechanism of enhanced DM/DR association that we describe here. Thus we find that the morphology and function of the Class II peptide loading compartment is affected by processes that affect lysosome morphology, indicating common mechanisms in their biogenesis and suggesting a role for compartment morphology in antigen presentation. Furthermore, the immune defects in CHS patients and the poor immune response to *Coxiella* infection may be exacerbated and/or partially explained by this morphologically-induced perturbation of the Class II MHC pathway.

RESULTS

Enlarged LAMP-1-staining vacuoles in B cells from Chediak-Higashi Sydrome patients contain both HLA-DR and HLA-DM

In human B cell lines, HLA-DM is a characteristic marker of the Class II loading compartment (Sanderson et al., 1994). To establish whether morphology of the loading compartment is altered in cells of CHS patients, we examined the distribution of HLA-DM relative to the enlarged CHS lysosomes. B lymphoblastoid cell lines from three unrelated CHS patients were double-stained for HLA-DM and the lysosomal marker LAMP-1 and analyzed by immunofluorescent microscopy (Fig. 2-1). The three CHS cell lines all contained significantly enlarged LAMP-1-staining vacuoles (Fig. 1 F, H, J), the majority of which co-stained for HLA-DM (Fig. 2-1 E, G, I). The wild-type B cells, JY and Jest

Hom, contained numerous small cytoplasmic LAMP-1-positive vesicles, indicated by a punctate staining pattern (Fig. 2-1 B, D), a subset of which also stained for HLA-DM (Fig. 2-1 A, C). In CHS cells, DM-staining vacuoles were consistently larger and fewer in number than those seen in wild type cells. Double-staining for HLA-DR and DM revealed that DR accumulated in the enlarged DM-containing vesicles, although staining of cell-surface DR was also observed in CHS cells (Fig. 2-2). The vesicular DR staining in wild-type cells was much more diffuse (Fig. 2-2 B, D). A similar immunofluorescent staining

---

Figure 2-1. Accumulation of HLA-DM in enlarged lysosome-like compartments in CHS B lymphoblastoid cell lines.

Wild type B cell lines JY (A, B), Jest Hom (C, D) and CHS B cell lines CHS-GG (E, F), GM02431A (G, H) and GM03365 (I, J) were double-stained for LAMP-1 (mouse mAb H4A3) (B, D, F, H, J) and HLA-DM (anti-DM rabbit serum) (A, C, E, G, I), followed by FITC goat anti-mouse Ig and Cy3 goat anti-rabbit Ig respectively. Each pair of adjacent photos shows staining of the same field for the different fluorophores.

Figure 2-2. Localization of HLA-DR with HLA-DM in enlarged CHS lysosome-like compartments.

Wild type B cell lines JY (A, B), Jest Hom (C, D) and CHS B cell lines CHS-GG (E, F), GM02431A (G, H) and GM03365 (I, J) were double-stained for HLA-DM (anti-DM rabbit serum) (B, D, F, H, J) and HLA-DR (mouse mAb L243) (A, C, E, G, I), followed by Cy3 goat anti-rabbit Ig and goat anti-mouse Ig respectively. Each pair of adjacent photos shows staining of the same field for the different fluorophores.

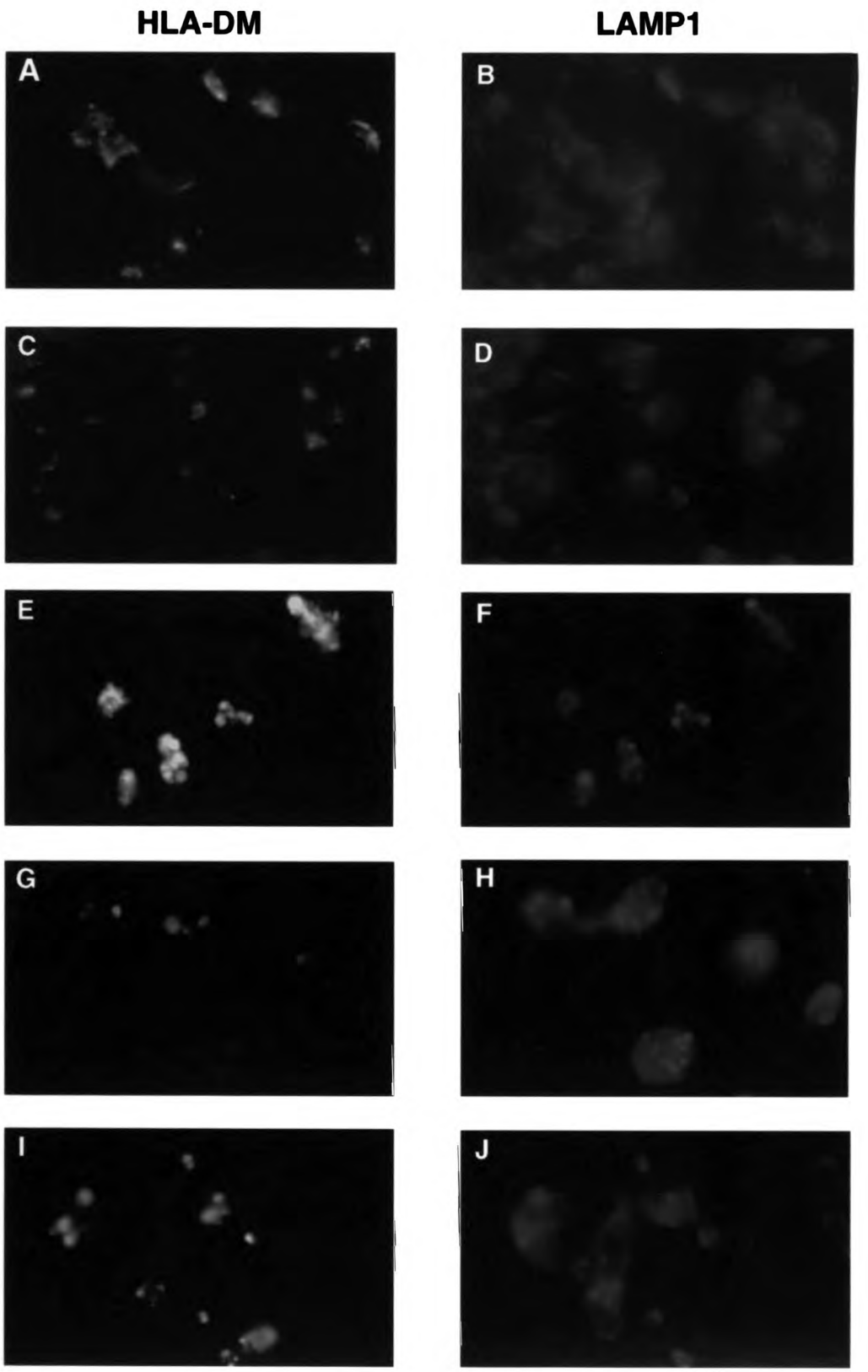

Figure 2-1

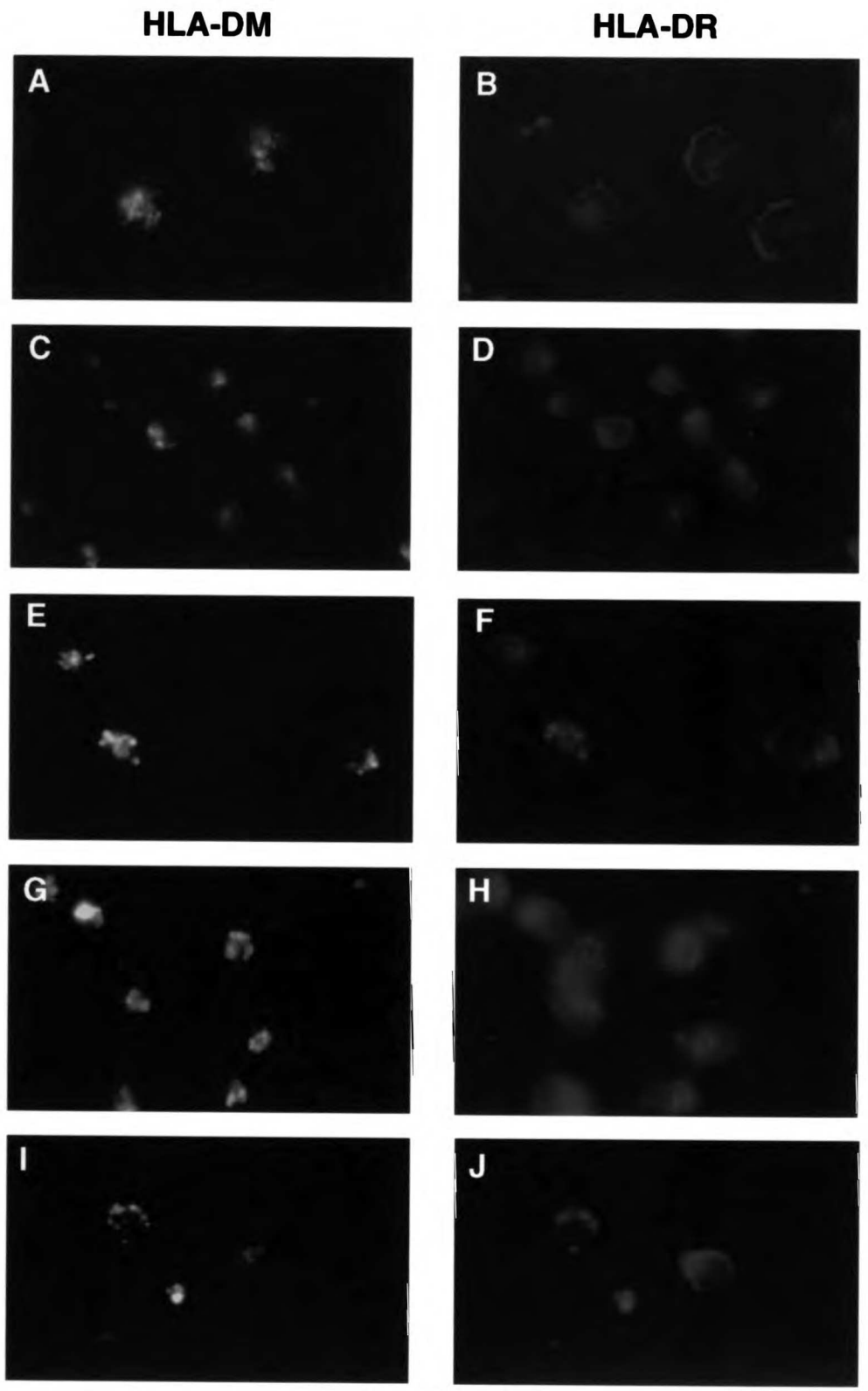

Figure 2-2

pattern of accumulated DM, DR and LAMP-1 was recently reported for two additional B cell lines derived from CHS patients (Faigle et al., 1998). We observed no significant difference in the distribution of Class I MHC molecules between the CHS and wild type B cells (data not shown), which demonstrates that the CHS mutation specifically affects molecules trafficking to the endocytic pathway, such as HLA-DM and HLA-DR, without disrupting the secretory pathway used by Class I molecules. These data are compatible with earlier observations (Burkhardt et al., 1993) that attribute the CHS pathology to disruption of late endocytic compartments.

Enlarged, lysosome-like Coxiella vacuoles accumulate both HLA-DR and HLA-DM

The swollen lysosomal compartments of *Coxiella burnetii*-infected cells are similar to the enlarged lysosomes seen in CHS cells. To determine whether alterations in lysosome morphology by mechanisms other than the CHS mutation would also affect DM and DR distribution, we analyzed their distribution in *Coxiella*-infected HeLa cells. HeLa cells do not normally express HLA-DR, invariant chain or HLA-DM, so expression of these molecules was induced by 48 hour treatment with IFN-γ. Induction was done simultaneous with *Coxiella* infection, and although IFN-γ treatment has been reported to slow the growth of *Coxiella* (Turco et al., 1984), it did not alter the vacuole morphology or

---

Figure 2-3. Localization of HLA-DR and HLA-DM to *Coxiella* but not *Chlamydia* vacuoles.

HeLa cells were treated with IFN-γ for 24 hours, then infected with *Coxiella burnetii* (A-D) or *Chlamydia trachomatis* serovar L2 (E-H) for 24 hours. Infected cells were fixed and stained for HLA-DR (B, F) or HLA-DM (D, H) with anti-DR mAb L243 or rabbit anti-DM. Nomarski imaging (A, C, E, G) distinguished the bacterial vacuoles (white arrows) from the HeLa nuclei (black arrows).

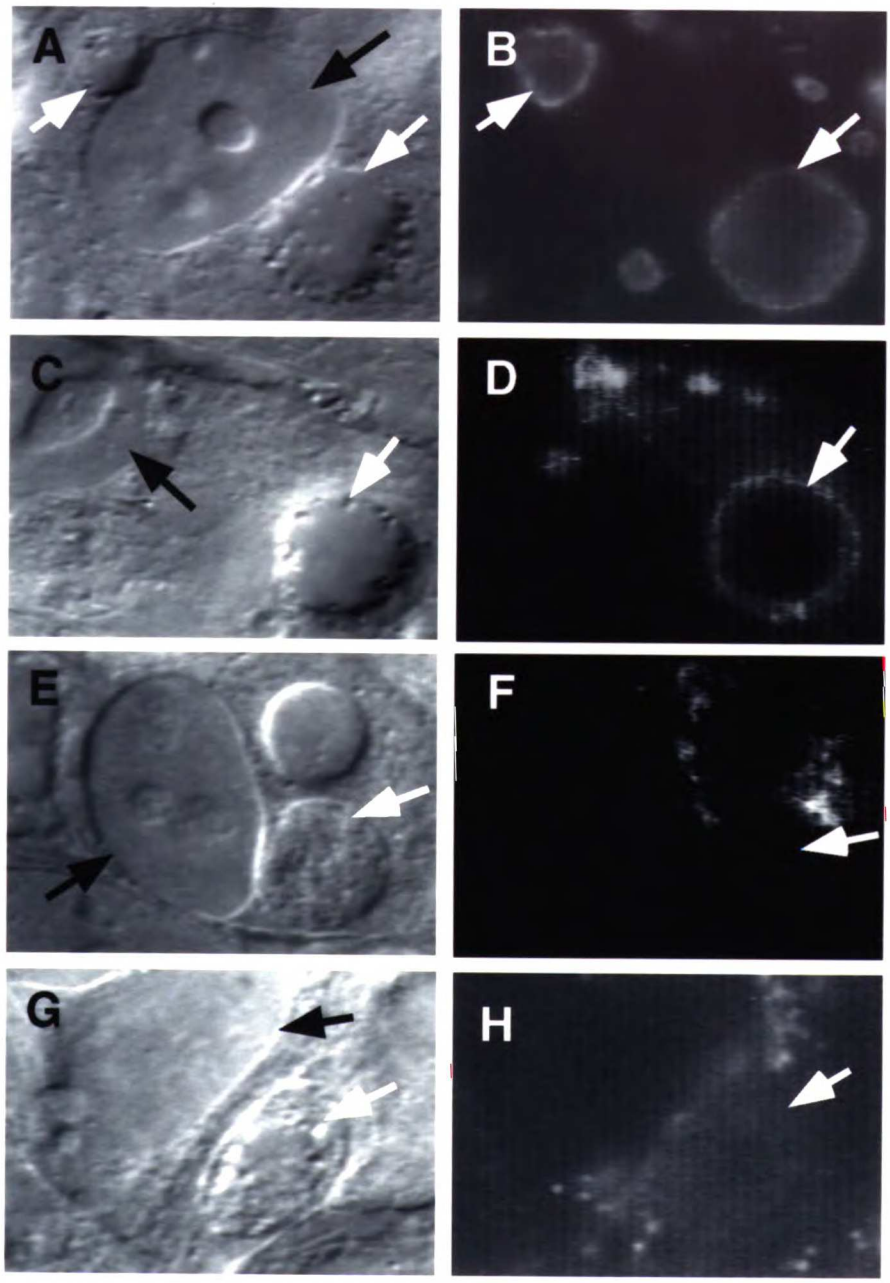

Figure 2-3

growth rate of the bacteria in our experience (data not shown). Uninfected and *Coxiella*-infected IFN-γ-treated HeLa 229 cells were then stained for HLA-DM and HLA-DR (Fig. 2-3). Immunofluorescent microscopy showed that the enlarged vacuoles of *Coxiella*-infected HeLa cells accumulated both HLA-DR (Fig. 2-3 B) and HLA-DM (Fig. 2-3 D). These vacuoles were identified as *Coxiella* vacuoles by paired Nomarski imaging of the same field (Fig. 2-3 A, C). In contrast, uninfected cells displayed a punctate cytoplasmic staining for both DR and DM indicative of numerous, small vesicles (data not shown). To control for possible nonspecific effects of infection by intracellular bacteria on Class II distribution, the same experiment was done with *Chlamydia trachomatis*, an organism which resides in a non-lysosomal vacuole (Heinzen et al., 1996). The chlamydial vacuoles (Fig. 2-3 E, G), did not label with antibodies against either HLA-DR (Fig. 2-3 F) or HLA-DM (Fig. 2-3 H). Thus, distortion of lysosome morphology by two independent mechanisms, the CHS mutation and *Coxiella* infection, correlated with distortion of the Class II loading compartment. These observations indicate that the biogenesis of the Class II loading compartment shares mechanisms with the biogenesis of lysosomes, suggesting that the Class II compartment is derived from the normal endocytic pathway rather than generated as a specialized compartment.

The steady state cell surface level of Class II molecules is normal in CHS B cells and Coxiella-infected cells

Cytotoxic T cells from CHS patients exhibit defective exocytosis of lysosomally-derived lytic granules (Baetz et al., 1995). Morphological studies have led to the suggestion that the exocytosis of the Class II loading compartment, in a manner similar to T cell degranulation, might be a mechanism of delivering peptide-loaded Class II molecules to the cell surface (Raposo et al., 1996; Wubbolts et al., 1996). If this is the case, the CHS mutation should affect the surface expression of Class II molecules. The concentrated staining of DR in *Coxiella* vacuoles also raised the possibility that the export of DR

molecules might be hindered. Surface expression of HLA-DR was analyzed in both disease states to investigate these issues (Fig. 2-4). Levels of DR on the surface of CHS B cells were compared to DR levels on a number of wild type B cells by flow cytometry of cells labeled with antibody under saturating conditions. Since lysosome size has been observed to vary within the cell cycle of CHS cells (Volkman et al., 1984), cell division of both CHS and wild-type B cells was synchronized by serum starvation followed by recovery in normal growth medium prior to analysis. HLA-DR staining with monoclonal antibody (mAb) L243 indicated that CHS B cells express wild-type levels of Class II

Figure 2-4. CHS B cells and *Coxiella*-infected cells express normal levels of HLA-DR.

(A) CHS B cells (GM03365 and GM02431A and CHS-GG), a wild-type B cell line Jest Hom (JH) and the DM-deficient B cell line 9.5.3 were stained for surface expression of HLA-DR with saturating concentrations of mAb L243 and analyzed by flow cytometry. Note that the three CHS lines were stained separately but their FACS plots are all displayed with a thin solid line and were essentially overlapping with the thick solid line representing staining of the wild-type B cell (JH). The units indicated for cell number and fluorescence are arbitrary.

(B) HeLa cells were simultaneously treated with IFN-γ and infected (Q samples) or not infected (U samples) with *Coxiella* for 48 hours. After surface biotinylation, cells were lysed and DR was immunoprecipitated with mAb DA6.147. Samples were divided in half for SDS-PAGE, transferred to nitrocellulose and immunoblotted with DA6.147 (total DRα chain) or probed with Streptavidin-HRP (surface HLA-DR). Note that in the surface DR lanes both the DRα and β chains were biotinylated and show up in the anti-DR immunoprecipitate. In the total DR lanes only DRα chain was probed for and the remaining bands are the immunoglobulin used for immunoprecipitation.

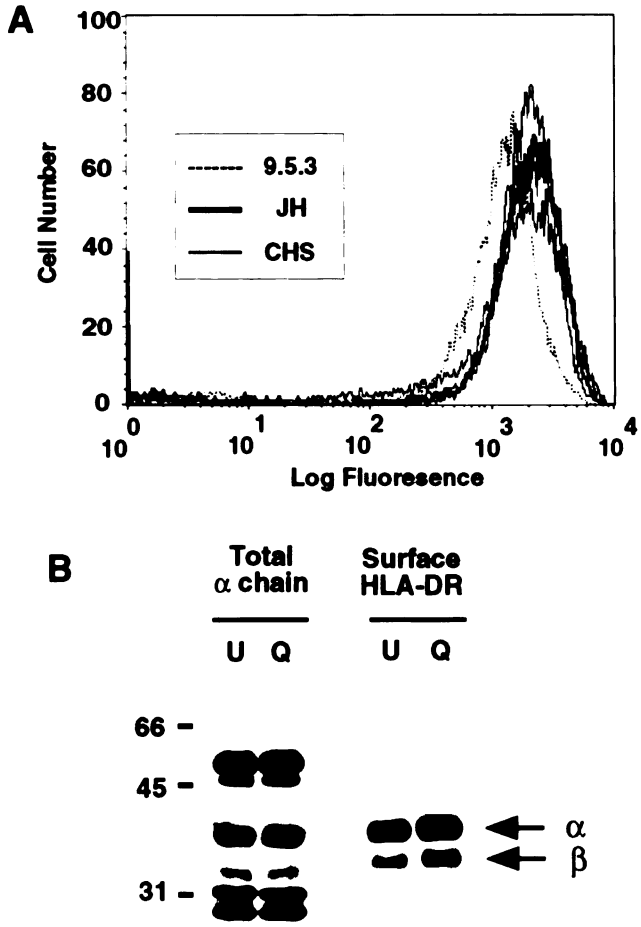
A
100
80
60
40
20
0
Cell Number
9.5.3
JH
CHS
10^0
10^1
10^2
10^3
10^4
Log Fluoresence
B
Total
α chain
Surface
HLA-DR
U Q
U Q
66 –
45 –
31 –
α
β

Figure 2-4

molecules on their surface (Fig. 2-4 A), about twice as much as the DR-hemizygous cell line 9.5.3 (Pious et al., 1985). According to this steady state measurement, the CHS mutation does not inhibit the expression of Class II molecules on the cell surface. The steady state surface levels of HLA-DR were measured biochemically in *Coxiella* -infected cells since infected cells were not amenable to FACS analysis. HeLa cells were exposed to IFN-γ and simultaneously either infected with *Coxiella* or mock-infected. After 48 hours in culture, surface molecules were labeled by biotinylation and HLA-DR molecules isolated from solubilized cells by immunoprecipitation with the mAb DA6.147, recognizing the a-chain of DR. These immunoprecipitates were analyzed for the proportion of DR derived from the cell surface by blotting with streptavidin and for the total level of DR by immunoblotting with mAb DA6.147. No substantial difference in the amount of surface HLA-DR was detected when *Coxiella*-infected cells were compared to uninfected cells, with total levels of HLA-DR being equivalent in both samples (Fig. 2-4 B). These results demonstrate that although DR appears to accumulate in the enlarged lysosomes present in both disease states, neither condition reduces the steady state surface levels of these Class II molecules.

Enhanced association of HLA-DR with DM in cells with enlarged lysosomes

While the CHS mutation or *Coxiella* infection did not decrease steady state surface levels of HLA-DR, it is possible that the accumulation of DR with DM in enlarged loading compartments might affect their interaction and consequently have an effect on antigen presentation. To assess whether DM/DR interactions were altered, HLA-DR was immunoprecipitated from the GM02431A CHS B cells and the level of associated DM was measured, in comparison to the level of DM/DR complexes in the haplotype-matched wild-type cell line Pala (Fig. 2-5). When either of two anti-DR mAbs were used to isolate these complexes, it was found that the DR from GM02431A had more DM associated with it

Figure 2-5. Increased number of DM/DR complexes in CHS B cells.
(A) DM/DR complexes were immunoprecipitated with the anti-DR mAbs L243 or DA6.147 from lysates of the CHS B cell line GM02431A (2431), or the wild-type B cell line Pala. Both cell lines are homozygous for HLA-DR3 and lysates were prepared in 1% CHAPS at pH 5.0. Samples were analyzed by SDS-PAGE, transferred to nitrocellulose and immunoblotted with a rabbit anti-DMβ serum (DMBS1). The presence of the DR-associated DMβ chain was detected by chemiluminescence. The same membrane was stripped and reprobed with mAb DA6.147 to detect the level of immunoprecipitated DRa chain.
(B) The blotting signals for DMβ and DRα in the immunoprecipitates were exposed to the linear range and then quantified from film scans, using NIH Image 1.61. Ratios of the quantified bands for DMβ/DRα are plotted for each mAb, for each cell line. The experiment shown is representative of three independent analyses of the GM02431A cells compared to Pala cells.

Figure 2-6. Increased DM/DR complexes in *Coxiella*-infected HeLa cells.
(A) DM/DR complexes were immunoprecipitated with the anti-DRα mAb DA6.147 from lysates of IFN-γ-treated HeLa cells which were either mock-treated (uninfected, U samples)) or infected with *Coxiella* (Q samples). Lysates were prepared in 1% digitonin at pH 5.0. Immunoprecipitates (DA6) were divided in half and each half analyzed by SDS-PAGE, adjacent to a sample of whole cell lysate (Lys), for separate immunoblotting with anti-DMβ serum (DMBS1) or anti-DRα mAb (DA6.147), after transfer to nitrocellulose.
(B) DMβ and DRα signals from the DA6 immunoprecipitate were quantitated, as described in the legend to Fig. 5, using NIH image 1.61, and the ratios of the two were graphed. The experiment shown is representative of results from four out of five independent infections of efficiency ≥65%.

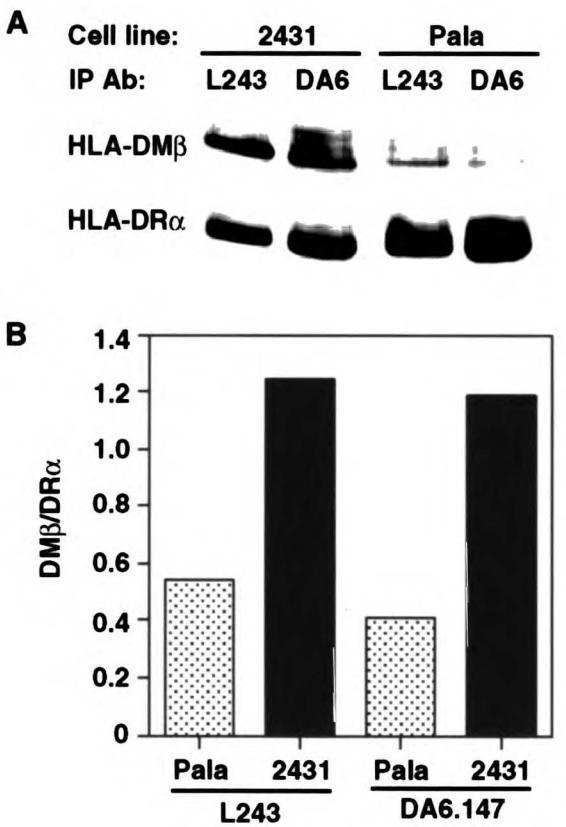
A
Cell line:
2431
Pala
IP Ab:
L243
DA6
L243
DA6
HLA-DMβ
HLA-DRα
B
DMβ/DRα
1.4
1.2
1.0
0.8
0.6
0.4
0.2
0
Pala
2431
Pala
2431
L243
DA6.147

Figure 2-5

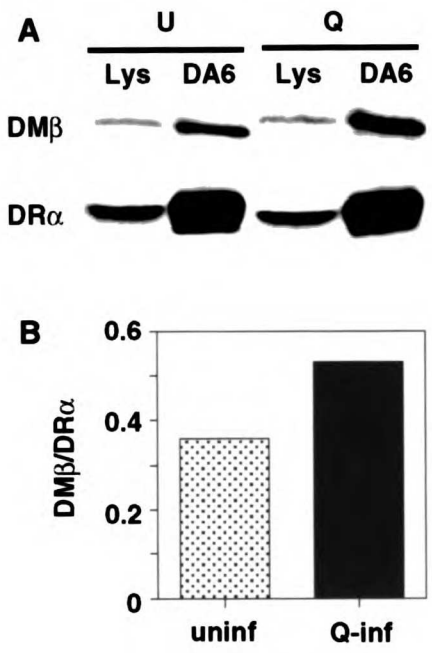

Figure 2-6

than the DR from Pala. This is demonstrated quantitatively by the ratios of the DM/DR blotting signals in the immunoprecipitates from each cell line (Fig. 2-5 B). The total levels of DM and DR were comparable in the cell lysates analyzed (data not shown), so the altered ratios in the immunoprecipitates represent skewed association of DM with DR in the CHS cells. A similar enhancement of DM/DR association was observed in cells infected with *Coxiella*. When DR was immunoprecipitated from infected cells, more DM was bound than the amount that co-immunoprecipitated with an equivalent amount of DR from uninfected cells (Fig. 2-6).

CHS B cells have decreased levels of total and cell surface CLIP-DR complexes

Prior to binding antigenic peptide, Class II molecules must first have the residual invariant chain peptide, CLIP, removed from the peptide binding site. This process is catalyzed when CLIP-DR complexes interact with HLA-DM, which stabilizes the unloaded form of DR (Denzin and Cresswell, 1995; Sherman et al., 1995; Sloan et al., 1995). To evaluate whether the enhanced interaction of DM with DR in CHS cells has a functional consequence, their levels of CLIP-DR complexes were analyzed in comparison to wild-type cells and to the DM-deficient cell line, 9.5.3, on which the majority of surface DR molecules are loaded with CLIP (Mellins et al., 1994; Riberdy et al., 1992; Sette et al., 1992). The CerCLIP.1 mAb, an antibody recognizing CLIP bound to HLA-DR molecules was used to measure surface levels of CLIP-DR complexes (Fig. 2-7). Wild-type, homozygous B cells with DR allelic types partially or fully matching the CHS types were used as controls, due to the unavailability of fully matched heterozygous cells. Allele matching was attempted because products of different DR alleles have been shown to have varying affinities for CLIP (Avva and Cresswell, 1994). Flow cytometry (Fig. 2-7 A) of synchronized cells stained with CerCLIP.1 indicated that the levels of CLIP-DR complexes on the surface of the three CHS B cell lines were lower than on the wild-type Jest Hom cell

line, which has a comparable level of DR on its surface (Fig. 2-4 A). In comparing the levels of CLIP on CHS cells to other control cell lines, it was necessary to account for varying levels of DR on the surface of these cell lines. Therefore the proportion of HLA-DR loaded with CLIP to total DR was calculated by taking the ratio of the geometric mean of the CerCLIP.1 staining intensity to the geometric mean of the anti-DR L243 staining intensity. As determined from the average ratios from multiple experiments (N=3), levels of CLIP-DR on the CHS cell lines were among the lowest in the panel of cells analyzed (Fig. 2-7 B), with the CHS line GM03365 always having the lowest ratio. Surface levels of CLIP on wild-type B cells were quite variable and on one cell line (Jest Hom) approached the level on the DM-deficient 9.5.3 cell line while on another (EA) approached CHS cell levels. The finding of high CLIP levels on wild type cells was unexpected since very little CLIP-DR is present on the surface of DM-deficient B cells that have been

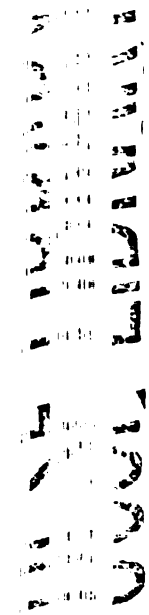

Figure 2-7. Decreased levels of DR-CLIP complexes on the surface of CHS B cells.

(A) CHS B cell lines (GM03365 (3365), GM02431A (2431), CHS-GG (Ched)), wild-type B cell line Jest Hom (JH) and the DM-deficient B cell line 9.5.3 were synchronized for cell cycle by serum starvation and 24 hour recovery. Cells were then stained for surface expression of DR-bound CLIP with mAb CerCLIP.1 and analyzed by flow cytometry. Cell number is indicated by on the y-axis and log fluorescence on the x-axis in arbitrary units.

(B) Average ratios of the geometric means of the flow cytometry peaks for CerCLIP.1 (CLIP-DR) and L243 (total DR) staining of each cell line, from two or three experiments, were plotted on the y-axis as a measure of the ratio of CLIP-associated DR to total DR. Data for wild-type (Jest Hom (JH), EA, AVL) and the DM-deficient cell line 9.5.3 are indicated with dotted bars while CHS cell lines are in solid black.

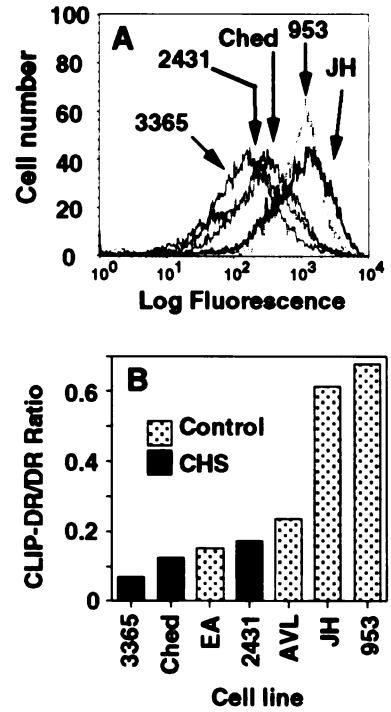
A
Ched
953
2431
JH
3365
Cell number
100
80
60
40
20
0
10^0
10^1
10^2
10^3
10^4
Log Fluorescence
B
Control
CHS
CLIP-DR/DR Ratio
0.6
0.4
0.2
0
3365
Ched
EA
2431
AVL
JH
953
Cell line

Figure 2-7

genetically rescued by transfection with DM (Denzin, 1994; Morris et al., 1994). However, it may be that when DM is present at wild-type levels and not over-expressed due to transfection, its unloading of CLIP is not particularly efficient, a process that might also vary for different DR types. The reduction of cell surface CLIP on CHS cells suggests an altered peptide repertoire is presented by these cells.

The decrease in CLIP-DR complexes in CHS cells was investigated further by immunoprecipitation experiments measuring total cellular levels of CLIP-DR. These complexes were isolated from solubilized cells using the CerCLIP.1 mAb and analyzed by quantitative immunoblotting for levels of DR co-immunoprecipitated with CLIP (Fig. 2-8). The GM03365 or GM02431A cell lysates had hardly any detectable CLIP-associated DR compared to the wild-type JY cell line or the DM-deficient 9.5.3 cell line. Thus by two

---

Figure 2-8. Reduced levels of CLIP-associated HLA-DR in CHS B cells. CerCLIP.1 mAb was used to immunoprecipitate CLIP/DR complexes from NP-40 lysates of the indicated B cell lines (CHS cells GM03365 labeled as 3365 and GM02431A labeled as 2431). (A) Samples were analyzed by SDS-PAGE and DR α-chain was detected by immunoblotting with DA6.147 mAb (lane 1). The supernatant from each CerCLIP.1 immunoprecipitation was used for a second precipitation with the same antibody (lane 2) to confirm that the majority of CLIP-DR complexes were depleted from the lysate. DR α-chain in a fixed amount of cell lysate was detected in the lanes marked "L." The portion of each blot containing the DR α chain is shown.

(B) The DR α-chain bands in each sample were quantified using a Molecular Dynamics Storm image processor, following development of the blot with the ECF substrate. Measurements were normalized to the protein content in the amount of lysate used for analysis. Ratios of the normalized DR α-chain signal in the CerCLIP.1 immunoprecipitate compared to the DR α-chain signal from total cell lysate are plotted.

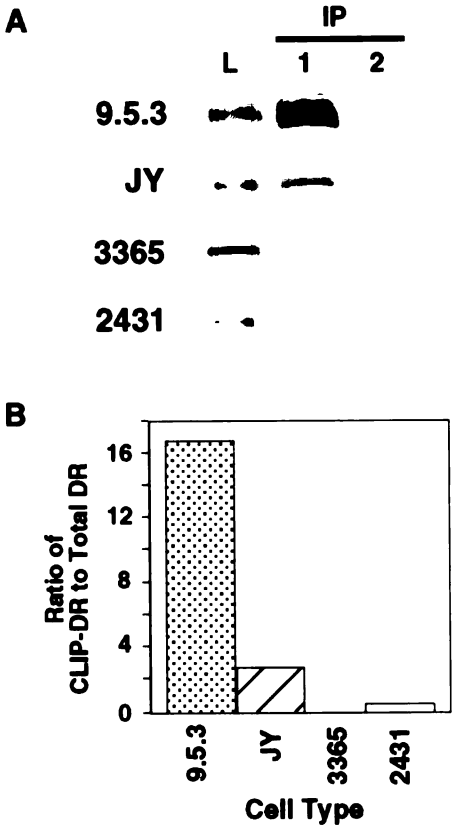
A
IP
L
1
2
9.5.3
JY
3365
2431
B
Ratio of
CLIP-DR to Total DR
16
12
8
4
0
9.5.3
JY
3365
2431
Cell Type

Figure 2-8

measures, the CHS B lymphoblastoid cells have fewer CLIP-DR complexes than their wild type counterparts, a difference seen most strikingly in the GM03365 line. The decrease in CLIP-DR on the cell surface of CHS cells, without a concomitant decrease in overall DR surface levels, suggests that the DR molecules observed in swollen lysosome-like compartments are transported through these compartments and out to the cell surface. Thus the swollen DR/DM-rich compartments are comparable to Class II loading compartments and are not merely dead-end lysosomes. In addition, these results indicate that the necessary conditions for DM to function are present in the enlarged lysosomes, including low pH, as would be predicted from previous studies demonstrating normal degradative function in lysosomes of CHS fibroblasts (Burkhardt et al., 1993).

To determine whether reduction of cell surface CLIP-DR complexes and enhanced DM/DR association was accompanied by an increase in expression of unloaded Class II, the peptide loading of surface DR molecules on CHS and *Coxiella*-infected cells was assessed. At room temperature, peptide-loaded Class II remains a stable heterodimer in sodium dodecyl sulfate (SDS), while unloaded or CLIP-occupied Class II molecules dissociate under the same conditions. When the SDS-stability of surface-biotinylated HLA-DR molecules was measured for the three CHS cells in this study, no difference in their steady state level of stable dimers was observed compared with the stability of surface DR molecules on our panel of allele-matched, wild-type homozygous B cell lines (data not shown). In *Coxiella* infected cells, results were highly variable, with a slight reduction of DR stability observed for about 50% of infections (data not shown). Thus, diseases which expand lysosomes cause the accumulation of HLA-DR and DM in enlarged compartments and thereby enhance their association, which can affect the peptide repertoire displayed by the diseased cells, without a cumulative effect on their surface DR stability.

DISCUSSION

Enlarged lysosome-like compartments, in cells with either the hereditary Chediak-Higashi Sydrome defect or cells infected with *Coxiella burnetii*, accumulate both HLA-DR and DM molecules, but not Class I molecules. The Class II molecules entering these compartments are not degraded but reach the plasma membrane, as indicated by normal surface levels of HLA-DR in both CHS B cells and *Coxiella*-infected cells. Enhanced interaction of DM and DR in the enlarged vacuoles of diseased cells seems to alter the dynamics of peptide loading. Collectively, these results provide several insights into the formation and function of the Class II loading compartment.

The fact that diseases which induce enlargement of lysosomes can also affect the morphology of the Class II loading compartment indicates that these two compartments share mechanisms of biogenesis. This suggests that the Class II loading compartment is part of the endocytic pathway, rather than an entirely specialized compartment. In two different cell lines, that are not specialized for antigen presentation, it has been previously demonstrated that the expression of Class II molecules along with invariant chain and DM is sufficient to generate compartments that resemble Class II loading compartments (Calafat et al., 1994; Karlsson et al., 1994). These experiments were interpreted to mean that Class II molecules and their associated proteins contained signals that allowed the *de novo* generation of a specialized compartment. An alternative interpretation could be that Class II, invariant chain and DM traffic to pre-existing endocytic compartments and simply accumulate there by virtue of retention or targeting signals in their cytoplasmic tails. This explanation would account for the observed distribution of Class II molecules throughout a number of endosomal compartments (Castellino and Germain, 1995; Guagliardi et al., 1990). Recent electron microscopy data, identifying a progression of endocytic, Class II-containing structures, also suggests an intimate relationship between pre-existing endocytic compartments and those used for antigen processing and presentation (Kleijmeer et al., 1997), a relationship corroborated by the findings reported here.

Although HLA-DR molecules accumulate in the CHS and *Coxiella*-induced vacuoles, a decrease in their steady state surface levels was not detected. We also found that the total levels of DR molecules in CHS cells were equivalent to those in normal B cells (data not shown). Thus the intense staining of the vacuoles in diseased cells does not reflect an increase in intracellular DR and DM, merely a redistribution, so they are are concentrated together in larger, but fewer, structures than in normal cells. This correlates with the report that the gross cellular volumes of lysosomes in normal and Chediak fibroblasts are similar (Burkhardt et al., 1993). The fact that DR molecules can reach the cell surface in CHS cells also indicates that secretion of Class II molecules is not exclusively via the same mechanism as regulated secretion of lytic granules, a process which is defective in CHS cytotoxic lymphocytes (Baetz et al., 1995). It is likely that the primary mechanism for Class II expression is via transport in small vesicles that bud from the loading compartment (Pond and Watts, 1997), and the expression of Class II on CHS cells is consistent with this mechanism. In CHS cells, enlarged lysosomes are apparently the consequence of a defective fission mechanism (Perou et al., 1997). Therefore, fission of Class II-containing compartments themselves does not seem to be required for Class II export to the cell surface. This fission mechanism is presumably distinct from budding of transport vesicles.

The co-localization of DM and DR in abnormally large structures has several measurable effects. Here we show that in both disease states, elevated levels of DM/DR complexes can be detected relative to levels in cells with a normal endocytic pathway. Faigle et al. (Faigle et al., 1998) have recently shown that the transit of DR through the endocytic pathway of CHS cells is slowed, suggesting that altered compartment morphology affects intracellular trafficking. Slower transit could be responsible for the enhanced association that we observe between the DM residing in enlarged vacuoles and the DR molecules trafficking through the vacuoles. Faigle et al. also described a slower acquisition of SDS stability by DR molecules in CHS cells, with an accompanying delay in

DR-restricted presentation of processed antigen to T cells (Faigle et al., 1998). These phenotypes can be explained by the enhanced DM/DR interaction that we report. Together these data support previous predictions that in vivo, as well as in vitro, DM does not actively load DR molecules, but rather stabilizes the unloaded conformation (Denzin and Cresswell, 1995; Sherman et al., 1995; Sloan et al., 1995). Enhancement of this predicted DM activity is consistent with the reduction in associated CLIP, shown here, and slower acquisition of stability and antigenic peptides by DR molecules in CHS cells (Faigle et al., 1998).

Enhanced interaction of DM with DR also alters the peptide repertoire that is ultimately expressed on the CHS cell surface, as indicated by the reduced proportion of CLIP-loaded Class II on the surface of these cells. It was not possible to test this effect for *Coxiella*-infected HeLa cells, induced with IFN-γ, because CLIP-DR complexes are undetectable in IFN-γ-treated uninfected HeLa cells. This is likely due to the absence of induction of DO expression by IFN-γ and the consequent heightened activity of DM (Denzin et al., 1997; Karlsson et al., 1991; Wake and Flavell, 1985). However, independent evidence of an altered peptide repertoire in CHS cells is indicated by the fact that their peptides are, on average, shorter than the peptides bound by Class II on wild-type cells (Faigle et al., 1998). This property, as well as the reduced CLIP, could reflect enhancement of DM's peptide-editing function, as a result of increased interaction with Class II molecules (Kropshofer et al., 1996). Here we show that, as also reported by Faigle et al. (Faigle et al., 1998), the surface DR molecules on CHS cells are stably loaded with peptide at steady state. This is not surprising because only peptide-loaded molecules will accumulate over time, even if DR stability takes longer to achieve in these cells. Interestingly, in a subset of *Coxiella* infections, it was possible to detect a decrease in the steady state stability of DR molecules (data not shown). The fact that unloaded complexes were even detectable at steady state may have been due to the combined effect of enhanced interaction of DM with DR and the hyperactivity of DM in these IFN-γ-induced HeLa cells,

which lack DO. Thus, both lysosomal diseases display defects that could result in altered peptide presentation to T cells.

B cells from the three CHS patients tested showed variability in their levels of surface CLIP-DR complexes, although low relative to most normal cells. This result hints at a range of CHS phenotypes and suggests that the more dramatic phenotypes may cause serious impairment in antigen presentation. Of the CHS lines examined, GM03365 showed the largest reduction in CLIP relative to wild type B cell lines, and by microscopy, GM03365 cells generally had the largest vacuoles (Figs. 2-1 and 2-2). Genetic analysis of GM03365 has revealed a nonsense mutation in the CHS gene, resulting in premature termination and loss of two thirds of the protein (Nagle et al., 1996). While only a handful of CHS patients have been genetically characterized, all have been shown to have homozygous nonsense mutations at various positions along the entire length of the 3801 aa gene, resulting in null alleles (Karim et al., 1997). Interestingly, early termination of the transcript does not correlate with an earlier age of onset or increased severity of the clinical disease, suggesting that other factors may be involved in the progression of CHS pathology.

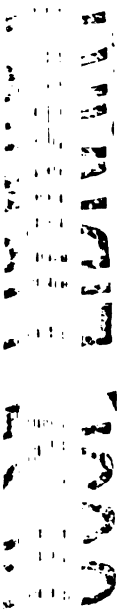

In conclusion, our data demonstrate that in both a hereditary and an infectious disease characterized by swollen lysosomes, the common phenotype correlates with accumulation of DM and DR in enlarged vacuoles. DR molecules apparently exit this vacuole and appear on the cell surface with decreased levels of CLIP peptide. Thus these enlarged vacuoles seem to represent morphologically expanded Class II loading compartments, indicating that the biogenesis of these compartments utilizes the same fusion and fission mechanisms that control lysosome formation. The interaction between DM and DR was measurably enhanced in these cells and appears to be a function of the altered morphology, the only feature common to both disease states. This enhanced DM/DR interaction suggests a mechanism for delays in antigenic peptide presentation, characteristic of CHS cells (Faigle et al., 1998). Thus the morphological effects on the Class II transport

pathway occuring in these lysosomal diseases contributes to the immune deficiencies seen in CHS patients and may very well do so in *Coxiella*-infected individuals.

Materials and Methods

Cell Lines: EBV-transformed B cell lymphoblastoid lines, JY, Jest Hom, AVL, EA, 9.5.3 (Pious et al., 1985) and CHS-GG (Baetz et al., 1995), were cultured in RPMI 1640 supplemented with 2 mM L-glutamine, 10% fetal bovine serum (FBS, Gemini, Bio-Products, Calabasas, CA) in 5% CO_2 at 37°C. Pala cells were grown in Iscove's medium with 5% FBS and GM03365 and GM02431A (Human Genetic Mutant Cell Repository, Camden, NJ) were grown in RPMI 1640 with 20% FBS. The HLA-DR types of the cells are as follows: AVL, DRb1*03011; EA, DRb1*1501; CHS-GG, DRb1*1501/0701; GM02431A, DRb1*0301; GM03365, DRb1*1501/1001; Jest Hom DRb1*0101, JY DRb1*1301/0402. Cell cycle synchronization was achieved by starving the cells in medium with 0.1% FBS for 32 hours followed by a 20 h recovery in normal medium before analysis. HeLa 229 cells (ATCC, Rockville, MD) were cultured in Eagle MEM with Earle's balanced salt solution (Mediatech) with 10% FBS in 5% CO_2 at 37°C.

Antibodies: The specificities of anti-HLA-DR-αβ mAb L243 (Blum and Cresswell, 1988; Lampson and Levy, 1980), anti-HLA-DR α-chain mAb DA6.147 (Guy et al., 1982), anti-class I MHC mAb W6/32 (Barnstable et al., 1978), anti-CLIP-HLA-DR complex CerCLIP.1 mAb (Denzin, 1994), anti-LAMP-1 mAb H4A3 (Chen et al., 1985), and anti-HLA-DM rabbit serum (Sloan et al., 1995) have been previously described. The antiserum DMBS1, against DMβ, used for immunoblotting was produced by rabbit immunization with a peptide (CYTPLPGSNYSEGWHIS) from the cytoplasmic domain of the DMβ chain.

Bacterial Infections: Infections were done as previously described (Heinzen et al., 1996). HeLa 229 cells were washed with Hank's BSS and overlaid with *Coxiella burnetti* Nine Mile strain clone II or *Chlamydia trachomatis* serovar L2 diluted into SPG (0.22 M sucrose, 20 mM sodium phosphate, 5 mM L-glutamic acid) and incubated at 37°C for 1 hr. Cells were then washed with HBSS and supplemented with medium and 0.5 mg/ml L-tryptophan (Shemer et al., 1987). HeLa cells were incubated in the presence of 100 u/ml human IFN-γ either 24 hours prior to infection and during infection or simultaneous with infection, as specified. Infections were allowed to progress for 24-48 hrs before cell lysis in NP-40 lysis buffer. Experiments were performed with Hela cultures having infection efficiencies greater than 65%.

Immunofluorescent Microscopy: The indirect immunofluorescence procedure for the EBV-B cell lines was modified from a published procedure (Denzin, 1994). 200 µl of B cells suspended at 5 x 10^5 cells/ml medium were plated onto 12 mm poly-L lysine coated coverslips and incubated for 1hr at 37°C. Coverslips were then washed in PBS, fixed for 10 min in 4% paraformaldehyde/PBS, permeabilized for 10 min with 0.04% saponin, and blocked in a solution of 5% goat serum, 0.02% SDS, 0.1% NP-40 in PBS-NaN_3. Coverslips were incubated with primary antibody diluted in blocking solution for 1 hr at room temperature, washed with PBS-N_3 and incubated for 1 hr with the appropriate Cy3 or FITC-conjugated secondary antibodies (Jackson Immunoresearch Labs Inc., West Grove, PA), then mounted in 0.1% *p*-phenylene diamine (Sigma, St. Louis, MO) in Fluromount G (Fisher Scientific, Pittsburgh, PA) and viewed with a Zeiss Axiophot fluorescence microscope. Indirect immunofluorescence for the adherent HeLa cells was carried out in the same manner, except the cells were grown on uncoated coverslips, infected with bacteria (see infection protocol) and then fixed, permeabilized and stained as described above. Paired immunofluorescence/Nomarski imaging was done on a Nikon fluorescence microscope.

Flow Cytometry: 5 x 10^5 B cells were washed in ice-cold PBS-N_3 containing 2% BSA, resuspended in 200 µl primary antibody diluted into PBS/BSA and incubated on ice for 45 min. Cells were washed in PBS/BSA and resuspended in FITC-conjugated goat-anti-mouse immunoglobulin (Dako, Carpinteria, CA) diluted in PBS/BSA for 30 min at 4°C. After washing, cell samples were analyzed on a Becton-Dickinson FACScan (Mountain View, CA). The CLIP/DR to total DR ratios was calculated by taking the ratios of the geometric means of the CerCLIP.1 peak and the L243 peak. Geometric means were calculated by CellQuest software (Becton-Dickinson) and are a measure of both mean values of all events and the range of distribution of the events. Staining with secondary antibody only was equivalent in all cells. Concentrations of the L243 mAb and CerCLIP.1 mAb used were established to be saturating by independent titration experiments.

Immunoprecipitations: To isolate CLIP-DR complexes, cells were lysed in NP-40 lysis buffer (1% NP-40, 50 mM Tris, pH 7.2, 150 mM sodium chloride, 0.2 mM PMSF, 2.5 mg/ml aprotinin, 1 mg/ml leupeptin) for 1 hr on ice. After pelleting the nuclei, lysates were incubated with protein G-bound CerCLIP.1. Immunoprecipitates were washed, boiled in SDS-sample buffer, and analyzed by SDS-PAGE (12%). The gels were transferred to nitrocellulose and immunoblotted with DA6.147. Total DR levels were obtained by quantifying DRα chain in whole lysates in the same manner. Bands were detected and quantified using an alkaline phosphatase conjugated-goat anti-mouse immunoglobulin and enhanced chemifluorescence (ECF) substrate (Amersham) on the Storm system (Molecular Dynamics, Sunnyvale, CA). To detect levels of DR/DM complexes, cells were lysed in 1% CHAPS or 1% digitonin in 150 mM NaCl, 50 mM sodium acetate, pH 5.0. MAbs L243 or DA6.147 were used to immunoprecipitate HLA-DR, as above. Samples were analyzed by SDS-PAGE (12%), transferred to nitrocellulose and immunoblotted with DMBS1 (anti-DMβ chain), and signals detected by ECF on film,

as above. Blots were then stripped of antibody by incubating in 100 mM β-mercaptoethanol, 2% SDS, 62.5 mM Tris, pH 6.7 at 55°C for 20 min and then re-probed with DA6.147 to quantify the level of DRα chain immunoprecipitated. Blotting signals were scanned and then quantitated using the program NIH Image 1.61.

Cell Surface Biotinylation: The biotinylation procedure was modified from a published report (Bonnerot et al., 1995) . Infected cells were washed three times with ice-cold PBS and then biotinylated for 10 min on ice with 0.5 mg/ml sulfo-NHS-LC-biotin (Pierce, Rockford, IL) in cold PBS. After washing the cells, the reaction was quenched with 50 mM NH_4Cl in PBS for 10 min. NP-40 lysates were made as described earlier. Immunoprecipitations were carried out using L243 mAb and analyzed by SDS-PAGE. Equivalent lanes were blotted with either DA6.147 or streptavidin conjugated to horseradish peroxidase (HRP) (Zymed) followed by detection with the ECL substrate (Amersham).

Chapter 3

A *Chlamydia trachomatis* Protease Degrades Invariant chain and Class II MHC Molecules *in vitro*

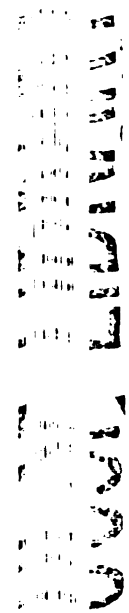

The work presented here will be submitted as a manuscript pending the outcome of some additional experiments discussed at the end of this chapter.

ABSTRACT

Class II MHC molecules stimulate CD4 T helper cells to initiate an antigen specific immune response. En route to the cell surface, class II MHC molecules travel from the TGN into the endocytic pathway where they bind antigenic peptides resulting from proteolytic degradation of endocytosed antigens. Invariant chain binds class II dimers in the ER and directs this trafficking through its cytoplasmic tail as well as serving a chaperone function in conveying stability to the empty heterodimer. Absence of invariant chain results in defective class II presentation and a severe immunodeficiency. *Chlamydia trachomatis* is an obligate intracellular pathogen that escapes the degradative endocytic pathway to form a compartment seemingly devoid of host molecules. Here we demonstrate that *Chlamydia* produce a protease capable of rapid degradation of the invariant chain *in vitro*. The protease can also degrade class II and DM molecules but not class I. Moreover, the protease is inhabitable by the proteasome inhibitor LLnL, but not inhibitors of cysteine, aspartic or serine lysosomal proteases or metalloproteases. This invariant chain degradation may serve as an immune evasion mechanism that prevents the loading and surface expression of class II molecules, thus explaining the asymptomatic infections characteristic of *Chlamydia*.

INTRODUCTION

Class II major histocompatibility molecules serve the essential role of initiating the body's helper T cell response to infection. They accomplish this function through the capture and display of antigenic peptides on the cell surface for recognition by antigen-specific T cell receptors. The production and class II-binding of these pathogen-derived antigenic peptides occurs in the endocytic pathway where they encounter newly synthesized class II molecules en route to the cell surface.

Both the generation of antigenic peptides and the maturation of class II molecules require the action of proteases in the endocytic pathway. As antigens descend the endocytic pathway through increasingly acidic compartments, they are cleaved by the multiple proteases and hydrolases present therein. The cumulative activities of these degradative enzymes break down internalized protein aggregates and microorganisms into short peptides, some of which are capable of binding class II molecules (Bennett et al., 1992; Matsunaga et al., 1993; van Noort and van der Drift, 1989).

The biosynthesis of class II molecules also requires the action of a number of endocytic proteases. Newly synthesized class II heterodimers are bound and stabilized by trimers of the invariant chain (Roche et al., 1991). Acting as a chaperone, the invariant chain confers stability to assembling class II molecules by occupying the peptide binding grooves of the heterodimers (Cresswell, 1996). At the same time, the invariant chain doubles as a delivery agent by directing class II molecules into the endocytic pathway from the trans-Golgi network (TGN) by means of a targeting signal in its N-terminal cytoplasmic tail (Odorizzi et al., 1994; Pieters et al., 1993). Both of these functions are intimately linked to the activities of proteases. Peptide loading of class II molecules requires that the invariant chain be progressively degraded, leaving a residual peptide termed CLIP, which is later exchanged for an antigenic peptide through the action of the class II-like HLA-DM (Denzin and Cresswell, 1995; Sherman et al., 1995; Sloan et al., 1995). This degradation is accomplished by cysteine proteases present in the loading compartments, such as

cathepsin S in dendritic cells and B cells (Riese et al., 1996) and cathepsin L (Nakagawa et al., 1998) in thymic epithelium. Inhibition of this degradation prevents the separation of class II molecules from the endosomal targeting signal in the invariant chain tail resulting ultimately in intracellular retention of the class II molecules (Amigorena et al., 1995; Brachet et al., 1997; Neefjes and Ploegh, 1992).

As mentioned in Chapter 1, this entire process of class II antigen presentation is subverted by many intracellular pathogenic bacteria. Some pathogens, such as *Listeria* (Cossart and Lecuit, 1998) and *Shigella* (High et al., 1992) escape the membrane vacuole and reside in the cytoplasm, thus avoiding membrane-bound class II molecules. Others, such as *Salmonella*, prevent their vacuoles from maturing into lysosomes by inhibiting phagosome fusion with lysosomes or endosomes (Uchiya et al., 1999). *Chlamydia trachomatis* forms an isolated compartment that has limited interaction with the endocytic pathway after its entry into the cell. This mechanism seemingly prevents *Chlamydia* from ever encountering class II molecules (Lem et al., 1999) or host proteases. Despite its isolation from class II molecules, *Chlamydia* somehow induce a down regulation of class II expression in infected cells. One mechanism used by *Chlamydia* to accomplish this down regulation is the degradation of an interferon-γ-inducible transcription factor necessary for expression of CIITA, the transcription factor directly responsible for class II gene expression (Zhong et al., 1999). The data presented in this chapter demonstrate the distinct possibility of a second mechanism of *Chlamydia*-induced class II down regulation, degradation of the invariant chain, class II and DM.

RESULTS

Chlamydia do not co-localize with Class II or invariant chain but induce their decreased expression.

To investigate the effects of *Chlamydia trachomatis* infection on class II MHC antigen presentation, we selected HeLa 229 cells for our model *Chlamydia* infection

system. As cervical epithelial cells, HeLa are the natural host cells for *Chlamydia trachomatis* infections. HeLa 229 are also readily responsive to IFN–γ and upon stimulation, produce class II molecules and its associated machinery for antigen presentation. To determine where intracellular pools of class II molecules reside in HeLa cells with chlamydial inclusions, we infected IFN–γ-stimulated HeLa cells with *Chlamydia trachomatis*, serovar L2 EB's for 20 hours, after which the cells were fixed and prepared for fluorescent microscopy (20 hours post-infection, hpi). Infected and mock infected cells were double-stained with antibodies for chlamydial LPS and either the DRα chain (Fig. 3-1 A), the N-terminus of the invariant chain (B), the lysosomal marker, CD63 (C), or the late endosomal marker, mannose-6-phosphate receptor (D). As shown previously (Lem et al., 1999), neither HLA-DR nor HLA-DM are detectable in or on the inclusion membrane. Moreover, it is striking that the cells harboring chlamydial inclusions seem to have the lowest staining for class II and invariant chain positive vesicles seem to redistribute to a peri-vacuolar region. A decrease in staining was not observed for the lysosomal marker CD63, which is associated with class II molecules (Hammond et al., 1998), or the late endosomal marker, M6PR. CD63 also seems to redistribute to a perivacuolar region. The decreased staining may be interpreted to mean that less class II and invariant chain are present in the *Chlamydia*-infected cells than in uninfected cells.

Figure 3-1: *Chlamydia*-infected cells contain fewer Class II/invariant chain-containing vesicles.

HeLa 229 stimulated with IFN-γ for 20 hrs were infected with *Chlamydia trachomatis* serovar L2 and paraformaldehyde fixed at 20 hpi. Cells were than stained for *C. trachomatis* (rabbit anti-EB), class IIαβ dimers (L243 mAb, A), invariant chain (Pin1.1, B), cation-independent mannose-6-phosphate receptor (rabbit anti-CI-M6PR, C), CD63 (anti-CD63, D) and examined by confocal microscopy. chlamydial inclusions are in green, other markers are shown in red.

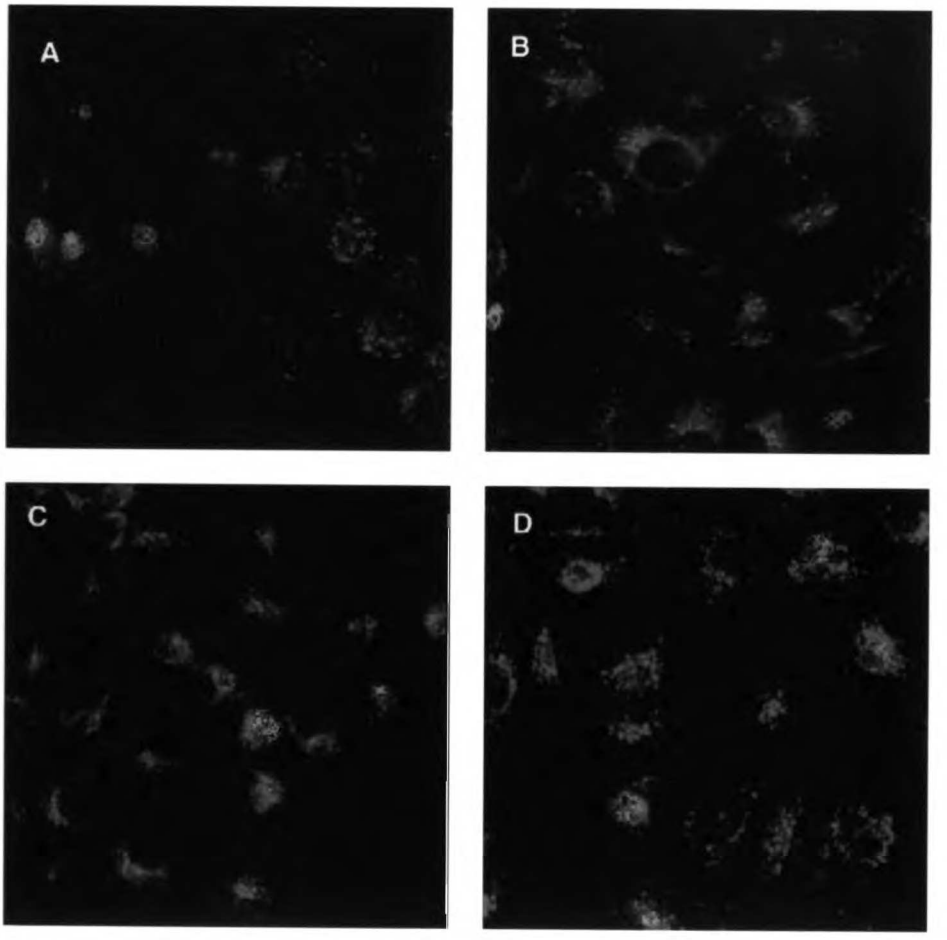

Figure 3-1

Chlamydia-infected cells contain decreased levels of DR, DM and invariant chain but not Class I MHC molecules

To confirm that lower amounts of class II and invariant chain are present in infected cells, NP-40 detergent lysates of mock or *Chlamydia*-infected HeLa cells were immunoblotted with antibodies to class IIα chain, invariant chain and the DMβ chain. As controls for general protein levels and infection, the lysates were also immunoblotted for class I heavy chain and *Chlamydia* major outer membrane protein (MOMP), respectively. As seen in Fig. 3-2 A, *Chlamydia*-infected lysates have markedly decreased levels of class IIα chain, DMβ chain and invariant chain. All isoforms of invariant chain are present in lower levels than in mock-infected cells. Disappearance of p42 and p35 invariant chain isoforms also coincides with the appearance of a 25 kD band recognized by the anti-KESL rabbit serum, presumably an invariant chain fragment. The decreased levels of class II, DM and invariant chain do not indicate a generalized decrease of protein synthesis or degradation since the immunoblot for class I heavy chain shows equivalent amounts of class I in both infected and mock-infected lysates.

Figure 3-2: *Chlamydia*-infected HeLa contain decreased levels of HLA-DR, HLA-DM and invariant chain, but not class I, despite normal synthesis rates.

(A) *Chlamydia*-infected HeLa downregulate expression of HLA-DR, HLA-DM and invariant chain. *Chlamydia*-infected HeLa were lysed in 1% NP-40 lysis buffer at 20 hpi. Equivalent amounts of protein were run in each lane and quantities of class I heavy chain (Rabbit anti-A2), DRα (DA6.147 mAb), invariant chain (KESL), DMβ (DMBS1) and major outer membrane (1-45 mAb) were determined by western blot. (B) *Chlamydia*-infected cells synthesize HLA-DRα at a normal rate. Mock and *Chlamydia*-infected HeLa were labeled with 35S-translabel for 1 hr., lysed and used for DRα immunoprecipitations for analysis on SDS-PAGE and autoradiography.

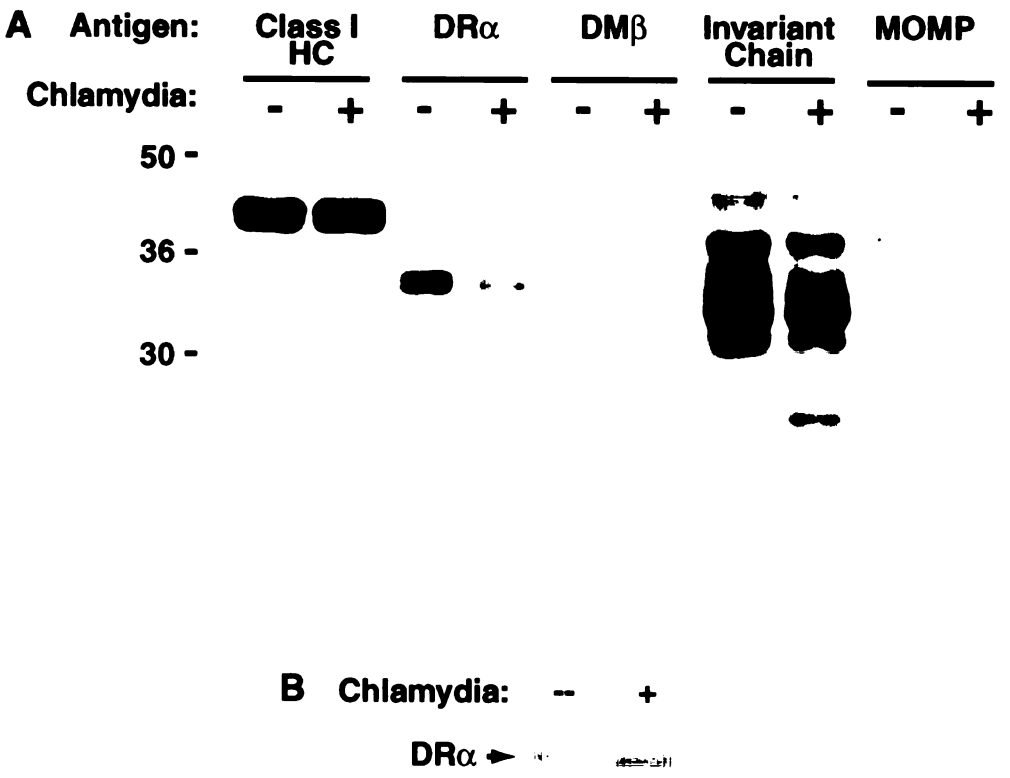
A
Antigen:
Class I HC
DRα
DMβ
Invariant Chain
MOMP
Chlamydia:
- + - + - + - + - +
50 -
36 -
30 -
B
Chlamydia: -- +
DRα
DRβ

Figure 3-2

Down regulation of the class II machinery is not predominantly due to decreased synthesis

The decreased levels of class II, DM and invariant chain may result from either a decreased rate of synthesis or a degradation of the polypeptides after synthesis. A synthetic labeling experiment was done to address the first possibility. HeLa cells were stimulated with IFN–γ and either mock-infected or infected with *Chlamydia*. After 19 hours of infection, the cells were labeled with ^{35}S-translabel and immediately lysed in NP-40 for class II or class I immunoprecipitations. The amounts of radiolabeled class IIα or β chain are roughly similar between the infected and mock-infected lysates (Fig. 3-2 B) while the synthesis of class I heavy chain is not appreciably altered (data not shown), as the Western blots showed. This data suggests that the large decrease seen in the class II levels is not likely due to a significant inhibition of synthesis of class IIα and β chain polypeptides. The unaltered levels of class I also suggest that, in general, host cell protein synthesis in this system is not inhibited by *Chlamydia* infection.

While class II molecules can be found through the endocytic pathway, significant populations of class II molecules exist in several distinct subcellular locations throughout the endocytic pathway. Because the half-life of class II molecules is relatively long, a significant proportion of the total class II pool resides at the plasma membrane. Subcellular fractionation studies show that lysosomes or lysosome-like class II loading compartments

---

Figure 3-3: Surface Class II molecules are not down regulated by *Chlamydia* infection.

IFN-γ stimulated HeLa were surface-biotinylated and then infected with *Chlamydia* for 24 hrs. before lysis. DRα and class I molecules were immunoprecipitated, analyzed by SDS-PAGE and Western blot and quantified (A). The DRα blot was stripped of antibody and blotted with streptavidin HRP and quantified (B).

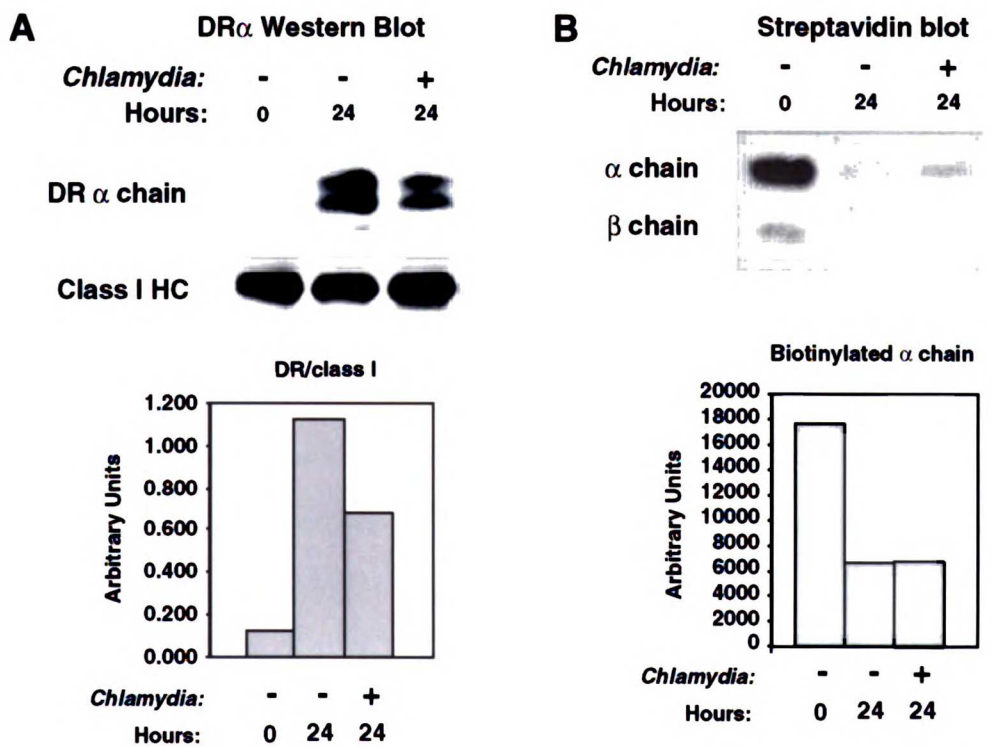
A
DRα Western Blot
Chlamydia: - - +
Hours: 0 24 24
DR α chain
Class I HC
DR/class I
Arbitrary Units
1.200
1.000
0.800
0.600
0.400
0.200
0.000
Chlamydia: - - +
Hours: 0 24 24
B
Streptavidin blot
Chlamydia: - - +
Hours: 0 24 24
α chain
β chain
Biotinylated α chain
Arbitrary Units
20000
18000
16000
14000
12000
10000
8000
6000
4000
2000
0
Chlamydia: - - +
Hours: 0 24 24

Figure 3-3

also contain large amounts of class II (Amigorena et al., 1994; Qiu et al., 1994; Tulp et al., 1994). We sought to determine which of these populations of class II molecules was being affected by *Chlamydia* infection by examining the effects of infection on surface class II molecules. We biotin-labeled surface class II molecules and examined their persistence in infected cells after a 24 hour chase. If *Chlamydia* decrease the total levels of class II molecules by causing the internalization of class II molecules, the levels of biotin-labeled class II should substantially decrease. Class II down regulation effected by degradation or synthesis inhibition should not alter levels of surface biotinylated class II. Western blot analysis of class II immunoprecipitates showed that *Chlamydia*-infected cells contained less total class IIα chain than infected cells 24 hours after inoculation (Fig. 3-3 A). The same membranes were then stripped of antibody and reprobed with streptavidin HRP to detect the biotinylated class IIα chain. The infected and mock-infected lysates contained the same levels of biotinylated class II molecules (Fig. 3-3 B), indicating that while infected cells contain less total class II, the population of class II being affected is not the class II that has already reached the cell surface prior to infection. In concert with Fig. 3-2B, this data suggests that an internal pool of class II is being degraded in *Chlamydia*-infected cells.

Anti-invariant chain antiserum precipitates a rapidly formed, 25 kD protein Chlamydia-infected cells

Given that the class II synthesis rate was not drastically affected by chlamydial infection, we also examined invariant chain synthesis rates and its degradation rate by a pulse-chase labeling. Mock and *Chlamydia*-infected cells were pulse-labeled with ^{35}S translabel at 20 hpi and chased over the course of an hour. The invariant chain was immunoprecipitated using the C-terminus specific serum, KESL, and analyzed by SDS-PAGE and autoradiography. The majority of ^{35}S-labeled invariant chain in the mock-infected cells consisted of the full length, p33-35 forms throughout the one hour chase period (Fig. 3-4 A). In contrast, the KESL immunoprecipitates from infected lysates

appeared at time 0 as a 25 kD polypeptide which slowly decreased in intensity over the one hour chase. Virtually no full length invariant chain was detected in the *Chlamydia*-infected cells at any point in the chase period. The amount of immunoprecipitated class I molecules was consistent between all samples and served as a control for the protein levels of lysate used in the invariant chain immunoprecipitations (Fig. 3-4 B). The appearance of the small KESL-reactive protein immediately after the pulse labeling may be explained in one of several ways. The invariant chain may not be synthesized as a full length protein in infected cells. Alternatively, the protein may be a *Chlamydia* protein that is fortuitously reactive with the KESL serum, or the invariant chain may be very rapidly degraded by proteases.

The 25 kD protein is not a prematurely terminated invariant chain

The first possibility was eliminated by immunoblotting the KESL immunoprecipitates with an antibody against amino acid residues 12-28 of the invariant chain, Pin.1.1 (Roche et al., 1991). The anti-KESL rabbit serum used in the immunoprecipitations was generated to a peptide corresponding to residues 192-216 of the p33 invariant chain, its C-terminus (Lem et al., 1999). The Pin.1.1 Western blot showed (data not shown) that the 25 kD KESL-reactive protein did not blot with the N-terminus

---

Figure 3-4: Invariant chain antiserum immunoprecipitates a rapidly formed, 25 kD protein in *Chlamydia*-infected cells.

Mock or *Chlamydia*-infected HeLa were pulsed labeled with 35S translabel for 5 min and chased for the indicated times before harvest in NP-40 lysis buffer. (A) KESL immunoprecipitations from *Chlamydia*-infected pulse/chase samples do not contain any full length invariant chain. (B) Class I heavy chain immunoprecipitations from the same samples indicate equivalent amounts of protein were used for the immunoprecipitations.

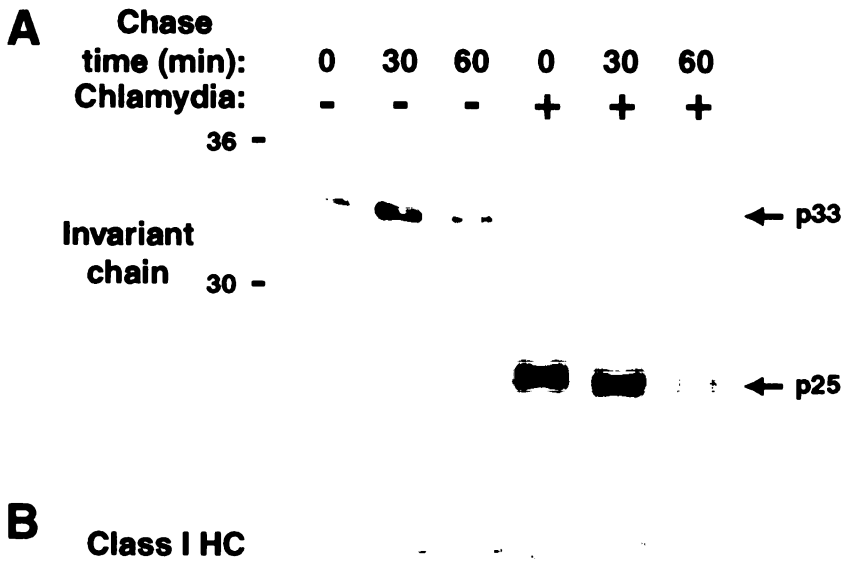
A
Chase
time (min):
Chlamydia:
0
30
60
0
30
60
-
-
-
+
+
+
36 -
Invariant
chain
30 -
p33
p25
B
Class I HC

Figure 3-4

monoclonal antibody. The lack of antibody reactivity to the N-terminus combined with antibody binding to its C-terminus suggests that the polypeptide is an N-terminally cleaved invariant chain, and not a prematurely terminated or alternately spliced form.

The 25 kD protein is not a Chlamydia protein

The possibility of KESL reactivity with a *Chlamydia* protein was addressed using chloramphenicol inhibition of bacterial protein synthesis. Infected cells were treated with a high dose of chloramphenicol for an hour before labeling with ^{35}S translabel. Cells were maintained in the presence of drug or the control carrier ethanol during the pulse labeling. The cells were then chased for one hour in the presence of chloramphenicol before harvest in NP-40 lysis buffer. KESL immunoprecipitates from infected lysates still showed a disappearance of full length invariant chain and the presence of a 25 kD protein (Fig. 3-5 A). *Chlamydia* major outer membrane protein was immunoprecipitated from the supernatants of the KESL precipitations and prepared for immunoblotting.

Figure 3-5. The 25-kD KESL precipitated fragment is not a *Chlamydia* protein.

Mock or *Chlamydia*-infected HeLa were labeled with 35S-translabel in the presence or absence of 200 μg/ml chloramphenicol and chased for 1 hr. (A) Chloramphenicol treatment during labeling did not affect the pattern of invariant chain bands. Radiolabeled invariant chain was immunoprecipitated with KESL and analyzed by 12% SDS-PAGE. (B) Chloramphenicol treatment prevented bacterial protein synthesis during the invariant chain labeling. *Chlamydia* major outer membrane protein (MOMP) was immunoprecipitated from the same lysates using 1-45 mAb. All immunoprecipitates were transferred to nitrocellulose for autoradiography. The same MOMP membrane was then immunoblotted with 1-45 to confirm the presence of MOMP protein in the chloramphenicol treated cells. MOMP band is indicated by the arrows.

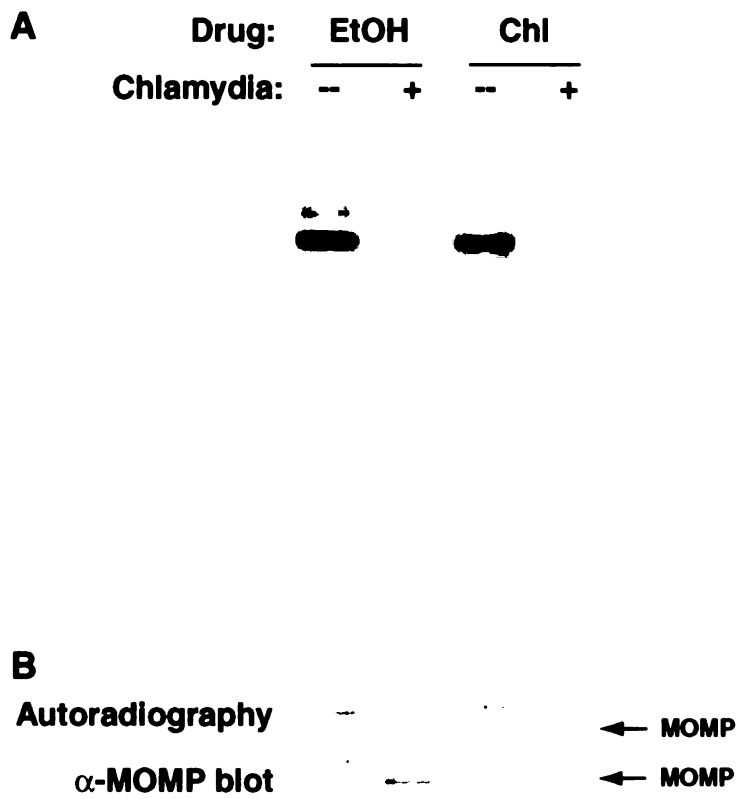
A
Drug:
EtOH
Chl
Chlamydia:
--
+
--
+
B
Autoradiography
α-MOMP blot
MOMP
MOMP

Figure 3-5

Autoradiography of the nitrocellulose membrane before blotting showed the presence of radiolabeled MOMP in infected cells treated with the ethanol control but not in lysates of infected cells treated with chloramphenicol (Fig. 3-5 B). To demonstrate that the anti-MOMP antibody precipitated MOMP out of the lysates, the same membrane was immunoblotted with an anti-MOMP antibody. The anti-MOMP immunoblot showed that unlabeled MOMP was present in the lysates from infected cells treated with chloramphenicol (Fig. 3-5 B), despite the absence of radiolabeled MOMP. Given the demonstrated effectiveness of chloramphenicol-mediated inhibition of *Chlamydia* protein synthesis, the newly synthesized 25 kD protein must be a host protein and is very likely invariant chain.

A possible explanation to the idea that a decrease in invariant chain levels is due to degradation is offered by the Germain lab (Romagnoli and Germain, 1995). They reported that the invariant chain is degraded when the cell is unable to properly glycosylate the protein. N-linked glycosylation of invariant chain is necessary for its association with calnexin, without which invariant chain does not properly assemble with class II heterodimers in the endoplasmic reticulum. I tested this idea in the *Chlamydia*-infected cells to see if *Chlamydia* cause a change in glycosylation patterns of invariant chain. Infected cultures were treated with tunicamycin to prevent all N-linked glycosylation. *Chlamydia* grew normally under these conditions and lysates still contained an invariant chain fragment downshifted to about 20-22 kD, presumably because of the lack of glycosylation of the 25 kD fragment (data not shown).

Figure 3-6. Invariant chain can be degraded in vitro by a *Chlamydia*-infected lysate.

Mock or *Chlamydia*-infected HeLa were harvested in lysis buffer at 22 hpi and mixed with uninfected, ^{35}S-labeled lysate and used for invariant chain immunoprecipitations with KESL.

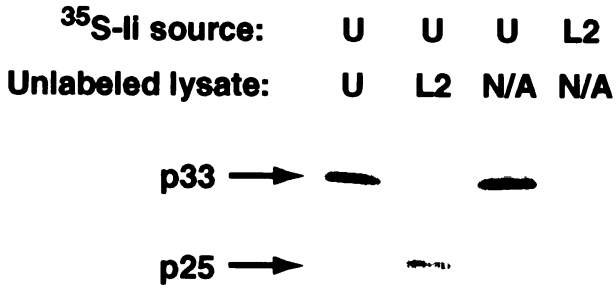

Figure 3-6

Invariant chain can be cleaved to the 25 kD fragment by Chlamydia-infected lysates in vitro

Since the 25 kD protein was likely the C-terminus fragment of a proteolytically cleaved invariant chain, we then addressed the question of how the newly synthesized invariant chain was so rapidly degraded as to be seen at time 0 of a pulse-chase. We conducted a lysate mixing experiment to determine if the invariant chain protease could remain active in the detergent lysate. IFN-γ stimulated HeLa cells were mock or *Chlamydia*-infected and harvested as detergent lysates. A parallel mock-infected HeLa culture was pulse labeled with ^{35}S-translabel and immediately harvested by detergent lysis. Using the radiolabeled lysate as a source of labeled invariant chain, equal volumes of uninfected, labeled lysate were mixed with aliquots of the unlabeled mock or *Chlamydia*-infected lysates. These mixtures were used for invariant chain immunoprecipitations with the KESL serum. If the invariant chain protease is functioning in vitro, the radiolabeled invariant chain should be cleaved in mixtures of labeled full length invariant chain with infected lysates. Autoradiographs of the gels indicate that the labeled invariant chain is indeed cleaved to its 25 kD form by a protease in the infected lysate (Fig. 3-6). In contrast, labeled invariant chain mixed with uninfected lysate predominantly remains as a full length, 35 kD protein. Invariant chain precipitated from radiolabeled uninfected and infected cells confirms the observed sizes of the invariant chain forms in the mixed lysates. Thus, the protease can readily cleave invariant chain in detergent lysate. This data raised the possibility that the observed proteolytic activity may have occurred post-lysis.

Invariant chain cleavage is prevented by immediate protease denaturation

To distinguish between in vivo and post-lysis cleavage of invariant chain, we harvested infected cells in NP-40 lysis buffer followed by immediate dilution with reducing sample buffer (RSV) and boiling. The high SDS concentration coupled with the heat-induced denaturation would likely destroy any proteolytic activity and prevent post-lysis

degradation. Mock and *Chlamydia*-infected cells were harvested with NP-40 and half was incubated on ice for 30 minutes while the other half was boiled with RSV. After the second half of lysate was boiled in RSV, all the samples were analyzed by SDS-PAGE and immunoblotting for invariant chain (KESL), class IIα chain (DA6.147 mAb) and the DMβ chain (DMBS1). No 25 kD invariant chain fragment was observed in the invariant chain blots of immediately boiled lysates whereas lysates maintained on ice for 30 minutes before boiling contained the fragment previously seen (Fig. 3-7 A). The immediate boiling thus prevented the cleavage of invariant chain in infected lysates. It indicated that much of the observed 25 kD fragment is a result of post-lysis degradation, presumably when proteases in membranous compartments are released by addition of detergent.

In addition, the lysates showed no difference in the amount of DRα chain between the infected and uninfected lysates at either time of boiling. There was also no decrease in the DR levels between the 0' and 30' infected lysates (Fig. 3-7 B). Thus, DR molecules are not as susceptible to this particular degradation as the invariant chain, despite the presence of active protease in the lysate of 30' boiled lysates.

Interestingly, both the 0' and 30' boiled, infected lysates showed a decrease in the level of DMβ seen, relative to the uninfected lysates (Fig. 3-7 C). Moreover, the amount of DMβ present in the 0' boiled infected lysate was roughly the amount seen in the 30' infected lysate. In contrast to the invariant chain, the decrease in DMβ seen in previous experiments cannot be ascribed to post-lysis degradation since a decreased level of DMβ

Figure 3-7. A *Chlamydia* protease degrades invariant chain post-lysis. Mock or *Chlamydia*-infected HeLa were harvested in 1% NP-40 lysis buffer; half the sample was immediately boiled (0'), the other half was incubated at 4°C for 30' before boiling. All samples were analyzed by 12% SDS-PAGE and immunoblotting with KESL (A), DA6.147 (B) or DMBS1 (C).

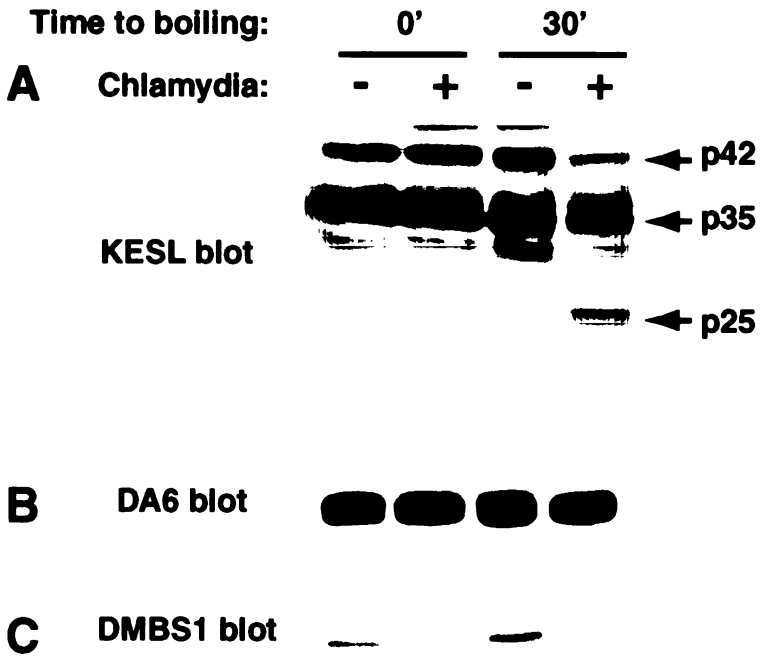
Time to boiling:
0'
30'
A
Chlamydia:
-
+
-
+
p42
p35
KESL blot
p25
B
DA6 blot
C
DMBS1 blot

Figure 3-7

was seen even in the immediately boiled samples. These results indicate that the DR and DM molecules are not readily degraded by the protease in 30 minutes at low temperature, even after it is released into the cytosol by detergent lysis, while the invariant chain is a readily susceptible substrate under the same conditions. It also suggests that the decrease in DM levels in the *Chlamydia*-infected cells must be due to a mechanism that occurs in vivo, before detergent lysis of the cells.

Immediate protease denaturation also prevents USF-1 degradation

IFN–γ stimulation of cells induces expression of the transcription factor USF-1, which in turn upregulates expression of the class II transcription factor, CIITA. CIITA is directly responsible for the transcription of the HLA-DR and HLA-DM genes. A previous report has suggested that *Chlamydia* produce a protease that degrades USF-1, thus preventing IFN–γ induction of HLA-DR and the related genes (Zhong et al., 1999). Since the methods used there mirrored the ones used for our invariant chain degradation assays, we investigated whether the disappearance of USF-1 could also be prevented by harvesting infected cells in sample buffer. Infected cells were either harvested directly in RSV and immediately boiled or in NP-40 lysis buffer and incubated on ice for 30 min. before boiling in RSV. The samples were run on SDS-PAGE and immunoblotted for USF-1. The

---

Figure 3-8. USF-1 degradation is prevented by immediate denaturation of lysate.

Mock or *Chlamydia*-infected cultures were harvested directly in reducing sample buffer (RSB) and immediately boiled or in 1% NP-40 lysis buffer boiled after 30' on ice. Samples were analyzed by SDS-PAGE and immunoblotted for USF-1 (A, left arrowhead). Quantitation and normalization of the USF-1 bands in RSB to background bands 1 or 2 (right arrowheads) was graphed (B).

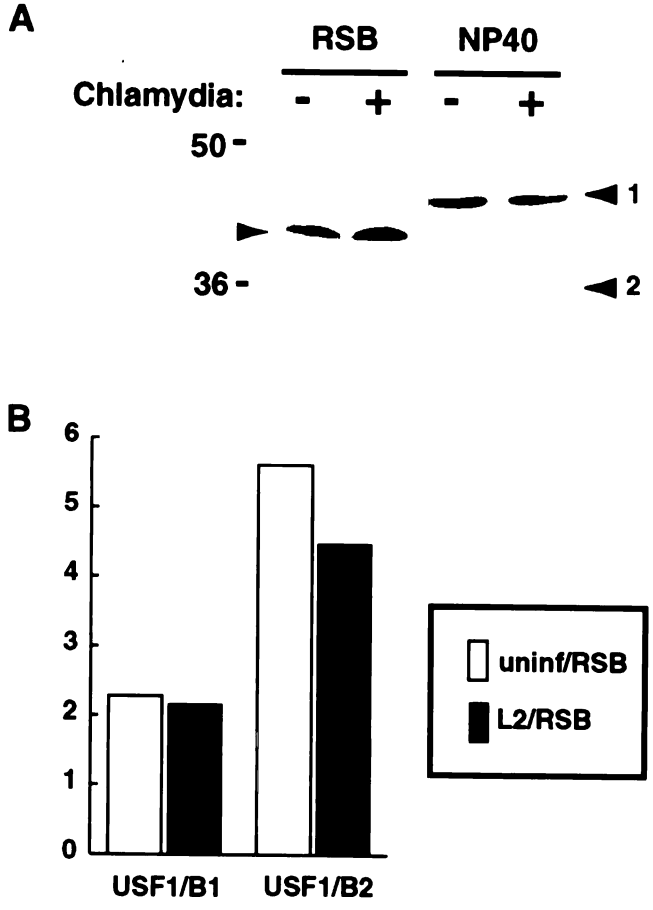
A
RSB
NP40
Chlamydia:
-
+
-
+
50 -
36 -
1
2
B
6
5
4
3
2
1
0
USF1/B1
USF1/B2
uninf/RSB
L2/RSB

Figure 3-8

Western blot demonstrates a near complete disappearance of the 42 kD USF-1 in infected lysate harvested in NP-40 (Fig. 3-8 A). In contrast, the parallel sample harvested in RSV showed only a slight decrease when normalized to the background band 1 or 2 (Fig. 3-8 B). Thus, proteolytic activity in *Chlamydia*-infected lysates have the capacity to degrade the invariant chain, class II molecules, DM and USF-1 in the lysates. The activities degrading these molecules may or may not be the same protease.

The invariant chain protease is a Chlamydia-encoded gene product

Having identified the invariant chain as a ready substrate for the proteolytic activity, we then sought to identify the source of the protease. The protease could logically have been a bacterially encoded gene product or a host protease induced by *Chlamydia* infection. If one could eliminate the production of the protease, a lysate mixing experiment would produce full-length, uncleaved invariant chain. This was accomplished using cycloheximide and chloramphenicol as mammalian and bacterial protein synthesis inhibitors, respectively. Treatment of *Chlamydia*-infected cells with cycloheximide for 12 hours produced a lysate that still contained a proteolytic activity for invariant chain (data not shown). In contrast, chloramphenicol treatment resulted in a significant increase in the amount of full length invariant chain. Chloramphenicol-containing media was fed to mock and infected cells at 18 hpi and again at 30 hpi before harvest at 42 hpi. The double treatment was to allow for turnover of proteases that were synthesized before the addition of the inhibitor. Cultures treated a single time, at 30 hpi, were also harvested simultaneously along with control cultures treated with ethanol at 18 hpi. A lysate mixing experiment performed with these lysates showed that the double-treated sample contained a significant amount of full-length invariant chain with a concomitant decrease in the level of 25 kD fragment present (Fig. 3-9). Much less full length invariant chain was seen in samples mixed with 30 hpi-treated infected cells. This data conclusively demonstrates that the invariant chain protease is a *Chlamydia* gene product and not an induced host protein.

Surprisingly, the control cells treated with ethanol contain an intermediate amount of full length invariant chain (Fig. 3-9). Since these were not treated with drug, the infections had progressed to a more advanced stage than the treated cultures. Both treated cultures contained large chlamydial inclusions that contained a significant number of large RB's that lined the inclusion membrane. The untreated culture contained even larger inclusions which consisted mainly of the smaller, metabolically inactive EB's, as the culture neared the time of lysis and release of the infectious EB's (data not shown). Because the majority of bacteria had differentiated back to the inert EB form, less protein should have been produced and thus the lysate likely contained a relatively low amount of protease, accounting for the lower level of degradation seen, relative to the 30 hpi-treated culture.

LLnL but not lactacystin inhibits invariant chain cleavage by the Chlamydia protease

It was of interest to us to characterize the invariant protease since it specifically cleaved invariant chain at what appears to be a single site. We attempted to identify an inhibitor of the protease that would allow us to classify the type of activity it had. All of the aforementioned data was done in the presence of leupeptin, aprotinin, pepstatin A and

---

Figure 3-9. *Chlamydia* protein synthesis is necessary for invariant chain degradation.

Mock or *Chlamydia*-infected cells were fed medium with 200 μg/ml chloramphenicol or ethanol at 18 hpi and again at 30 hpi before harvest in 1% NP-40 lysis buffer at 42 hpi. These lysates were mixed with uninfected 35S-labeled HeLa lysate and used for invariant chain immunoprecipitations with KESL, SDS-PAGE and autoradiography.

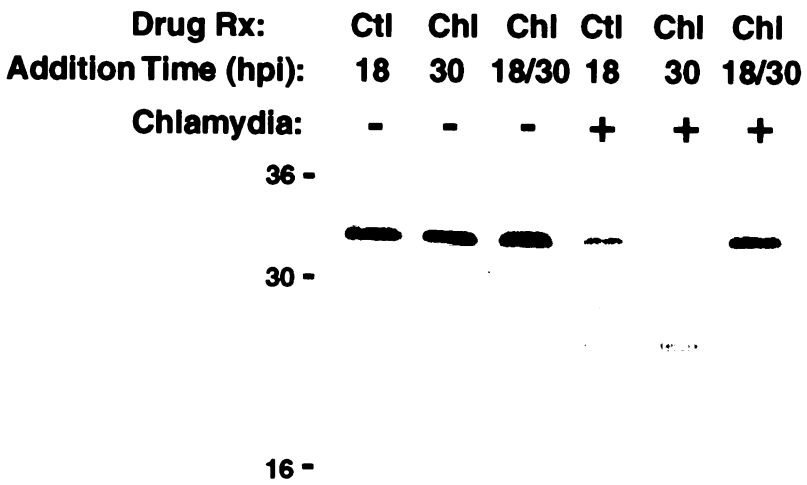
Drug Rx: Ctl Chl Chl Ctl Chl Chl
Addition Time (hpi): 18 30 18/30 18 30 18/30
Chlamydia: - - - + + +
36 -
30 -
16 -

Figure 3-9

PMSF. These protease inhibitors inhibit serine, cysteine and aspartic proteases and none prevented the cleavage of invariant chain in lysates. Double doses of these inhibitors and the addition of E-64, another serine/cysteine protease inhibitor, also did not prevent proteolysis (data not shown). Addition of EDTA to inhibit metalloproteinases likewise did not prevent the degradation (data not shown). Zhong et al. (Zhong et al., 1999) published a study demonstrating the presence of a proteasome-like activity in *Chlamydia*-infected HeLa. The protease was characterized as proteasome-like on the basis of its being inhibited by lactacystin. We treated *Chlamydia*-infected lysates with either lactacystin or LLnL to determine if the activity we have described was also proteasome-like. Infected cells were harvested in NP-40 lysis buffer containing either an inhibitor or a DMSO control. After a 30 minute incubation on ice, the lysates were analyzed by SDS-PAGE and immunoblotting for invariant chain or DRα chain. Virtually no decrease was seen in the amount of full length invariant chain in lysates containing LLnL (Fig. 3-10 A). Also, a faint 25 kD band was detectable in infected lysates with LLnL, indicating that a small amount of proteolysis had occurred. Lactacystin was not as effective as LLnL since a significantly larger amount of fragment was detected at 25 kD and a notable decrease was observed in all of the full length forms of invariant chain. Levels of the 25 kD fragment were comparable to the amount of seen in the DMSO control infected sample. Thus, the activity does seem to be proteasome-like in that is it inhibited by LLnL. However, it is not sensitive to lactacystin inhibition like the previously described activity (Zhong et al., 1999).

Figure 3-10. Invariant chain degradation by a *Chlamydia* protease is inhibited by LLnL, but not lactacystin.

Mock or *Chlamydia*-infected HeLa were harvested at 22 hpi in 1% NP-40 lysis buffer with ethanol, 250 μM LLnL or 75 μM lactacystin. After 30 minutes at 4°C, the lysates were run on SDS-PAGE and analyzed by immunoblotting with KESL (A) or DA6.147 (B).

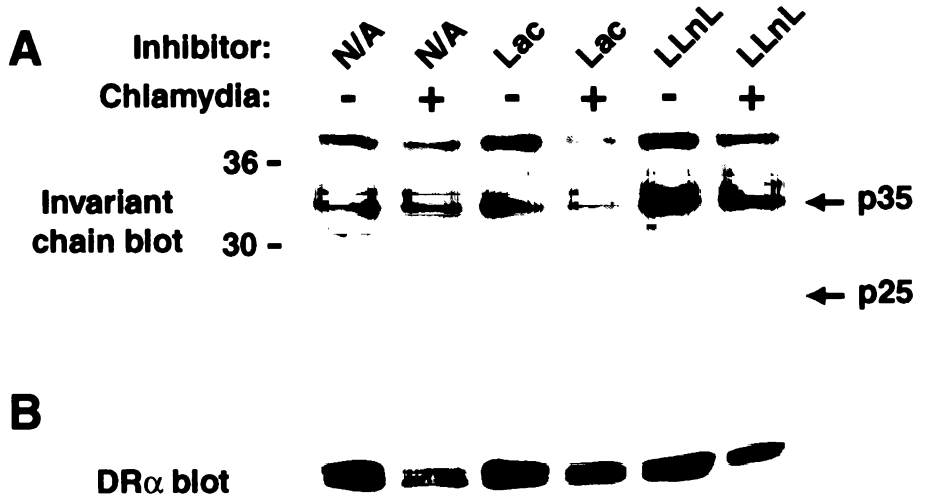
A
Inhibitor:
N/A
N/A
Lac
Lac
LLnL
LLnL
Chlamydia:
-
+
-
+
-
+
36 -
Invariant
chain blot
30 -
p35
p25
B
DRα blot

Figure 3-10

Immunoblots of these same lysates for DRα chain showed that all of the infected samples contained less DRα than the matched uninfected lysates (Fig. 3-10 B). Given the mixed performance of the inhibitors, it is difficult to determine if the decreases were due to inhibition of DR synthesis or a degradation of the protein.

DISCUSSION

Chlamydia, like other intracellular bacteria, evade the host antibody-mediated response by reproducing within the confines of a host cell. Host cells normally respond to such an invasion by digestion of internalized particles and presentation of their antigens as peptides bound by class II MHC molecules on the cell surface. However, bacteria specialized to live in intracellular compartments have also developed mechanisms to evade that defense by either preventing lysosomal maturation of the compartments they inhabit, such as *Mycobacterium spp.* (Sinai and Joiner, 1997; Sturgill-Koszycki et al., 1994), escaping from the membrane compartment as *Listeria* does (Cossart and Lecuit, 1998) or isolating their vacuole from the endocytic pathway entirely. *Chlamydia* (Heinzen et al., 1996; Taraska et al., 1996) and *Legionella* (Vogel and Isberg, 1999) are prominent examples of bacteria using the last mechanism.

Our data demonstrates that *Chlamydia* possess an additional mechanism for evading the class II MHC antigen presentation defense. *Chlamydia* contain a protease or set of proteases that are able to specifically degrade the protein components of the class II loading and processing machinery. Cells infected with *Chlamydia* contain lower levels of HLA-DR, HLA-DM and invariant chain. Since there is not an accompanying decrease in the steady state levels of class I molecules or the cytosolic protein clathrin, the effect appears to be specific to proteins related to class II MHC antigen presentation or, at least, those in the endocytic pathway. The decrease in class II and its related proteins is most easily monitored through the degradation of invariant chain. We have demonstrated that in lysates

of *Chlamydia*-infected cells, invariant chain is specifically cleaved into a 25 kD fragment before its degradation into untraceable smaller pieces. The proteolytic activity generating this 25 kD fragment is present after *Chlamydia* infection and can be eliminated by preventing bacterial protein synthesis for an extended period of time during an active infection. We also characterized this *Chlamydia*-encoded activity as a proteasome-like protease inhabitable by LLnL, but not by lactacystin.

The chlamydial protease specifically cleaves invariant chain at a single site in *in vitro* assays. Infected lysate immediately denatured in RSB did not show any appreciable decrease in the total amount of full length invariant chain at steady state, while the NP-40-harvested infected sample contained the 25 kD fragment. This experiment indicated that the synthesis of invariant chain was not significantly decreased by the presence of *Chlamydia* during the infection period. It also indicated that the degradation observed in previous experiments was occurring post-lysis, when invariant chain and the protease, normally sequestered in separate membrane compartments, are released by detergent into the cytosol. A similar degradation may also be occurring in vivo, but at much smaller quantities not detectable by our assays.

However, it is very reasonable to expect that invariant chaing might be degraded *in vivo*. In order to be effective in preventing antigen presentation, degradation need only occur on invariant chain/class II complexes that reach the vacuole. *Chlamydia* are very effective in preventing host proteins from accumulating on the vacuole membrane (Taraska et al., 1996) although they do acquire host lipids from the TGN (Hackstadt et al., 1995). *Chlamydia* are known to insert proteins into the vacuole membrane that interfere with the fusion of the vacuole and host endocytic vesicles (Scidmore-Carlson et al., 1999; Suchland et al., 2000) and to this same end, it is likely that they secrete proteins into the cytosol as well (Hsia et al., 1997). Studies on the trafficking of class II MHC molecules have found complexes throughout the endocytic pathway (Kleijmeer et al., 1997). If a class II-containing membrane vesicle from the TGN or endocytic pathway fuses with the vacuole,

any host proteins entering the inclusion, including class II/invariant chain complexes, may be rapidly degraded by the bacteria. Rapid elimination of invariant chain/class II complexes that reach the vacuole ensures that fewer *Chlamydia* -derived peptides will be presented at the cell surface.

The rapidity of invariant chain cleavage in vitro also suggests that the same may occur *in vivo*. The speed with which the invariant chain is cleaved in the lysate mixing experiments suggests a very powerful proteolytic activity is accomplishing the cutting, especially since it occurs at 4°C. At physiological temperature, the activity is undoubtedly much more rapid. Moreover, the 25 kD fragment is degraded into smaller untraceable fragments over time, a process which is also undoubtedly speedier at 37°C. Thus, it is not unreasonable to infer that degradation of the 25 kD fragment might occur so rapidly *in vivo* that it is not present at detectable levels. It is also plausible that the initial cleavage to 25 kD occurs rapidly at 4°C while further degradation is slowed at such temperatures, allowing detection of the fragment only *in vitro*.

Interestingly, the degradation of the invariant chain leaves a 25 kD C-terminus fragment. This cleavage site should be close to the CLIP region of the invariant chain, as calculated by molecular weight. The 25 kD fragment does not contain the CLIP region (data not shown) as indicated by immunoblotting with anti-CLIP antiserum. Such a cleavage would occur on the lumenal side of the membrane compartments and would leave the class II molecules with a piece of invariant chain containing CLIP and the N-terminal cytoplasmic tail. Were the N-terminal portion of the invariant chain to be degraded so as to release the CLIP region, the class II molecule would be unstable without a peptide in its binding groove. Given that there is not a high concentration of DM molecules in the vacuole as there is in class II loading compartments, it is unlikely that a DM molecule would be present to stabilize the empty class II molecules as it does in the loading compartment. Consequently, the empty class II molecule would disassociate into single α

and β chains, which are more susceptible to degradation individually than as a heterodimer [Dusseljee, 1998 #1247].

That the cleavage might occur within the lumen of the vacuole is consistent with the observation that no gross protein degradation is occurring in lysates of infected cells. Comparison of banding patterns of mock or infected lysates on SDS-PAGE gels are remarkably similar and indicate that most host proteins are not susceptible to degradation by the invariant chain protease (unpublished data, L.L., F.M.B.). In addition, the majority of invariant chain is degraded after the lysis, suggesting that the protease does not have access to the majority of invariant chain in the cell until the membranes have been dissolved with detergent.

Our data also demonstrates that the synthesis of DM molecules is hindered in the presence of *Chlamydia*.Western blotting of the RSB harvested lysates also indicates that the levels of DMβ chain are decreased, even in immediately denatured lysates (Fig. 3-7C). This correlates with previously published data showing that the transcription factor USF-1 is degraded in *Chlamydia* -infected cells (Zhong et al., 1999). Loss of such a factor prevents transcription of the class II, DM and invariant chain genes. In our hands, the immediately denatured, infected lysates contained slightly less USF-1 than the mock-infected lysates. It is not clear if the decreased level of DM in RSB harvested lysates is due to degradation of DM molecules or a loss of transcription due to USF-1 degradation. A minute decrease in the amount of USF-1 in the infected cells seems to affect DM synthesis much more than that of class IIα or invariant chain, which were only slightly decreased, if at all. Differences between synthesis of these three loci can be explained by fact that the upstream regulatory elements of the three are different. While the DMβ and DRα promoters are similar in structure, the DMβ promoter is much weaker than the DRα promoter as reflected in both transcription levels and amount of translated protein (Ting et al., 1997). The two loci that normally produce the most protein, the invariant chain and

class II loci, are the ones that are the least sensitive to a minute decrease in USF-1 while DM, normally the least abundant of the three proteins, displays a detectable decrease.

The apparent discrepancy regarding the presence of USF-1 in our RSB harvested, infected cells and the published data (Zhong et al., 1999) can be readily explained by the time of IFN–γ stimulation. In the present system, we used HeLa cells that were stimulated with IFN–γ 18-20 hours prior to infection, a period long enough for USF-1 to expressed and translocated to the nucleus where it would presumably be protected from chlamydial proteases. In our system, class II and invariant chain synthesis are minimally affected by the presence of the bacteria. Previously published work focused on cells that had been stimulated with IFN–γ long after the establishment of infection, an environment which contained proteases before USF-1 production began. Consequently, USF-1 would not likely have a chance to be translocated into the nucleus before encountering bacterial proteases, accounting for the near complete absence of class II, DM and invariant chain synthesis.

An additional comparison is warranted between the microscopy data and the RSB harvested blots. The microscopy data indicated that the *Chlamydia*-infected cells contain significantly less class II dimers while the lysates showed approximately equivalent levels between mock and infected cells. However, an anti-αβ dimer was used in the microscopy while the α chain levels were measured in the blotting experiment. If significantly less class II dimers were present at the time of harvest, as indicated by microscopy, while the α chains were still present in significant numbers, the *Chlamydia* may very well have been inducing destabilization of the class II dimers with a significant level of unpaired α chains awaiting degradation. The hypothesis of the removal of invariant chain would very well correlate these two pieces of data.

Although *Chlamydia* infections result in the degradation of invariant chain and USF-1, the two activities are not likely to be the same protein. Invariant chain degradation is inhibited by LLnL but not by lactacystin, which effectively prevents USF-1 degradation.

Both inhibitors are able to inhibit proteases other than the proteasome. LLnL will inhibit cysteine proteases, like cathepsin B and calpain, at a thousand-fold greater efficiency than the proteasome (Rock et al., 1994). Lactacystin, on the other hand, does not inhibit these cysteine proteases nor trypsin or chymotrypsin, even at concentrations greater than necessary for proteasome inhibition (Fenteany et al., 1995). The great difference in sensitivity to the inhibitors points to different proteases being responsible for the invariant chain and USF-1 degradations. Further characterization will be necessary to identify the activities.

The data support a model of *Chlamydia* infection in which the bacteria display multiple mechanisms to evade the immune response. Initially, the bacteria are endocytosed and through synthesis of early gene products, modify the early endosome in which it is contained so as to prevent its maturation into a late endosome/lysosome. This mechanism prevents the bacteria from ever reaching the acidic, degradative lysosome where proteolytic degradation by acid hydrolases would result in bacterial peptides being loaded onto the class II MHC molecules present there. Thus, the bacteria avoid both class II molecules and lysosomal proteases by isolating itself from the endocytic pathway. Once the bacteria are safely isolated, they begin producing all the proteins necessary for metabolic activity and rapidly multiply within the vacuole. During this time, the *Chlamydia* recruit sphingomyelin-containing vesicles from the trans-Golgi network as a source of membrane (unpublished data, L.L, F.M.B) (Hackstadt et al., 1995). Perhaps, included among these vesicles are small amounts of class II/invariant chain complexes. Those complexes that are shuttled to the vacuole are quickly degraded by bacterial proteases in the vacuole, accounting for the observed absence of host membrane proteins on the inclusion membrane. The degradation first results in rapid cleavage of invariant chain, with a subsequent destabilization of class II molecules and an eventual disruption of empty heterodimers. The separated α and β chains are then degraded. The vast majority of class II/invariant chain complexes that are not trafficked to the vacuole will travel to the early

endosome from the TGN and progress through its normal trafficking pathway. This scenario would explain the apparent lack of invariant chain degradation when the lysates are immediately denatured. How would the degradation of a small amount of invariant chain and class II be beneficial to the bacteria? Because the bacteria are sequestered in its inclusion, the only class II molecules that encounter chlamydial antigen are those that traffic into the inclusion. If those are degraded, no antigens will be presented on class II molecules, resulting in an impaired class II-mediated stimulation of T cells. This model is also consistent with characterizations of the chlamydial inclusion as a bare vacuole with no detectable host membrane markers. Any markers transported into the vacuole from the TGN are immediately degraded, preventing vacuole fusion with host compartments.

Concomitant with this parasitic redirecting of sphingomyelin trafficking and class II degradation is the production of a cytosolic protease which can degrade USF-1 that has not yet translated to the nucleus. Normally, the host cell will respond to IFN-γ by decreasing the synthesis of L-tryptophan to prevent bacterial growth and upregulating the synthesis of class II and its related molecules. However, degradation of USF-1 serves to prevent the latter step and further minimize the possibility that chlamydial antigens will be presented on class II molecules.

While data supporting the idea of USF-1 degradation has been published, several additional experiments are necessary to prove to validity of this model for the location and function of the novel invariant chain protease identified here. First, it must be demonstrated that the *Chlamydia* protease cleaves invariant chain *in vivo*. A simple experiment can be done using LLnL as an *in vivo* inhibitor. If *Chlamydia*-infected cells are treated with LLnL *in vivo*, the protease should be inhibited and any proteins trafficking to the inclusion should remain intact, assuming there are not more than one protease in the vacuole. This assumption is reasonable for the invariant chain, since the *in vitro* cleavage shows primarily a single fragment. One should be able to observe the accumulation of host proteins on the vacuole membrane over a prolonged (e.g. 6 hour) treatment with LLnL by

using immunofluorescent confocal microscopy or immunoelectron microscopy. A very long treatment (12 hours) with LLnL will cause apoptosis in HeLa cells so a balance must be maintained between facilitating protein accumulation and keeping the host cells healthy. Titration of LLnL might also help to determine the optimal dose and length of treatment necessary to observe the expected accumulation of host proteins.

To confirm the distinction between the protease degrading USF-1 and the invariant chain protease, a comparative inhibitor study must be done. In this study, mock and infected cells will be lysed in detergent lysis buffer containing either LLnL or lactacystin. The lysates can be incubated on ice to allow cleavage and degradation of USF-1 and invariant chain in samples not treated with inhibitors. Samples can be analyzed by SDS-PAGE and immunoblotted for USF-1 and invariant chain. The lactacystin-treated lysates should confirm the published lactacystin-inhibitable degradation of USF-1. They should also show that degradation of invariant chain still occurs in the presence of lactacystin. By contrast, invariant chain degradation should be inhibited in the LLnL-treated lysates while USF-1 degradation should continue to occur.

Much work remains to be done to elucidate the exact mechanisms of *Chlamydia* evasion of the immune system. However, it is clear from the emerging work that intracellular pathogenic bacteria, like *Chlamydia*, will often possess multiple mechanisms for its defense against host immunity, much as viruses have been found to have multiple mechanisms of defense evasion (Abendroth and Arvin, 1999; Mahr and Gooding, 1999). The multiple evasion strategies provides researchers with a complicated picture to unravel, while at the same time giving tools with which to probe the molecular mechanisms of the immune system.

Materials and Methods

Cells and antibodies: HeLa 229 cells (American Type Cell Collection) were cultured in Eagle minimal essential medium with Earle's BSS and 10% fetal bovine serum in 5% CO_2 at 37°C. Stimulation with recombinant human IFN-γ (Genzyme) was done at concentrations of 100 U/ml. The specificities of anti-HLA-DRαβ mAb antibody L243 (Blum and Cresswell, 1988; Lampson and Levy, 1980), anti-HLA-DRα mAb DA6.147 (Guy et al., 1982), anti-N terminus invariant chain mAb Pin 1.1 (Roche et al., 1991), anti-C terminus invariant chain rabbit serum KESL (Lem et al., 1999), anti-DMβ tail serum DMBS1 (Lem et al., 1999), anti-class I heay chain mAb W6/32 (Barnstable et al., 1978), anti-cation independent mannose-6-phosphate receptor serum was a gift from Linton Traub, anti-major outer membrane protein (MOMP) mAb 1-45 (Baehr et al., 1988; Zhang et al., 1987), anti-*Chlamydia trachomatis* serovar L2 serum (Heinzen et al., 1996), rabbit anti-class I A2 (Bresnahan et al., 1997) have all been previously described.

***Chlamydia* Infections:** HeLa 229 cells were stimulated with 100 u/ml recombinant human IFN-γ (Genzyme) in Eagle MEM with Earle's BSS, 10% fetal bovine serum for 18-20 hrs. Cells were then mock-infected or infected with *Chlamydia trachomatis* LGV-434 serovar L2 at a MOI of a 100 in HBSS. Infections were then fed with medium containing 100 U/ml r-hu IFN-γ and 0.05 mg/ml L-tryptophan (Sigma) for 18-40 hrs, as experiments required.

Immunofluorescent confocal microscopy: Infections were performed on HeLa plated on coverslips. Cells were fixed for 10 min in 4% paraformaldehyde/PBS, permeabilized for 10 min with 0.04% saponin and blocked in blocking solution (1% BSA, 1% cold water fish gelatin, 0.02% SDS, 0/1% Nonidet P-40 (NP-40), 0.02% sodium azide in PBS) for 1 hr, RT. Cells were stained with primary antibody diluted in blocking buffer for 1 hr, washed with PBS and incubated with fluorophore-conjugated secondary

antibody in blocking buffer for 1 hr. Coverslips were then washed in PBS and mounted in Fluoromount G (Fisher Scientific) with 0.1% *p*-phenylenediamine (Sigma) and examined with a Nikon microscope equipped with a BioRad MRC 1024 confocal setup.

Immunoprecipitations and Western blotting: Mock or *Chlamydia*-infected HeLa were harvested in 1% NP-40 lysis buffer at 21 hpi, and equivalent volumes of lysate were analyzed by 12% SDS-PAGE, transferred to nitrocellulose and immunoblotted with primary antibody diluted in 10 mM Tris, pH 7.4, 150 mM NaCl, 0.05% Tween-20 (TBST) and HRP-conjugated secondary antibody in the same manner before visualization using ECL (Amersham Pharmacia). Quantitations were done using the National Institutes of Health (NIH) Image 1.61 software.

Surface biotin chase: IFN-γ stimulated HeLa 229 were washed with PBS and labeled with 0.5 mg/ml sulfo-NHS-LC-biotin in PBS on ice for 10 min and then washed extensively with cold PBS. Cells were then mock or *Chlamydia*-infected and fed with medium with 100 U/ml IFN-γ and 0.05 mg/ml L-tryptophan. Cells were lysed in NP40 lysis buffer + protease inhibitors 24 hpi and used for class II immunoprecipitations with DA6.147 mAb. Class II molecules were analyzed by SDS-PAGE, transferred to nitrocellulose and immunoblotted with DA6.147 mAb. The nitrocellulose was then stripped of Ab by incubation in 100 mM 2-mercaptoethanol, 2% SDS, and 62.5 mM Tris, pH 6.7 at 55°C for 20 minutes before reprobing with streptavidin HRP to determine the amount of surface labeled class II molecules.

^{35}S-metabolic labeling: Mock or infected HeLa were starved in cysteine/methionine deficient medium for 1 hr. and then labeled with 0.5 mCi/10 cm dish for the appropriate time. If necessary, labeled proteins were chased for the requisite time in medium with 5X methionine before harvesting in NP-40 lysis buffer.

Lysate mixing experiments: Mock or *Chlamydia*-infected, IFN-γ treated HeLa cultures were labeled with ^{35}S-translabel and lysed in NP-40 lysis buffer/protease inhibitors. A set of unlabeled cultures were harvested simultaneously. All lysates were precleared with protein G sepharose (PGS); aliquots of each labeled lysate were mixed with an unlabeled lysate in a 1:1 ratios for use in KESL immunoprecipitations. After a 2 hr precipitation step, the immunoprecipitates were analyzed by SDS-PAGE, transferred to nitrocellulose and developed by autoradiography to locate the labeled invariant chain fragments.

In vitro degradation of invariant chain: Mock or *Chlamydia*-infected HeLa were harvested at 23 hpi in 1% NP-40 lysis buffer/protease inhibitors. The lysate was split into half; one half was immediately boiled with 5X reducing sample buffer (RSB) while the other was incubated on ice for 30 minutes before addition of RSB and boiling. Samples were analyzed by 12% SDS-PAGE, transferred to nitrocelluose and immunoblotted for invariant chain (KESL), DRα chain (DA6.147 mAb) or DMβ (DMBS1). The appropriate 2° Ab was used with ECL to develop the blot.

Extended chloramphenicol treatment: IFN-γ stimulated, mock or *Chlamydia*-infected HeLa were fed new medium with 200 μg/ml chloramphenicol or an equivalent volume of ethanol either at 18 hpi only or at both 18 and 30 hpi and harvested at 43 hpi in 1% NP-40 lysis buffer. Parallel mock-infected HeLa cultures were labeled with ^{35}S-translabel for 10 min and immediately harvested in lysis buffer. Aliquots of the labeled lysate were mixed with equivalent volumes of drug-treated lysates and used for KESL immunoprecipitations, which were analyzed on SDS-PAGE, and transferred to nitrocelluose for autoradiography.

Proteasome inhibitor treatments: Mock or *Chlamydia*-infected HeLa were harvested at 22 hpi in 1% NP-40 lysis buffer + protease inhibitors. In addition to the usual 5 inhibitors, either 250 μM LLnL (Roche Molecular Biochemicals), 75 μM lactacystin (Calbiochem) or DMSO (Sigma) were added. Lysates were incubated on ice for 1 hr before pelleting the nuclei. Aliquots of the lysates were analyzed by 12% SDS-PAGE, transferred to nitrocellulose, immunoblotted with KESL and developed with goat anti-rabbit HRP (Jackson Antibodies) and ECL (Amersham).

Chapter 4

Discussion and Future Directions

This work of this thesis was designed to address the question of how the presence of disruptions in the endocytic pathway would affect class II trafficking and antigen presentation. More specifically, the disruptions were due to a genetic disease leading to disabled fission of lysosomes or the presence of intracellular bacteria occupying two very different membrane compartments. In all of the systems studied, class II antigen presentation was negatively altered. In CHS B lymphoblasts and *Coxiella*-infected epithelial cells, HLA-DR and HLA-DM were redistributed to the enlarged lysosomes in which a prolonged association between DR and DM molecules occurred. The prolonged association resulted in a greater proportion of class II molecules having CLIP exchanged, presumably, for peptides. This population of peptides is different than that seen in control cells (Faigle et al., 1998). *Chlamydia* synthesize a protease that can readily cleave invariant chain in vitro and is likely to do so *in vivo*. Rapid removal of invariant chain *in vivo* could lead to dissociation of the αβ heterodimer and subsequent degradation of the separated chains.

Future Directions

A variety of questions remain regarding the effects of these vacuoles on class II trafficking. In the Chediak system, the molecular function of the Chediak/Lyst protein has not yet been identified. Neither has its subcellular location been conclusively demonstrated. It is likely that the function of this proteins and others that it may interact with will shed new light on the regulation of lysosomal fission. It is also not clear how preventing the fission of lysosomes into smaller vesicles would allow for prolonged association of class II and DM molecules, particularly when other functions of the lysosome appear to be unaffected. The answer may lie in understanding how trafficking of class II-containing vacuoles to the surface is regulated, an answer somehow associated with the function of this protein.

Coxiella vacuoles fuse and do not split, much like the CHS lysosomes. Given that *Coxiella* vacuoles affected class II molecules in a manner similar to CHS vacuoles, it would be interesting to investigate if a *Coxiella* protein was able to bind the CHS protein and were able to prevent lysosome fusion in a recombinant form without other bacterial gene products. A number of the experiments done in the CHS B lymphoblasts were attempted in *Coxiella* -infected cells as well but in many of those experiments the class II levels in the immunoprecipitates were below detection level. Those experiments still need to be done to confirm the correlations with the CHS results, particularly the increased association of HLA-DR with HLA-DM in *Coxiella*-infected cells.

The increased efficiency of CLIP removal in the CHS B lymphoblasts suggests that an increased proportion of cells are loaded with peptide. This effect should be detectable by an SDS stability assay on CHS lysates. Despite repeated attempts to observe this phenomena, no increase in the amount of SDS stable class II was detected. It may be that the two to three-fold differences seen in CLIP removal resulted in a two-fold increase in the amount of peptide loaded class II, an amount that might not be detectable by blotting. It may also be that the class II molecules loaded with alternative peptides carry peptides that are only weak binders and do not survive SDS treatments. It is also possible that $\alpha\beta$ heterodimers associated with DM for a prolonged period of time bind CLIP in a manner that does not allow recognition by the anti-CLIP/dimer antibodies.

A wholy different explanation involves the populations of cells sampled in the assays in question. The SDS stability assay measures the total class II population, both internal and external. The CLIP flow cytometry accounts only for surface molecules. The class II/DM complexes in the CHS lysosome are SDS sensitive. An increased amount of these complexes coupled with the decreased amount of CLIP/class II complexes at the surface might result in the same total amount of SDS unstable class II molecules. This explanation would reconcile all of the observations.

The serendipitous discovery of the *Chlamydia*-induced downregulation of class II in *Chlamydia*-infected cells presents a wealth of opportunities for further research. First of all, it must be demonstrated that *Chlamydia* degrade the invariant chain *in vivo*. This might be addressed by treating live cells with the proteasome inhibitor LLnL early during the infection and observing if invariant chain and class II begin to accumulate on the vacuole membrane by immunofluorescent microscopy.

While the data correlates the invariant chain degradation with the disappearance of class II molecules over time, it did not demonstrate a direct connection between the two. Cells normally contain a significant excess of invariant chain that ensures that all the formed heterodimers are transported to the endocytic pathway from the ER (Marks et al., 1990). The data presented did not distinguish between class II-associated invariant chain or excess free invariant chain. This distinction is important since degradation of free invariant chain would be expected to have few effects on class II trafficking, unless the invariant chain in the ER was being degraded to an extent that an excess no longer existed. Degradation experiments using purified class II/invariant chain complexes can readily provide this answer.

During the work of this thesis, pulse/chase experiments to examine the persistence of class II molecules in *Chlamydia*-infected cells were performed but not presented in Chapter 3. Those experiments hinted that a faster rate of degradation might occur for the DRα chain in *Chlamydia*-infected cells than in uninfected cells. Since those experiments focused specifically on the α chain, the outcome for class II dimers still needs to be investigated. The degradation observed may have been specific to unpaired α chains and, in that event, would suggest that *Chlamydia* affected the outcome of misfolded proteins, perhaps through the proteasome with a bacterial subunit added.

Identifying the *Chlamydia* protease responsible for the in vitro degradation of invariant chain is another piece of the puzzle yet to be solved. Knowledge about the bacterial protease will enable the design of inhibitors that when administered may allow

class II/invariant chain complexes to progress normally through the loading pathway and present chlamydial antigens without inhibiting antigen presentation on class I MHC molecules. Such a response could result in true elimination of the bacteria rather than mere control of the infection. Actual clearance of a *Chlamydia* infection would prevent some of the pathology of chronic infections, such as the associated reactive arthritis (Bas et al., 1995; Rahman et al., 1992; Silveira et al., 1993) or in the case of *Chlamydia. pneumoniae*, atherosclerosis (Gura, 1998).

While the benefits of a strong immune response are evident, the problems must also be considered. Since some of the pathology of *Chlamydia* infections emanates from the destructive immune response (Ward, 1995), as seen in ocular trachoma scarring, a more vigorous response may also prove to be detrimental to the host unless it can clear the *Chlamydia* before too much damage is done. As a parasite in kind, *Chlamydia* are relatively non-toxic to the host cell until the latter stages of infection when the cell is lysed (Moulder, 1991). This low toxicity accounts for the ability of the host cell to maintain fairly normal metabolic activity during infections. It may also partially account for the asymptomatic infections seen. Without an immune response, the symptoms are fairly mild, if present at all, until infections become chronic. In this sense, current antibiotic regimens may prove to be more successful than a drug that disables the immune evasion mechanisms of *Chlamydia*. If that proves to be reality, inhibitors of this *Chlamydia* protease may be better used to decrease the immunopathologic effects of infection when used in conjunction with antibiotics.

Such talk is, of course, premature without a definitive identification of the protease. The protease can be identified in two ways. The first approach is to use proteomic information gathered by 2-D gels of fractionated, *Chlamydia*-infected HeLa lysate. Fractionation of lysate into membrane and cytosolic components will allow one to narrow down the number of proteins from which the protease must be fished out. Using invariant chain as the substrate and the appearance of the 25 kD fragment as evidence of activity,

there is a ready in vitro assay to detect active fractions. At this point, the lysates can be run on 2-D gels and compared with uninfected lysates. The non-overlapping spots will be *Chlamydia* proteins. They can then be sequenced directly or compared with predicted characteristics, such as MW and pI, from sequence data of the predicted proteases in the *C. trachomatis* genome (Stephens et al., 1998) (see classifications of the genes at "http://*Chlamydia*-www.berkeley.edu:4231/"). The classifications list twenty putative proteases based on sequence homology. Sequence data could be used to match the pI and MW of the identified spots with those of the putative proteases in the database with confirmation done by mass spectrometry analysis of a tryptic digest of the purified protease.

An alternative mechanism takes advantage of the fact that we have identified an inhibitor for the protease. By using a radiolabeled form of LLnL, one can specifically label proteases in whole cell lysate and identify the bands in a gel, as was done in the purification of cathepsin S (Riese et al., 1996). A possible drawback to this approach is that LLnL does not covalently bind to the protease it inhibits (Lee and Goldberg, 1998). This problem may be avoided if one can identify the radioactive peaks in a chromatography purification. Given the tight association of the inhibitor with the protease, the inhibitor should remain bound to the protease in solution and allow for purification of a small number of proteins co-eluting with the radioactivity. The possibility of the radioactivity diffusing from the protease is a very real one due to gradual dissociation. In order for this approach to be significantly reliable, an irreversible inhibitor for the protease must be identified.

The intracellular location of the *Chlamydia* protease is another interesting subject for speculation. The *in vitro* assays presented here do not characterize the protease since all membrane compartments are dissolved and mixed during the detergent lysis. A simple initial characterization might begin with isolating membrane and cytosol fractions for invariant chain digest assays. Results from this assay would indicate whether the protease

is membrane associated or cytosolic. Several initial observations suggest that the protease is likely enclosed in a membrane compartment, either as an integral membrane protein or a soluble protein in a compartment lumen. The first is that examination of banding patterns in SDS-PAGE of *Chlamydia*-infected lysates shows little or no change from uninfected controls, indicating that a massive degradation of cytosolic proteins is not occurring in infected cells (data not shown). Also, metabolism seems to progress normally and host cells, with low multiplicity of infections, shows no slowdown in protein synthesis or the cell cycle. Cytosolic degradation would be expected to be reflected in changes in some or all of these areas. The fact that invariant chain cleavage is detected in 4°C-incubated lysis buffer but not immediately denatured lysates also indicates that invariant chain is not accessible to the protease until detergent dissolution of host membranes.

Perspectives

The results of this thesis highlight the fact that intracellular pathogens often contain a number of methods for evading the host cellular immune response in addition to avoiding the humoral response. *Coxiella* are not only able to avoid proteolytic degradation in the acidic lysosomes, but they also shift the antigenic peptide repertoire. Shifting the peptide repertoire may alter the T cell response from a protective Th1 to a pathogenic Th2 response. *Chlamydia* may also have multiple mechanisms of evasion. Besides the degradation of an IFN-γ responsive transcription factor to prevent class II synthesis and upregulation of radical oxygen producing enzymes, *Chlamydia* produce a protease that is likely to degrade invariant chain and prevent peptide loading of class II molecules that reach the vacuole.

Perhaps these mechanisms might have been anticipated by observing the multiple mechanisms of viral immune evasion. Several persistent pathogenic viruses are known to establish chronic infections which are controlled but not eliminated by the host immune response. Human cytomegalovirus (HCMV) is a prime example of an organism having multiple immune evasion mechanisms. Two of its gene products, US2 and US11 have

been shown to induce reverse translocation of class I molecules back into the cytoplasm where they are degraded (Wiertz et al., 1996; Wiertz et al., 1996). Another gene product, US6, interferes with peptide translocation into the ER by the TAP transporter (Ahn et al., 1997; Früh et al., 1995). If those were not sufficient, CMV also produce a kinase, pp65, which modifies an antigenic CMV protein to prevent its proteolysis (Gilbert et al., 1996). Even the class II MHC pathway is targeted by HCMV through degradation of JAK1, a kinase necessary for IFN-γ inducible expression of class II molecules (Miller et al., 1998). In addition, IFN-γ inducible class II expression is inhibited partially by the induction of IFN-β by HCMV (Sedmak et al., 1994). Clearly, the persistence of HCMV demonstrate that it is advantageous to have multiple evasion mechanisms in the establishment of chronic infections.

The results also point out that alteration of membrane trafficking can be a potent method for immune evasion. All three of the systems studied in this thesis showed how membrane trafficking can alter class II trafficking. Because class II loading and antigenic processing rely heavily on trafficking through various intracellular compartments, disruptions of trafficking can have distinct effects on surface expression of class II molecules. Other pathogenic intracellular bacteria also reorganize membrane trafficking for their own growth and defense (Meresse et al., 1999). For example, *Salmonella typhimurium* induces aggregation of host surface proteins during its invasion of host cells and seems to specifically direct class I MHC molecules into the bacterial vacuole (Garcia-del Portillo et al., 1994). Presumably, such a mechanism might allow the bacteria to escape class I-mediated recognition by T cells. In contrast, *Salmonella enterica* contain a mechanism to prevent trafficking of its vacuoles to lysosomes. A type III-secreted gene product, SpiC, inhibits fusion of vacuoles with lysosomes and even endosome/endosome fusion (Uchiya et al., 1999). This evasion prevents *S. enterica* from entering the lysosomes where proteolysis and peptide loading of class II can occur. Such examples suggest that other intracellular bacteria, when examined, may also display similar

mechanisms for altering host membrane trafficking that, perhaps not coincidentally, hinders antigen presentation.

It is also likely that other intracellular bacteria use proteases as mechanisms of immune evasion. Several pathogens have already been demonstrated to degrade immune system molecules. As shown in this thesis, *Chlamydia* likely have at least two proteases that serve to downregulate class II molecules. *Leishmania amazonensis* is also known to degrade class II molecules that reach their parasitophorous vacuoles (De Souza Leao et al., 1995). As mentioned earlier, HCMV utilize a protease defense that prevents IFN-γ stimulation through JAK1 (Miller et al., 1998). Closer examination of other intracellular pathogens is likely to yield other instances of proteolytic defenses against the host immune response. Identification and characterization of such proteases will be an important contribution to understanding the pathogenesis and chronic infections by these organisms. Also, if relatively specific inhibitors for these bacterial proteases can be identified, the inhibitors could prove to be a veritable goldmine for scientists in drug development.

In conclusion, it must be reiterated that pathogens know us better than we know ourselves. The rapidly growing field of bacterial pathogenesis is likely to continue to present many surprises to us in the future, surprises both of the complexity of bacterial evasion systems and the normal workings of host cells that pathogens reveal to us through their disruption. And for as short a time as antibiotics have been utilized in human civilization, we have already observed a slow adaptation of the pathogens to drugs intended to eliminate them. Far from being ominous, the situation rings out as a challenge to better understand the pathogens that plague humankind. For as long as there are humans, there will be infectious disease and a dazzling array of nature's intricate entanglements of host/pathogen interactions for scientists to discover.

Chapter 5

Experimental Procedures

This chapter contains detailed descriptions of the general procedures used in the experiments of this thesis that are not documented elsewhere in the laboratory. Methods used for particular experiments are detailed in Chapter 2 and 3. The descriptions here are written so as to be easily replicated by following the step-by-step protocol and being mindful of the hints noted herein.

Induction of Class II MHC molecules with interferon-γ

Materials:

- Cell medium without fetal calf serum, prewarmed to 37°C
- recombinant human IFN-γ, lyophilized, (Genzyme)

- Cells to be stimulated, human (e.g. HeLa 229)
- Appropriate cell medium with fetal calf serum, prewarmed to 37°C
- L-tryptophan stock, 0.5 mg/ml in HBSS, if infections are to be done

Procedure:

Making stocks:

1. Sterilize the outside of the tube of IFN-γ with ethanol and place in biosafety hood. Perform the reconstitution in the hood to maintain sterility.
2. Aliquot the appropriate amount of medium (no serum) to a sterile tube. Use 1 ml of medium to resuspend the lyophilized IFN-γ. Pipet up and down VERY SLOWLY, since foaming and vigorous shaking results in loss of active IFN. Transfer to larger tube of medium and SLOWLY pipet up and down to ensure even mixing.
3. Aliquot in 0.5 ml aliquots and freeze at -20°C. Aliquots are stable for 6 months at -20°C. Thawed aliquots can be stored at 4°C for 1-2 months. DO NOT repeatedly freeze/thaw aliquots. Aliquots can also be stored at -80°C.

Cell stimulations:

1. Aliquot the prewarmed cell medium with serum to a tube.
2. Use a pipetman to add the appropriate amount of IFN-γ stock to the medium. Usually 100 units/ml medium is appropriate for induction of class II, invariant chain and DM in HeLa 229 cells. Add the stock directly into the medium rather than on the side of the tube.

3. Cap tube and mix gently by inverting tube several times. Take care not to generate froth by hard shaking since the IFN activity is lost in vigorously shaken solutions.

4. Remove old medium from cells and add medium/IFN to cells. Incubate for 18-24 hours for optimal induction of class II.

Chlamydia Infection

Materials Needed:

- HeLa 229 cells or other cells to be infected
- sterile Hank's Balanced Salt solution (HBSS), prewarmed to 37°C
- small (50 ml) beaker of ice
- Frozen *Chlamydia trachomatis*, LGV 434, serovar L2 stock (50 µl), kept on ice
- 14" x 19" red biohazard autoclave bag in 4 liter plastic beaker (autoclave safe)
- autoclavable tube rack, for 50 ml tubes
- Eagle MEM with Earle's BSS, 10% fetal calf serum, supplemented with 2 mM L-glutamine, prewarmed to 37°C
- recombinant human interferon-γ, 1000X stock (100,000 Units/ml), if necessary
- L-tryptophan in HBSS, 0.5 mg/ml (10X)
- P-200 pipteman with sterile filter tips
- waste bottle containing approx. 100 ml of bleach (use an old 1 L or 500 ml plastic bottle with a screw cap)

Procedure:

1. Split cells into 10 cm plates, the day before infection, aiming for 60% confluency on the day of infection.
2. Thaw the frozen tube of *Chlamydia* stock (henceforth referred to as 'L2') in 37°C water bath and transfer to beaker of ice when tube has nearly thawed. (Keep cold: infectivity is lost when the sample warms up)
3. Do all steps in the hood, for sterile transfers and user safety. Place biohazard bag and large beaker into hood for a disposal bin. Aliquot warm HBSS to a 50 ml tube, 5 ml for each 10 cm dish to be infected.

4. Pipet the L2 stock up and down to be sure that L2 is well mixed and add the appropriate amount of stock to the 50 ml tube of HBSS. Dilutions of 1:1000 are commonly used to make the innoculum. Mix well by inverting tube several times; do not shake vigorously.

5. Rinse cells once with 5 ml of warm HBSS. Remove HBSS and add 5 ml of innoculum/10 cm dish. Use 5 ml of sterile HBSS for parallel mock-infections.

6. Incubate cells at 37°C for 1 hour in premarked incubator.

7. During incubation, prepare medium for cells, aiming for 10 ml medium/ 10 cm plate. Dilute L-tryptophan stock with Eagle MEM/FCS/L-glut, adding 1 ml L-tryp to 10 ml Eagle MEM. Mix well. Add the appropriate amount of IFN-γ and SLOWLY invert the tube to mix well. You may pipet up and down SLOWLY with a serological pipet to ensure good mixing.

8. Pipet off the innoculum and dispose of in waste bottle with bleach.

9. Wash cells once with 5 ml warm HBSS. Feed cells with 10 ml of prepared medium/IFN/L-tryptophan.

10. Incubate cells at 37°C for 20 hours. Vacuoles should be visible by microscope 12-14 hours post infection (hpi).

11. Wash cells once with warm HBSS and photograph with Polaroid camera on the Nikon TMS microscope as needed. Wipe down surfaces of microscope (but not the objectives) with 70% ethanol when finished.

12. Harvest cells as needed for biochemistry. Dispose of all materials in the biohazard bags. Seal the bag with tape while it is still in the biosafety cabinet/hood and carry to the autoclave in a medium-sized, plastic Nalgene (autoclavable) tray. Label with autoclave tape and leave it for kitchen staff. Autoclave tube racks also.

13. Assess the infectivity by counting nuclei in one quadrant of the photograph. The nuclei are light gray spots with several darker gray spots in the center ad are surrounded by the darker cytoplasm (see the white arrow, Figure 5-1A). Also, count all the vacuoles (bright spots) in the same quadrant (see black arrows in Figure 5.1A and B for examples).

The large gray circles rimmed with a bright border (black arrowhead, Figure 5-1A) are rounded-up cells on top of the monolayer and should not be mistaken for vacuoles. Do not count these in the cell count since it is difficult to determine whether or not these cells are infected. Use an overhead transparency with a photograph-sized box and quadrants drawn with permanent marker as an overlay to help delineate a quadrant on the photographs. A non-permanent transparency pen can be used to dot the vacuoles or nuclei on the transparency when one is counting. Dotting can be done on the opposite side of the transparency as the quadrant to avoid rubbing off the lines. The numbers obtained can be used to calculate the percentage of cells infected ((number of vacuoles/number of nuclei) X 100 = % cells infected). While some cells have two nuclei and some cells have two vacuoles, the frequency is low enough that the assumption of one nucleus/one vacuole will provide a relatively quick and accurate determination of the efficiency of the infection.

NOTES:

• L-tryptophan stocks: These stocks should be made fresh, if possible. Stocks can be made and stored away from light at 4°C for about 1 week. Aliquots can be frozen at -20°C and thawed for each infection if they are flash frozen in liquid nitrogen before being transferred to the freezer. When using frozen aliquots, be sure to check the tube for precipitates upon thawing since L-tryptophan will sometimes precipitate upon thawing, leaving an inadequate concentration of tryptophan in solution, resulting in poor infections.

• IFN-γ stocks: See IFN-γ stimulation protocol for cautions and tips.

• *Chlamydia* stocks can be stored after their initial thaws for several days, though infectivity is lost over time. Use previously thawed stocks when MOI is not crucial (e.g. microscopy experiments). DO NOT freeze/thaw stocks since infectivity dramatically decreases with repeated thawings.

• Plating cells on coverslips for microscopy: In general, cells must be plated at a lower density than on plates and infections must be done at a lower MOI than on plates (typically 25-50% of that used for infections on plates). Because microscopy gives data on individual cells, it is not necessary to get 100% infection. MOI's in the range of plate infections will usually cause large scale apoptosis on coverslips.

SAFETY PRECAUTIONS:

Do **ALL** steps in the hood except those not possible, e.g. thawing tubes. Dispose of all pipets, plates and tubes in the red bag in the hood and seal bag with tape before removing from the hood. Use double gloves and a lab coat and wash hands after the work, even when double gloves were used. Notices of the days and times of infectious work MUST be posted to inform others when work is in progress. UV irradiate the hood for 15 minutes when work is completed.

Figure 5-1. High efficiency *Chlamydia* infections of HeLa 229 cells.

(A) Polaroid photograph of a high efficiency infection of HeLa 229 cells with *Chlamydia trachomatis* LGV 434, serovar L2. Cells were plated in a 10 cm dish and infected as indicated in the procedure above. Photograph was taken with the 20X objective on a Nikon TMS microscope mounted with a Polaroid camera, using Polaroid Polapan 57 black and white film. Final magnification is 80X. The black arrow indicates a typical Chlamydia vacuole/inclusion; the white arrow indicates a nucleus; black arrowhead indicates a balled-up cell on top of the monolayer.

(B) Black and white Polaroid photograph of a late stage *Chlamydia trachomatis* infection of Hela 229 cells. Note the size of the inclusions is much larger than those in (A). Final magnification is 80X.

(C) Polaroid photograph of a parallel culture of mock-infected HeLa 229 cells.

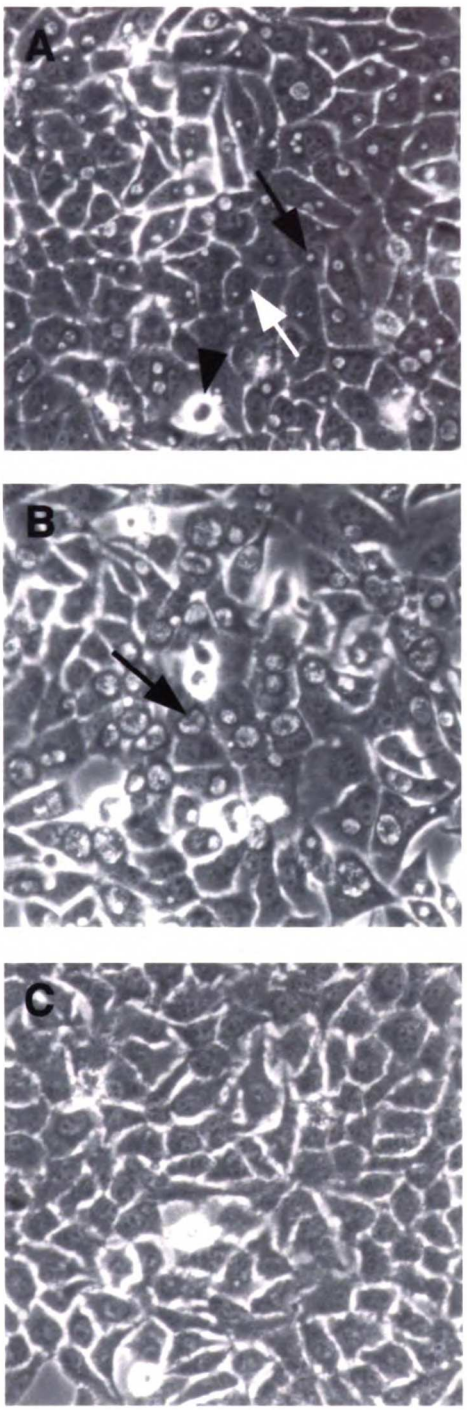

Figure 5-1

Coxiella Infection

Materials Needed:

- HeLa 229 cells or other cells to be infected
- sterile Hank's Balanced Salt solution (HBSS), prewarmed to 37°C
- small (50 ml) beaker of ice
- Frozen *Coxiella burnetii*, Nine mile II, clone 4 stock (50 µl), kept on ice
- 14" x 19" red biohazard autoclave bag in 4 liter plastic beaker (autoclave safe)
- autoclavable tube rack, for 50 ml tubes
- Eagle MEM with Earle's BSS, 10% fetal calf serum, supplemented with 2 mM L-glutamine, prewarmed to 37°C
- recombinant human interferon-γ, 1000X stock (100,000 Units/ml), if necessary
- L-tryptophan in HBSS, 0.5 mg/ml (10X)
- P-200 pipetman with sterile filter tips
- waste bottle containing approx. 100 ml of bleach (use an old 1 L or 500 ml plastic bottle with a screw cap)

Procedure:

1. Split cells into 10 cm plates, the day before infection, aiming for 60% confluency on the day of infection.
2. Thaw the frozen tube of *Coxiella* stock (henceforth referred to as 'Q') in 37°C water bath and transfer to beaker of ice when tube has nearly thawed. (Keep cold: infectivity lost when the sample warms up)
3. Do all steps in the hood, for sterile transfers and user safety. Place biohazard bag and large beaker into hood for a disposal bin. Aliquot warm HBSS to a 50 ml tube, 5 ml for each 10 cm dish to be infected.

4. Pipet the Q stock up and down to be sure that Q is well mixed and add the appropriate amount of stock to the 50 ml tube of HBSS. Dilutions of 1:50 are commonly used to make the innoculum. Mix well by inverting tube several times; do not shake vigorously.

5. Rinse cells once with 5 ml of warm HBSS. Remove HBSS and add 5 ml of innoculum/10 cm dish. Use 5 ml of sterile HBSS for parallel mock-infections.

6. Incubate cells at 37°C for 1 hour in premarked incubator.

7. During incubation, prepare medium for cells, aiming for 10 ml medium/ 10 cm plate. Dilute L-tryptophan stock with Eagle MEM/FCS/L-glut, adding 1 ml L-tryp to 10 ml Eagle MEM. Mix well. Add the appropriate amount of IFN-γ and SLOWLY invert the tube to mix well. You may pipet up and down SLOWLY with a serological pipet to ensure good mixing.

8. Pipet off the innoculum and dispose of in waste bottle with bleach.

8. Wash cells once with 5 ml warm HBSS. Feed cells with 10 ml of prepared medium/IFN/L-tryptophan.

10. Incubate cells at 37°C for 48 hours. Vacuoles should be visible by microscope 12-14 hours post infection (hpi). Remove medium and add freshly prepared medium/IFN/L-tryptophan. Incubate another 24 hours.

11. Wash cells once with warm HBSS and harvest as needed at 72 hpi. Dispose of all materials in the biohazard bags. Seal the bag with tape while it is still in the biosafety cabinet/hood and carry to the autoclave in a medium-sized, plastic Nalgene (autoclavable) tray. Label with autoclave tape and leave it for kitchen staff. Autoclave tube racks also.

NOTES:

• L-tryptophan stocks: These stocks should be made fresh, if possible. Stocks can be made and stored away from light at 4°C for about 1 week. Aliquots can be frozen at -20°C and thawed for each infection if they are flash frozen in liquid nitrogen before being transferred to the freezer. When using frozen aliquots, be sure to check the tube for

precipitates upon thawing since L-tryptophan will sometimes precipitate upon thawing, leaving an inadequate concentration of tryptophan in solution, resulting in poor infections.

• IFN-γ stocks: See IFN-γ stimulation protocol for cautions and tips.

• Repeated freeze/thaws of stocks decreases infectivity. Given the low dilution factor necessary for good innocula, previously thawed stocks are not recommended for later infections.

SAFETY PRECAUTIONS:

• *Coxiella* is resistant to harsh environmental conditions, including desiccation, making it a dangerous organism should it be released from the laboratory by aerosol or on clothing. It is normally a Biosafety level 3 organism, but the strain listed above is considered to be a non-reverting attenuated strain which can be used under level 2 conditions with great caution. **Extra precautions above normal BSL3 standards should be taken when working with *Coxiella*.**

• Do **ALL** steps in the hood except those not possible, e.g. thawing tubes. Dispose of all pipets, plates and tubes in the red bag in the hood and seal bag with tape before removing from the hood. Use double gloves and a lab coat and wash hands after the work, even when double gloves were used. Notices of the days and times of infectious work MUST be posted to inform others when work is in progress.

• Remove the outer gloves and dispose in the biohazard bag in the hood before removing ones hands from the hood during the work. It is essential to autoclave all the materials in the hood (e.g. tube racks) or to UV irradiate the items in the hood for at least 20 minutes before removing them (e.g. pipetman and ethanol bottles). When finished with work, wipe the hood surface with enough 10% bleach or Wescodyne disinfectant to thoroughly wet the surface and leave wet for 10 minutes. Dry the surface and wipe with 70% ethanol before UV irradiating the hood for a minimum of 20 minutes. Keep lab coat separate from other lab materials in a red biohazard bag. Coats can be cleaned normally, with steam washes.

• Have a respirator mask fitted before commencement of any work with *Coxiella*. The respirator is to be used in event of a spill. EH&S also requires annual blood monitoring for those working with *Coxiella*.

NBD-ceramide labeling/chase in *Chlamydia*-infected cells

(adapted from protocol of Ted Hackstadt)

Materials needed:

C6-NDB-ceramide (Molecular Probes, N-1154)

Defatted BSA

Eagle minimal essential medium (no serum), prewarmed to 37°C

Hank's Balanced salt solution (HBSS)

5 mM C6-NBD-ceramide stock solution

Dissolve 1 mg of C6-NBD-ceramide in 0.34 ml ethanol.

5 μM working C6-NBD-ceramide solution

1 ml Eagle MEM + 0.34% defatted BSA

9 ml Eagle MEM

10 ml 5 μM C6-NBD-ceramide

Mix the above three ingredients together. Do not store more than one day at 4°C.

Procedure:

1. Infect HeLa cells that were plated on 12 mm coverslips in 24 well dish. Use normal infection procedure except use 6 drops (approximately 200 μl) of innoculum/well in a 24-well plate. After the hour incubation, wash with cold HBSS.
2. Place the plate on ice.
3. Add 200 μl of 5 mM C6-NBD-ceramide in Eagle's + 0.034% BSA/well.
4. Incubate 30 minutes at 4°C (on ice). (10 minutes at 37°C will work, if no synchronization is necessary).
5. Rinse with cold HBSS.
6. Add 1 ml pre-warmed Eagle's + 0.34% defatted BSA/well.

7. Incubate at 37°C for the necessary chase times. Chase times of 1, 2 and 3 hours are ideal for following the lipid into the *Chlamydia* vacuoles.

8. To photograph the coverslips at time 0, wash twice with cold HBSS. Transfer the coverslip to the slide using 10 ml of HBSS as mounting medium. Store slide in a moist chamber at room temperature while you prepare other slides and photograph within 10 minutes to avoid desiccation of samples. Use a very small drop of oil on the oil lenses so that the oil does not come off the coverslip onto the slide. Photograph the slides quickly since the NBD fades rapidly. It helps to use the rhodamine filter to adjust the focus and then shifting to the fluorescein filter immediately before the photograph.

9. Repeat step 8.

NOTES:

Do NOT use normal mounting medium for the coverslips (e.g. Vectashield or Fluoromount G), especially those that contain organic solvents as they will extract the NBD-ceramide from the cell into the mounting medium. Cells will also begin to detach from the coverslip after a short time. Fixing of the cells is not recommended since the fixing does not prevent diffusion of the lipid.

References

Abendroth, A., and Arvin, A. (1999). Varicella-zoster virus immune evasion. Immunol. Rev. *168*.

Ahn, K., Bruhler, A., Galocha, B., Jones, T. R., Wiertz, E. J. H. J., Ploegh, H. L., Peterson, P. A., Yang, Y., and Früh, K. (1997). The ER-luminal domain of the HCMV glycoprotein US6 inhibits peptide translocation by TAP. Immunity *6*, 613-621.

Amigorena, S., Drake, J. R., Webster, P., and Mellman, I. (1994). Transient accumulation of new class II MHC molecules in a novel endocytic compartment in B lymphocytes. Nature *369*, 113-120.

Amigorena, S., Webster, P., Drake, J., Newcomb, J., Cresswell, P., and Mellman, I. (1995). Invariant chain cleavage and peptide loading in major histocompatibility complex class II vesicles. J. Exp. Med. *181*, 1729-1741.

Arneson, L. S., and Miller, J. (1995). Efficient endosomal localization of major histocompatibility complex class II-invariant chain complexes requires multimerization of the invariant chain targeting sequence. J Cell Biol *129*, 1217-28.

Avva, R. R., and Cresswell, P. (1994). In vivo and in vitro formation and dissociation of HLA-DR complexes with invariant chain-derived peptides. Immunity *1*, 763-774.

Baehr, W., Zhang, Y. X., Joseph, T., Su, H., Nano, F. E., Everett, K. D., and Caldwell, H. D. (1988). Mapping antigenic domains expressed by Chlamydia trachomatis major outer membrane protein genes. Proc Natl Acad Sci U S A *85*, 4000-4.

Baetz, K., Isaaz, S., and Griffiths, G. M. (1995). Loss of cytolytic T lymphocyte function in Chekdiak-Higashi syndrome that prevents lytic granule exocytosis. J. Immunol. *154*, 6122-6131.

Bakke, O., and Dobberstein, B. (1990). MHC class II-associated invariant chain contains a sorting signal for endosomal compartments. Cell *63*, 707-716.

Bannantine, J. P., Stamm, W. E., Suchland, R. J., and Rockey, D. D. (1998). Chlamydia trachomatis IncA is localized to the inclusion membrane and is recognized by antisera from infected humans and primates. Infect Immun *66*, 6017-21.

Barak, Y., and Nir, E. (1987). Chediak-Higashi syndrome. Am. J. Ped. Hem. Onc. *9*, 42-55.

Barbosa, M. D., Barrat, F. J., Tchernev, V. T., Nguyen, Q. A., Mishra, V. S., Colman, S. D., Pastural, E., Dufourcq-Lagelouse, R., Fischer, A., Holcombe, R. F., Wallace, M. R., Brandt, S. J., de Saint Basile, G., and Kingsmore, S. F. (1997). Identification of mutations in two major mRNA isoforms of the Chediak- Higashi syndrome gene in human and mouse. Hum Mol Genet *6*, 1091-8.

Barbosa, M. D. F. S., Nguyen, Q. A., Tchernev, V. T., Ashley, J. A., Detter, J. C., Blaydes, S. M., Brandt, S. J., Chotai, D., Hodgman, C., Solari, R. C. E., Lovett, M., and Kingsmore, S. F. (1996). Identification of the homologous beige and Chediak-Higashi syndrome genes. Nature *382*, 262-265.

Barnstable, C. J., Bodmer, W. F., Brown, G., Galfre, G., Milstein, C., Williams, A. F., and Ziegler, A. (1978). Production of monoclonal antibodies to group A erythrocytes, HLA and other human cell surface antigens--new tools for genetic analysis. Cell *14*, 9-20.

Bas, S., Griffais, R., Kvien, T. K., Glennas, A., Melby, K., and Vischer, T. L. (1995). Amplification of plasmid and chromosome *Chlamydia* DNA in synovial fluid of patients with reactive arthritis and undifferentiated seronegative oligoarthropathies. Arth. & Rheum. *38*, 1005-1013.

Benaroch, P., Yilla, M., Raposo, G., Ito, K., Miwa, K., Geuze, H. J., and Ploegh, H. L. (1995). How MHC class II molecules reach the endocytic pathway. Embo J *14*, 37-49.

Bennett, K., Levine, T., Ellis, J. S., Peanasky, R. J., Samloff, I. M., Kay, J., and Chain, B. M. (1992). Antigen processing for presentation by class II major histocompatibility complex requires cleavage by cathepsin E. Eur J Immunol *22*, 1519-24.

Blum, J. S., and Cresswell, P. (1988). Role for intracellular proteases in the processing and the transport of class II HLA antigens. Proc. Natl. Acad. Sci. USA *85*, 3975-3979.

Blume, R. S., and Wolff, S. M. (1972). The Chediak-Higash syndrome: studies in four patients and a review of the literature. Medicine *51*, 247-280.

Bonnerot, C., Lankar, D., Hanau, D., Spehner, D., Davoust, J., Salamero, J., and Fridman, W. H. (1995). Role of B Cell Receptor Igα and Igβ subunits in MHC Class II-restricted antigen presentation. Immunity *3*, 335-347.

Brachet, V., Raposo, G., Amigorena, S., and Mellman, I. (1997). Ii chain controls the transport of major histocompatibility complex class II molecules to and from lysosomes. J. Cell. Biol. *137*, 51-65.

Bresnahan, P. A., Barber, L. D., and Brodsky, F. M. (1997). Localization of class I histocompatibility molecule assembly by subfractionation of the early secretory pathway. Hum. Immunol. *53*, 129-139.

Brodsky, F. M., Lem, L., Solache, A., and Bennett, E. M. (1999). Human pathogen subversion of antigen presentation. Immunol Rev *168*, 199-215.

Burkhardt, J. K., Wiebel, F. A., Hester, S., and Argon, Y. (1993). The giant organelles in *Beige* and Chediak-Higashi fibroblasts are derived from late endosomes and mature lysosomes. J. Exp. Med. *178*, 1845-1856.

Busch, R., Cloutier, I., Sekaly, R. P., and Hammerling, G. J. (1996). Invariant chain protects class II histocompatibility antigens from binding intact polypeptides in the endoplasmic reticulum. Embo J *15*, 418-28.

Byrne, G. I., Lehmann, L. K., Kirschbaum, J. G., Borden, E. C., Lee, C. M., and Brown, R. R. (1986). Induction of tryptophan degradation in vitro and in vivo: a gamma-interferon-stimulated activity. J Interferon Res *6*, 389-96.

Calafat, J., Nijenhuis, M., Janssen, H., Tulp, A., Dusseljee, S., Wubbolts, R., and Neefjes, J. (1994). Major histocompatibility complex class II molecules induce the formation of endocytic MIIC-like structures. J. Cell Biol. *126*, 967-977.

Campbell, S., Larsen, J., Knight, S. T., Glicksman, N. R., and Wyrick, P. B. (1998). Chlamydial elementary bodies are translocated on the surface of epithelial cells. Am J Pathol *152*, 1167-70.

Castellino, F., and Germain, R. N. (1995). Extensive trafficking of MHC class II-invariant chain complexes in the endocytic pathway and appearance of peptide-loaded class II in multiple compartments. Immunity *2*, 73-88.

Chen, J. W., Murphy, T. L., Willingham, M. C., Pastan, I., and August, J. T. (1985). Identification of two lysosomal membrane glycoproteins. J. Cell Biol. *101*, 85-95.

Cossart, P., and Lecuit, M. (1998). Interactions of Listeria monocytogenes with mammalian cells during entry and actin-based movement: bacterial factors, cellular ligands and signaling. Embo J *17*, 3797-806.

Cresswell, P. (1996). Invariant chain structure and MHC class II function. Cell *84*, 505-7.

De Souza Leao, S., Lang, T., Prina, E., Hellio, R., and Antoine, J.-C. (1995). Intracellular *Leishmania amazonensis* amastigotes internalize and degrade MHC class II molecules of their host cells. J. Cell Sci. *108*, 3219-3231.

Denzin, L. K., Robbins, N.F., Carboy-Newcomb, C., and Cresswell, P. (1994). Assembly and intracellular transport of HLA-DM and correction of the class II antigen-processing defect in T2 cells. Immunity *1*, 595-606.

Denzin, L. K., and Cresswell, P. (1995). HLA-DM induces CLIP dissociation from MHC class II αβ dimers and facilitates peptide loading. Cell *82*, 155-165.

Denzin, L. K., Hammond, C., and Cresswell, P. (1996). HLA-DM interactions with intermediates in HLA-DR maturation and a role for HLA-DM in stabilizing empty HLA-DR molecules. J. Exp. Med. *184*, 2153-2165.

Denzin, L. K., Sant'Angelo, D. B., Hammond, C., Surman, M. J., and Cresswell, P. (1997). Negative regulation by HLA-DO of MHC class II-restricted antigen processing. Science *278*, 106-109.

Deussing, J., Roth, W., Saftig, P., Peters, C., Ploegh, H. L., and Villadangos, J. A. (1998). Cathepsins B and D are dispensable for major histocompatibility complex class II-mediated antigen presentation. Proc Natl Acad Sci U S A *95*, 4516-21.

Dunn, W. A. (1994). Autophagy and related mechanisms of lysosome-mediated protein degradation. Trend Cell Biol *4*, 139-143.

Faigle, W., Raposo, G., Tenza, D., Pinet, V., Vogt, A. B., Kropshofer, H., Fischer, A., de Saint-Basile, G., and Amigorena, S. (1998). Deficient peptide loading and MHC class II endosomal sorting in a human genetic immunodeficiency disease: the Chediak-Higashi syndrome. J. Cell Bio. *141*, 1121-1134.

Fenteany, G., Standaert, R. F., Lane, W. S., Choi, S., Corey, E. J., and Schreiber, S. L. (1995). Inhibition of proteasome activities and subunit-specific amino-terminal threonine modification by lactacystin. Science *268*, 726-31.

Fling, S. P., Arp, B., and Pious, D. (1994). HLA-DMA and -DMB genes are both required for MHC class II/peptide complex formation in antigen-presenting cells. Nature *368*, 554-558.

Früh, K., Anh, K., Djaballah, H., Sempé, P., van Edert, P. M., Tampé, R., Peterson, P. A., and Yang, Y. (1995). A viral inhibitor of peptide transporters for antigen presentation. Nature *375*, 415-418.

Fung-Leung, W.-P., Surh, C. D., Liljedahl, M., Pang, J., Leturcq, D., Peterson, P. A., Webb, S. R., and Karlsson, L. (1996). Antigen presentation and T cell development in H2-M-deficient mice. Science *271*, 1278-1281.

Galan, J. E., and Collmer, A. (1999). Type III secretion machines: bacterial devices for protein delivery into host cells. Science *284*, 1322-8.

Garcia-del Portillo, F., Pucciarelli, M. G., Jefferies, W. A., and Finlay, B. B. (1994). Salmonella typhimurium induces selective aggregation and internalization of host cell surface proteins during invasion of epithelial cells. J Cell Sci *107*, 2005-20.

Ghosh, P., Amaya, M., Mellins, E., and Wiley, D. C. (1995). The structure of an intermediate in class II MHC maturation: CLIP bound to HLA-DR3. Nature *378*, 457-462.

Gilbert, M. J., Riddell, S. R., Plachter, B., and Greenberg, P. D. (1996). Cytomegalovirus selectively blocks antigen processing and presentation of its immediate-early gene product. Nature *383*, 720-722.

Gorvel, J. P., Escola, J. M., Stand, E., and Bakke, O. (1995). Invariant chain induces a delayed transport from early to late endosomes. J. Biol. Chem. *270*, 2741-2746.

Greendale, G. A., Haas, S. T., Holbrook, K., Walsh, B., Schachter, J., and Phillips, R. S. (1993). The relationship of Chlamydia trachomatis infection and male infertility. Am J Public Health *83*, 996-1001.

Griffiths, G. M. (1996). Secretory lysosomes - a special mechanism of regulated secretion in haemopoietic cells. Trends Cell Biol. *6*, 329-332.

Guagliardi, L. E., Koppelman, B., Blum, J. S., Marks, M. S., Cresswell, P., and Brodsky, F. M. (1990). Co-localization of molecules involved in antigen processing and presentation in an early endocytic compartment. Nature *343*, 133-139.

Gura, T. (1998). Infections: a cause of artery-clogging plaques? [news] [published erratum appears in Science 1998 aug 14;281(5379):923]. Science *281*, 35,37.

Guy, K., van Heyningen, V., Cohen, B. B., Deane, D. L., and Steel, C. M. (1982). Differential expression and serologically distinct subpopulations of human Ia antigens detected with monoclonal antibodies to Ia alpha and beta chains. Eur. J. Immunol. *12*, 942-948.

Hackstadt, T., Scidmore, M. A., and Rockey, D. D. (1995). Lipid metabolism in *Chlamydia trachomatis*-infected cells: directed trafficking of Golgi-derived sphingolipids to the chlamydial inclusion. Proc. Natl. Acad. Sci., USA *92*, 4877-4881.

Hackstadt, T., and Williams, J. C. (1983). pH dependence of the Coxiella burnetii glutamate transport system. J Bacteriol *154*, 598-603.

Hammond, C., Denzin, L. K., Pan, M., Griffith, J. M., Geuze, H. J., and Cresswell, P. (1998). The tetraspan protein CD82 is a resident of MHC class II compartments where it associates with HLA-DR, -DM, and -DO molecules. J. Immunol. *161*, 3282-3291.

Harding, C. V., and Geuze, H. J. (1993). Immunogenic peptides bind to class II MHC molecules in an early lysosomal compartment. J. Immunol. *151*, 3988-3998.

Heinzen, R. A., Scidmore, M. A., Rockey, D. D., and Hackstadt, T. (1996). Differential interactions with endocytic and exocytic pathways distinguish parasitophorous vacuoles of *Coxiella burnetii* and *Chlamydia trachomatis*. Infect. Immun. *64*, 796-809.

High, N., Mounier, J., Prevost, M. C., and Sansonetti, P. J. (1992). IpaB of Shigella flexneri causes entry into epithelial cells and escape from the phagocytic vacuole. Embo J *11*, 1991-9.

Holtzman, E. (1989). Lysosomes (New York: Plenum Publishing Corporation).

Hsia, R. C., Pannekoek, Y., Ingerowski, E., and Bavoil, P. M. (1997). Type III secretion genes identify a putative virulence locus of Chlamydia. Mol Microbiol *25*, 351-9.

Igietseme, J. U., Magee, D. M., Williams, D. M., and Rank, R. G. (1994). Role for CD8+ T cells in antichlamydial immunity defined by Chlamydia- specific T-lymphocyte clones. Infect Immun *62*, 5195-7.

Karim, M. A., Nagle, D. L., Kandil, H. H., Burger, J., Moore, K. J., and Spritz, R. A. (1997). Mutations in the Chediak-Higashi syndrome gene (CHS1) indicate requirement for the complete 3801 amino acid CHS protein. Hum. Mol. Genet. *6*, 1087-1089.

Karlsson, L., Peleraux, A., Lindstedt, R., Liljedahl, M., and Peterson, P. A. (1994). Reconstitution of an operational MHC class II compartment in nonantigen-presenting cells. Science *266*, 1569-1573.

Karlsson, L., Surth, C. D., Sprent, J., and Peterson, P. A. (1991). A novel class II MHC molecule with unusual tissue distribution. Nature *351*, 485-488.

Kaufman, J. F., Auffray, C., Korman, A. J., Shackelford, D. A., and Strominger, J. (1984). The class II molecules of the human and murine major histocompatibility complex. Cell *36*, 1-13.

Kaufmann, S. H. E. (1999). Immunity to intracellular bacteria. In Fundamental Immunology, W. E. Paul, ed. (Philadelphia: Lippincott-Raven), pp. 1335-1371.

Kleijmeer, M. J., Morkowski, S., Griffith, J. M., Rudensky, A. Y., and Geuze, H. J. (1997). Major histocompatibility complex class II compartments in human and mouse B lymphoblasts represent conventional endocytic compartments. J. Cell Biol. *139*, 639-649.

Kraulis, P. J. (1991). Molscript - a Program to Produce Both Detailed and Schematic Plots of Protein Structures. Journal of Applied Crystallography *24*, 946-950.

Kropshofer, H., Arndt, S. O., Moldenhauer, G., Hammerling, G. J., and Vogt, A. B. (1997). HLA-DM acts as a molecular chaperone and rescues empty HLA-DR molecules at lysosomal pH. Immunity *6*, 293-302.

Kropshofer, H., Vogt, A. B., Moldenhauer, G., Hammer, J., Blum, J. S., and Hammerling, G. J. (1996). Editing of the HLA-DR-peptide repertoire by HLA-DM. EMBO J. *15*, 6144-6154.

Lampe, M. F., Wilson, C. B., Bevan, M. J., and Starnbach, M. N. (1998). Gamma interferon production by cytotoxic T lymphocytes is required for resolution of Chlamydia trachomatis infection. Infect Immun *66*, 5457-61.

Lampson, L. A., and Levy, R. (1980). Two populations of Ia-like molecules on a human B cell line. J.Immunol. *125*, 293-299.

Lee, D. H., and Goldberg, A. L. (1998). Proteasome inhibitors: valuable new tools for cell biologists. Trends Cell Biol *8*, 397-403.

Lem, L., Riethof, D. A., Scidmore, M., Griffiths, G., Hackstadt, T., and Brodsky, F. M. (1999). Enhanced interaction of HLA-DM with HLA-DR in enlarged vacuoles of hereditary and infectious lysosomal diseases. J. Immunol. *162*, 523-532.

Lindstedt, R., Liljedahl, M., Peleraux, A., Peterson, P. A., and Karlsson, L. (1995). The MHC class II molecule H2-M is targeted to an endosomal compartment by a tyrosine-based targeting motif. Immunity *3*, 561-72.

Liu, S.-H., Marks, M. S., and Brodsky, F. M. (1998). A dominant-negative clathrin mutant differentially affects trafficking of molecules with distinct sorting motifs in the class II major histocompatibility complex (MHC) pathway. J. Cell Biol. *140*, 1023-1037.

Lu, H., and Zhong, G. (1999). Interleukin-12 production is required for chlamydial antigen-pulsed dendritic cells to induce protection against live Chlamydia trachomatis infection. Infect Immun *67*, 1763-9.

Maekawa, Y., Himeno, K., Ishikawa, H., Hisaeda, H., Sakai, T., Dainichi, T., Asao, T., Good, R. A., and Katunuma, N. (1998). Switch of CD4+ T cell differentiation from Th2 to Th1 by treatment with cathepsin B inhibitor in experimental leishmaniasis. J Immunol *161*, 2120-7.

Magee, D. M., Williams, D. M., Smith, J. G., Bleicker, C. A., Grubbs, B. G., Schachter, J., and Rank, R. G. (1995). Role of CD8 T cells in primary Chlamydia infection. Infect Immun *63*, 516-21.

Mahr, J. A., and Gooding, L. R. (1999). Immune evasion by adenoviruses. Immunol. Rev. *168*.

Marks, M., Blum, J. S., and Cresswell, P. (1990). Invariant chain trimers are sequestered in the rough endoplasmic reticulum in the absence of association with HLA class II antigens. J. Cell Biol. *111*, 839-855.

Martin, W. D., Hicks, G. G., Mendiratta, S. K., Leva, H. I., Ruley, H. E., and Van Kaer, L. (1996). H2-M mutant mice are defective in the peptide loading of class II molecules, antigen presentation, and T cell repertoire selection. Cell *84*, 543-50.

Matsunaga, Y., Saibara, T., Kido, H., and Katunuma, N. (1993). Participation of cathepsin B in processing of antigen presentation to MHC class II. FEBS Lett *324*, 325-30.

Maurin, M., Benoliel, A. M., Bongrand, P., and Raoult, D. (1992). Phagolysosomes of *Coxiella burnetii*-infected cell lines maintain an acidic pH during persistent infection. Infect. Immun. *60*, 5013-5016.

Mellins, E., Cameron, P., Amaya, M., Goodman, S., Pious, D., Smith, L., and Arp, B. (1994). A mutant human histocomaptibility leukocyte antigen DR molecule associated with invariant chain peptides. J. Exp. Med. *179*, 541-549.

Meresse, S., Steele-Mortimer, O., Moreno, E., Desjardins, M., Finlay, B., and Gorvel, J. P. (1999). Controlling the maturation of pathogen-containing vacuoles: a matter of life and death. Nat Cell Biol *1*, E183-E188.

Merritt, E. A., and Murphy, M. E. P. (1994). Raster3d Version 2.0 - a Program For Photorealistic Molecular Graphics. Acta Crystallographica Section D-Biological Crystallography *50*, 869-873.

Miller, D. M., Rahill, B. M., Boss, J. M., Lairmore, M. D., Durbin, J. E., Waldman, W. J., and Sedmak, D. D. (1998). Human cytomegalovirus inhibits major histocompatibility complex class II expression by disruption of the Jak/Stat pathway. J. Exp. Med. *187*, 675-683.

Miyazaki, T., Wolf, P., Tourne, S., Waltzinger, C., Dierich, A., Barois, N., Ploegh, H., Benoist, C., and Mathis, D. (1996). Mice lacking H2-M complexes, enigmatic elements of the MHC class II peptide-loading pathway. Cell *84*, 531-41.

Mizuochi, T., Yee, S. T., Kasai, M., Kakiuchi, T., Muno, D., and Kominami, E. (1994). Both cathepsin B and cathepsin D are necessary for processing of ovalbumin as well as for degradation of class II MHC invariant chain. Immunol Lett *43*, 189-93.

Morris, P., Shaman, J., Attaya, M., Amaya, M., Goodman, S., Bergman, C., Monaco, J. J., and Mellins, E. (1994). An essential role for HLA-DM in antigen presentation by class II major histocompatibility molecules. Nature *368*, 551-554.

Morrison, R. P., Feilzer, K., and Tumas, D. B. (1995). Gene knockout mice establish a primary protective role for major histocompatibility complex class II-restricted responses in Chlamydia trachomatis genital tract infection. Infect Immun *63*, 4661-8.

Moulder, J. W. (1991). Interaction of chlamydiae and host cells in vitro. Microbiol. Rev. *55*, 143-190.

Nagle, D. L., Karim, M. A., Woolf, E. A., Holmgren, L., Bork, P., Misumi, D. J., McGrail, S. H., Dussalt, B. J., Perou, C. M., Boissy, R. E., Duyk, G. M., Spritz, R. A., and Moore, K. J. (1996). Identification and mutation analysis of the complete gene for Chediak-Higashi syndrome. Nature Gen. *14*, 307-311.

Nahn, M. H., Apicella, M. A., and Briles, D. E. (1999). Immunity to extracellular bacteria. In Fundamental Immunology, W. E. Paul, ed. (Philadelphia: Lippincott-Raven), pp. 1373-1386.

Nakagawa, T., Roth, W., Wong, P., Nelson, A., Farr, A., Deussing, J., Villadangos, J. A., Ploegh, H., Peters, C., and Rudensky, A. Y. (1998). Cathepsin L: critical role in Ii degradation and CD4 T cell selection in the thymus. Science *280*, 450-453.

Nakagawa, T. Y., Brissette, W. H., Lira, P. D., Griffiths, R. J., Petrushova, N., Stock, J., McNeish, J. D., Eastman, S. E., Howard, E. D., Clarke, S. R., Rosloniec, E. F., Elliott, E. A., and Rudensky, A. Y. (1999). Impaired invariant chain degradation and antigen presentation and diminished collagen-induced arthritis in cathepsin S null mice. Immunity *10*, 207-17.

Neefjes, J. J., and Ploegh, H. L. (1992). Inhibition of endosomal proteolytic activity by leupeptin blocks surface expression of MHC Class II molecules and their conversion to SDS resistant αβ heterodimers in endosomes. EMBO J. *11*, 411-416.

Odorizzi, C. G., Trowbridge, I. S., Xue, L., Hopkins, C. R., Davis, C. D., and Collawn, J. F. (1994). Sorting signals in the MHC class II invariant chain cytoplasmic tail and transmembrane region determine trafficking to an endocytic processing compartment. J. Cell Biol. *126*, 317-330.

Penner, J. D., and Prieur, D. J. (1987). A comparative study of lesions in cultured fibroblasts of humans and four species of animals with chediak-higashi syndrome. Am. J. Med. Gen. *28*, 445-454.

Perou, C. M., Leslie, J. D., Green, W., Li, L., McVey Ward, D., and Kaplan, J. (1997). The Beige/Chediak-Higashi syndrome gene encodes a widely expressed cytosolic protein. J. Biol. Chem. *272*, 29790-29794.

Perou, C. M., Moore, K. J., Nagle, D. L. M., D.J., Woolf, E. A., McGrail, S. H., Holmgren, L., Brody, T. H., Dussault, j., B.J., Monroe, C. A., Duyk, G. M., Pryor, R. J., Li, L., Justice, M. J., and Kaplan, J. (1996). Identification of the murine *beige* gene by YAC complementation and positional cloning. Nature Gen. *13*, 303-308.

Perry, L. L., Feilzer, K., Hughes, S., and Caldwell, H. D. (1999). Clearance of Chlamydia trachomatis from the murine genital mucosa does not require perforin-mediated cytolysis or Fas-mediated apoptosis. Infect Immun *67*, 1379-85.

Pierre, P., Denzin, L. K., Hammond, C., Drake, J. R., Amigorena, S., Cresswell, P., and Mellman, I. (1996). HLA-DM is localized to conventional and unconventional MHC class II- containing endocytic compartments. Immunity *4*, 229-39.

Pieters, J., Bakke, O., and Dobberstein, B. (1993). The MHC class II-associated invariant chain contains two endosomal targeting signals within its cytoplasmic tail. J. Cell Sci. *106*, 831-846.

Pious, D., Dixon, L., Levine, F., Cotner, T., and Johnson, R. (1985). HLA class II regulation and structure: analysis with HLA-DR3 and HLA-DP point mutants. J. Exp. Med. *162*, 1193-1207.

Pond, L., and Watts, C. (1997). Characterization of transport of newly assembled, T cell-stimulatory MHC Class II-peptide complexes from MHC Class II compartments to the cell surface. J. Immunol. *159*, 543-553.

Qiu, Y., Xu, X., Wandinger-Ness, A., Dalke, D. P., and Pierce, S. K. (1994). Separation of subcellular compartments containing distinct functional forms of MHC class II. J Cell Biol *125*, 595-605.

Rahman, M. U., Hudson, A. P., and Schumacher, H. R. (1992). Chlamydia and Reiter's syndrome (reactive arthritis). Spondyloarthropathies *18*, 67-79.

Raoult, D., and Marrie, T. (1995). Q fever. Clin. Infect. Dis. *20*, 489-496.

Raposo, G., Nijman, H. W., Stoorvogel, W., Leijendekker, R., Harding, C. V., Melief, C. J. M., and Geuze, H. J. (1996). B Lymphocytes secrete antigen-presenting vesicles. J. Exp. Med. *183*, 1161-1172.

Rasmussen, S. J., Timms, P., Beatty, P. R., and Stephens, R. S. (1996). Cytotoxic-T-lymphocyte-mediated cytolysis of L cells persistently infected with Chlamydia spp. Infect Immun *64*, 1944-9.

Reimer, L. G. (1993). Q fever. Clin. Microbiol. Rev. *6*, 193-198.

Reyes, V. E., Lu, S., and Humphreys, R. E. (1992). Cathepsin B cleavage of Ii from class II MHC a- and b-chains. J. Immunol. *146*, 3877-3880.

Riberdy, J. M., Avva, R. R., Geuze, H. J., and Cresswell, P. (1994). Transport and intracellular distribution of MHC class II molecules and associated invariant chain in normal and antigen-processing mutant cell lines. J Cell Biol *125*, 1225-37.

Riberdy, J. M., Newcomb, J. R., Surman, M. J., Barbosa, J. A., and Cresswell, P. (1992). HLA-DR molecules from an antigen-processing mutant cell line are associated with invariant chain peptides. Nature *360*, 474-477.

Riese, R. J., Wolf, P. R., Bromme, D., Natkin, L. R., Villadangos, J. A., Ploegh, H. L., and Chapman, H. A. (1996). Essential role for cathepsin S in MHC class II-associated invariant chain processing and peptide loading. Immunity *4*, 357-366.

Roche, P. A., and Cresswell, P. (1990). Invariant chain association with HLA-DR molecules inhibits immunogenic peptide binding. Nature *345*, 615-618.

Roche, P. A., Marks, M. S., and Cresswell, P. (1991). Formation of a nine-subunit complex by HLA class II glycoproteins and the invariant chain. Nature *354*, 392-394.

Rock, K. L., Gramm, C., Rothstein, L., Clark, K., Stein, R., Dick, L., Hwang, D., and Goldberg, A. L. (1994). Inhibitors of the proteasome block the degradation of most cell proteins and generation of peptides presented on MHC class I molecules. Cell *78*, 761-771.

Rodriguez, G. M., and Diment, S. (1992). Role of cathepsin D in antigen presentation of ovalbumin. J Immuno *149*, 2894-2898.

Romagnoli, P., and Germain, R. N. (1995). Inhibition of invariant chain (Ii)-calnexin interaction results in enhanced degradation of Ii but does not prevent the assembly of alpha beta Ii complexes. J Exp Med *182*, 2027-36.

Root, R. K., Rosenthal, A. S., and Balestra, D. J. (1972). Abnormal bactericidal, metabolic, and lysosomal functions of Chediak- Higashi Syndrome leukocytes. J Clin Invest *51*, 649-65.

Rothermel, C. D., Byrne, G. I., and Havell, E. A. (1983). Effect of interferon on the growth of Chlamydia trachomatis in mouse fibroblasts (L cells). Infect Immun *39*, 362-70.

Sadegh-Nasseri, S., Stern, L. J., Wiley, D. C., and Germain, R. N. (1994). MHC class II function preserved by low-affinity peptide interactions preceding stable binding. Nature *370*, 647-50.

Sanderson, F., Kleijmeer, M. J., Kelly, A., Verwoerd, D., Tulp, A., Neefjes, J. J., Geuze, H. J., and Trowsdale, J. (1994). Accumulation of HLA-DM, a regulator of antigen presentation, in MHC class II compartments. Science *266*, 1566-1569.

Sanderson, F., Thomas, C., Neefjes, J., and Trowsdale, J. (1996). Association between HLA-DM and HLA-DR in vivo. Immunity *4*, 87-96.

Schramm, N., Bagnell, C. R., and Wyrick, P. B. (1996). Vesicles containing Chlamydia trachomatis serovar L2 remain above pH 6 within HEC-1B cells. Infect Immun *64*, 1208-14.

Scidmore-Carlson, M. A., Shaw, E. I., Dooley, C. A., Fischer, E. R., and Hackstadt, T. (1999). Identification and characterization of a Chlamydia trachomatis early operon encoding four novel inclusion membrane proteins. Mol Microbiol *33*, 753-65.

Sedmak, D. D., Guglielmo, A. M., Knight, D. A., Birmingham, D. J., Huang, E. H., and Waldman, W. J. (1994). Cytomegalovirus inhibits major histocompatibility class II expression on infected endothelial cells [see comments]. Am J Pathol *144*, 683-92.

Sette, A., Ceman, S., R.T., K., Sakaguchi, K., Appella, E., Hunt, D. F., Davis, T. A., Michel, H., Shabanowitz, J., Rudersdorf, R., Grey, H. M., and DeMars, R. (1992). Invariant chain peptides in most HLA-DR molecules of an antigen-processing mutant. Science *258*, 1801-1804.

Shemer, Y., Kol, R., and Sarov, I. (1987). Tryptophan reversal of recombinant human gamma-interferon inhibition of Chlamydia trachomatis growth. Curr. Microbiol. *16*, 9-13.

Sherman, M. A., Weber, D. A., and Jensen, P. E. (1995). DM enhances peptide binding to class II MHC by release of invariant chain-derived peptide. Immunity *3*, 197-205.

Silveira, L. H., Gutierrez, F., Scopelitis, E., Cuellar, M. L., Citera, G., and Espinoza, L. R. (1993). Chlamydia-induced reactive arthritis. Infect. Arth. *19*, 351-362.

Sinai, A. P., and Joiner, K. A. (1997). Safe haven: the cell biology of nonfusogenic pathogen vacuoles. Annu Rev Microbiol *51*, 415-62.

Sloan, V. S., Cameron, P., Porter, G., Gammon, M., Amaya, M., Mellins, E., and Zaller, D. M. (1995). Mediation by HLA-DM of dissociation of peptides from HLA-DR. Nature *375*, 802-806.

Stein, A., and Raoult, D. (1995). Q fever endocarditis. Eur. Heart J. *16*, 19-23.

Stephens, R. S., Kalman, S., Lammel, C., Fan, J., Marathe, R., Aravind, L., Mitchell, W., Olinger, L., Tatusov, R. L., Zhao, Q., Koonin, E. V., and Davis, R. W. (1998). Genome sequence of an obligate intracellular pathogen of humans: Chlamydia trachomatis [see comments]. Science *282*, 754-9.

Sturgill-Koszycki, S., Schlesinger, P. H., Chakraborty, P. L., Haddix, P. S., Collins, H. L., Fok, A. K., Allen, R. D., Gluck, S. L., Heuser, J., and Russell, D. G. (1994). Lack of acidification in *Mycobacterium* phagosomes produced by exclusion of the vesicular proton-ATPase. Science *263*, 678-681.

Su, H., and Caldwell, H. D. (1995). CD4+ T cells play a significant role in adoptive immunity to *Chlamydia trachomatis* infection of the mouse genital tract. Infect. Immun. *63*, 3302-3308.

Suchland, R. J., Rockey, D. D., Bannantine, J. P., and Stamm, W. E. (2000). Isolates of Chlamydia trachomatis that occupy nonfusogenic inclusions lack IncA, a protein localized to the inclusion membrane. Infect Immun *68*, 360-7.

Taraska, T., Ward, D. M., Ajioka, R. S., Wyrick, P. B., Davis-Kaplan, S. R., Davis, C. H., and Kaplan, J. (1996). The late chlamydial inclusion membrane is not derived from the endocytic pathway and is relatively deficient in host proteins. Infect Immun *64*, 3713-27.

Ting, J. P., Wright, K. L., Chin, K. C., Brickey, W. J., and Li, G. (1997). The DMB promoter: delineation, in vivo footprint, trans-activation, and trans-dominant suppression. J Immunol *159*, 5457-62.

Tulp, A., Verwoerd, D., Dobberstein, B., Ploegh, H. L., and Peiters, J. (1994). Isolation and characterization of the intracellular MHC class II compartment. Nature *369*, 120-126.

Turco, J., Thompson, H. A., and Winkler, H. H. (1984). Interferon-g inhibits growth of Coxiella burnetti in mouse fibroblasts. Infect. Immun. *45*, 781-783.

Uchiya, K., Barbieri, M. A., Funato, K., Shah, A. H., Stahl, P. D., and Groisman, E. A. (1999). A Salmonella virulence protein that inhibits cellular trafficking. Embo J *18*, 3924-33.

van Noort, J. M., and van der Drift, A. C. (1989). The selectivity of cathepsin D suggests an involvement of the enzyme in the generation of T-cell epitopes. J Biol Chem *264*, 14159-64.

van Ooij, C., Apodaca, G., and Engel, J. (1997). Characterization of the Chlamydia trachomatis vacuole and its interaction with the host endocytic pathway in HeLa cells. Infect Immun *65*, 758-66.

Veras, P. S. T., de Chastellier, C., Moreau, M.-F., Villiers, V., Thibon, M., Mattei, D., and Rabinovitch, M. (1994). Fusion between large phagocytic vesicles: targeting of yeast and other particulates to phagolysosomes that shelter the bacterium *Coxiella burneti* or the protozoan *Leishmania amazonensis* in Chinese hamster ovary cells. J. Cell Sci. *107*, 3065-3076.

Veras, P. T., Moulia, C., Dauguet, C., Tunis, C. T., Thibon, M., and Rabinovitch, M. (1995). Entry and survival of *Leishmania amazonenis* Amastigotes within

phagolysosome-like vacuoles that shelter *Coxiella burnetti* in Chinese hamster ovary cells. Infect. and Immun. *63*, 3502-3509.

Vogel, J. P., and Isberg, R. R. (1999). Cell biology of Legionella pneumophila. Curr Opin Microbiol *2*, 30-4.

Vogt, A. B., Kropshofer, H., Moldenhauer, G., and Hammerling, G. J. (1996). Kinetic analysis of peptide loading onto HLA-DR molecules mediated by HLA-DM. Proc. Natl. Acad. Sci. USA *93*, 9724-9729.

Volkman, D. J., Buescher, E. S., Gallin, J. I., and Fauci, A. S. (1984). B cell lines as models for inherited phagocytic diseases: abnormal superoxide generation in chronic granulomatous disease and giant granules in chediak-higashi syndrome. J. Immunol. *133*, 3006-3009.

Wake, C. T., and Flavell, R. A. (1985). Multiple mechanisms regulate the expression of murine immune response genes. Cell *42*, 623-628.

Ward, M. E. (1995). The immunobiology and immunopathology of chlamydial infections. Apmis *103*, 769-96.

Warmerdam, P. A., Long, E. O., and Roche, P. A. (1996). Isoforms of the invariant chain regulate transport of MHC class II molecules to antigen processing compartments. J Cell Biol *133*, 281-91.

Weber, D. A., Evavold, B. D., and Jensen, P. E. (1996). Enhanced dissociation of HLA-DR-bound peptides in the presence of HLA-DM. Science *274*, 618-620.

West, M. A., Lucocq, J. A. M., and Watts, C. (1994). Antigen processing and class II MHC peptide-loading compartments in human B-lymphoblastoid cells. Nature *369*, 147-151.

Wiertz, E. J. H. J., Jones, T. R., Sun, L., Bogyo, M., Geuze, H. J., and Ploegh, H. L. (1996). The human cytomegalovirus US11 gene product dislocates MHC class I heavy chains from the endoplasmic reticulum to the cytosol. Cell *84*, 169-119.

Wiertz, E. J. H. J., Tortorella, D., Bogyo, M., Yu, J., Mothes, W., Jones, T. R., Rapoport, T. A., and Ploegh, H. L. (1996). Sec61-mediated transfer of a membrane protein from the endoplasmic reticulum to the proteasome for destruction. Nature *384*, 432-438.

Wubbolts, R., Fernandez-Borja, M., Oomen, L., Verwoerd, D., Janssen, H., Calafat, J., Tulp, A., Dusseljee, S., and Neefjes, J. (1996). Direct vesicular transport of MHC class II molecules from lysosomal structures to the cell surface. J. Cell Biol. *135*, 611-622.

Zhang, Y. X., Stewart, S., Joseph, T., Taylor, H. R., and Caldwell, H. D. (1987). Protective monoclonal antibodies recognize epitopes located on the major outer membrane protein of Chlamydia trachomatis. J Immunol *138*, 575-81.

Zhong, G., Castellino, F., Romagnoli, P., and Germain, R. N. (1996). Evidence that binding site occupancy is necessary and sufficient for effective major histocompatibility complex (MHC) class II transport through the secretory pathway redefines the primary function of class II-associated invariant chain peptides (CLIP). J Exp Med *184*, 2061-6.

Zhong, G., Fan, T., and Liu, L. (1999). Chlamydia inhibits interferon gamma-inducible major histocompatibility complex class II expression by degradation of upstream stimulatory factor 1. J Exp Med *189*, 1931-8.

Appendix

Cell, Vol. 96, 677–687, March 5, 1999, Copyright ©1999 by Cell Press

EGF Receptor Signaling Stimulates SRC Kinase Phosphorylation of Clathrin, Influencing Clathrin Redistribution and EGF Uptake

Andrew Wilde,[1,6] Eric C. Beattie,[2,7] Lawrence Lem,[1] David A. Riethof,[1] Shu-Hui Liu,[1] William C. Mobley,[3,8] Philippe Soriano,[4] and Frances M. Brodsky[1,5]
[1]The G. W. Hooper Foundation
Department of Immunology and Microbiology
Departments of Biopharmaceutical Sciences and Pharmaceutical Chemistry
[2]Department of Physiology
[3]Departments of Neurology and Anatomy
University of California, San Francisco
San Francisco, California 94143-0552
[4]Division of Basic Sciences
Fred Hutchinson Cancer Research Center
1100 Fairview Avenue North
Seattle, Washington 98109-1024

Summary

Epidermal growth factor (EGF) binding to its receptor causes rapid phosphorylation of the clathrin heavy chain at tyrosine 1477, which lies in a domain controlling clathrin assembly. EGF-mediated clathrin phosphorylation is followed by clathrin redistribution to the cell periphery and is the product of downstream activation of SRC kinase by EGF receptor (EGFR) signaling. In cells lacking SRC kinase, or cells treated with a specific SRC family kinase inhibitor, EGF stimulation of clathrin phosphorylation and redistribution does not occur, and EGF endocytosis is delayed. These observations demonstrate a role for SRC kinase in modification and recruitment of clathrin during ligand-induced EGFR endocytosis and thereby define a novel effector mechanism for regulation of endocytosis by receptor signaling.

Introduction

Receptor-mediated endocytosis allows the specific removal of cell surface receptors and their cargo from the plasma membrane and targets them to endosomes, where they are sorted for downregulation or recycling (Pearse and Robinson, 1990). This process is initiated by recruitment of the receptor into a clathrin-coated pit at the plasma membrane, a structure formed by assembly of clathrin and adaptors into a protein lattice on the membrane's cytosolic face. Polymerization of clathrin into a hexagonal array provides a scaffold for organizing the adaptors, which recognize sequence motifs in the cytoplasmic domains of internalized receptors (Schmid, 1997). Different receptors have different requirements for their entry into coated pits. Those binding nutrients or inert cargo, such as the transferrin receptor, are internalized in the presence or absence of bound ligand, whereas signaling receptors, such as receptor tyrosine kinases and G protein–coupled receptors, require ligand binding for uptake. In this study, we characterize a novel aspect of ligand-induced endocytosis of the epidermal growth factor receptor (EGFR) and demonstrate that receptor signaling, upon ligand binding, stimulates modification and recruitment of clathrin.

A partial explanation for the difference between constitutively endocytosed receptors and those whose endocytosis is ligand induced is that the adaptor recognition signal is constitutively accessible in the former, but cryptic in the latter, until ligand binding has occurred. For example, ligand binding to EGFR causes receptor tyrosine kinase activation and autophosphorylation (Schlessinger and Ullrich, 1992). This results in a structural change that exposes coated pit targeting motifs in the cytoplasmic domain (Cadena et al., 1994). However, there is considerable evidence that ligand-induced endocytosis involves additional regulatory events beyond the mere exposure of an internalization motif for adaptor binding. Downstream receptor signaling is necessary for EGFR internalization (Lamaze and Schmid, 1995) and also for internalization of G protein–coupled receptors (Ferguson et al., 1996; Freedman and Lefkowitz, 1996). In addition, endocytosis of both of these classes of ligand-gated receptors is associated with recruitment of clathrin to the plasma membrane. Activation of EGFR and other receptor tyrosine kinases causes an increase in the number of plasma membrane coated pits (Connolly et al., 1984; Corvera, 1990; Grimes et al., 1996). For the β2-adrenergic G protein–coupled receptor, agonist binding induces phosphorylation of its cytoplasmic domain, which then associates with β-arrestin 1, a clathrin-binding protein (Goodman et al., 1996). The implication of downstream signaling and effects on clathrin in several examples of ligand-induced endocytosis suggested a possible relationship between these processes, particularly in the case of the dramatic clathrin recruitment following receptor tyrosine kinase activation. To investigate this, we set out to establish how EGF binding to EGFR might affect clathrin distribution.

Ligand stimulation of EGFR activates the receptor tyrosine kinase and a number of downstream cellular kinases. Kinase activation and phosphorylation of clathrin-coated vesicle components have already been implicated directly and indirectly in the regulation of endocytosis (Fallon et al., 1994; Holen et al., 1995; Lamaze and Schmid, 1995; Wilde and Brodsky, 1996; Slepnev et al., 1998). We have previously shown that even during constitutive endocytosis, cytosolic phosphorylation of adaptors inhibits nonproductive clathrin–adaptor interactions (Wilde and Brodsky, 1996). In that study we noted a basal level of clathrin phosphorylation in cells, growing under standard tissue culture conditions. Clathrin is composed of three heavy chains of 192 kDa and three light chain subunits (25–29 kDa), of which there are two

[5]To whom correspondence should be addressed (e-mail: fmarbro@itsa.ucsf.edu).
[6]Present address: Department of Embryology, Carnegie Institution of Washington, 115 West University Parkway, Baltimore, Maryland 21210.
[7]Present address: Department of Psychiatry, University of California, San Francisco, California 94143.
[8]Present address: Department of Neurology, Stanford University School of Medicine, Stanford, California 94305.

types in mammalian cells, LCa and LCb (Brodsky, 1988). In cultured cells, both the clathrin heavy chain (CHC) and LCb were phosphorylated at low levels (Wilde and Brodsky, 1996). The CHC phosphorylation was on tyrosine residues, while LCb was serine phosphorylated. In an earlier study of chicken embryo fibroblasts transformed by Rous sarcoma virus (RSV) (Martin-Perez et al., 1989), an increase in the basal level of CHC tyrosine phosphorylation had been observed, which correlated with an increase in plasma membrane clathrin, relative to the clathrin phosphorylation and distribution in nontransformed cells. These observations suggested that CHC phosphorylation might be related to clathrin recruitment. Here we demonstrate that these molecular events both depend on EGFR activation of SRC kinase, which phosphorylates clathrin at a site that mediates critical intermolecular interactions during clathrin self-assembly (Blank and Brodsky, 1987; Näthke et al., 1992). Inhibition or genetic deletion of SRC kinase activity also delays EGF uptake, providing a molecular link between receptor signaling and induction of regulated endocytosis.

Results

EGF Stimulation Causes CHC Tyrosine Phosphorylation and Clathrin Redistribution

To investigate the role of CHC tyrosine phosphorylation in endocytosis and clathrin recruitment, we characterized these events during synchronized EGFR endocytosis by A431 cells. EGF was bound to A431 cells at 4°C, followed by warming the cells to 37°C, in the continued presence of EGF. Cells were lysed at various times after warming, CHC was immunoprecipitated, and its phosphorylation state assessed by immunoblotting with the phosphotyrosine-specific monoclonal antibody (mAb) 4G10. Within 10 min of initiating EGF endocytosis, the level of CHC tyrosine phosphorylation typically increased greater than 10-fold, with phosphorylation detectable as early as 2 min following warming (Figures 1A and 1B). This ligand-induced phosphorylation was followed by a dramatic redistribution of clathrin, visualized by immunofluorescent confocal microscopy within 10 min of initiation of endocytosis (Figures 1C and 1D). In the absence of EGF, clathrin had a punctate distribution throughout the cell with a typical crescent-shaped concentration in the *trans*-Golgi network (TGN) perinuclear region. In the presence of EGF, clathrin had a predominantly peripheral membrane distribution. In fact, the staining of the TGN region was rarely detectable, relative to the increased intensity of the peripheral staining. The change in overall immunofluorescent staining pattern likely reflects the quantitated increase in plasma membrane clathrin-coated pits reported in earlier electron microscopy studies of EGF effects (Connolly et al., 1984).

To establish a connection between tyrosine phosphorylation of CHC and the EGF-induced redistribution of clathrin, cells were treated with the kinase inhibitors H7, herbimycin A, and staurosporin prior to and during EGF stimulation. Only the tyrosine kinase inhibitors herbimycin A and staurosporin prevented EGF-induced clathrin redistribution and prevented CHC tyrosine phosphorylation (Figure 2). H7, which inhibits serine and threonine kinase activity, had no effect. Staurosporin and herbimycin A inhibit the activity of receptor tyrosine kinases and cytosolic tyrosine kinases. It was therefore necessary to determine which type of kinase was responsible for the direct phosphorylation of clathrin in the presence of EGF, in order to understand how ligand binding might influence clathrin recruitment.

EGFR Kinase Activity Is Necessary but Not Sufficient for CHC Phosphorylation

The cytoplasmic portion of EGFR is composed of a membrane-proximal tyrosine kinase domain, which becomes activated upon ligand binding, and a more distal regulatory domain, which is a target for phosphorylation by an adjacent activated EGFR (Chen et al., 1989; Schlessinger and Ullrich, 1992). The regulatory domain contains the binding sites for accessory proteins involved in initiation of signaling and activation of cytosolic kinases. EGFR kinase was isolated by immunoprecipitation from A431 cells and was tested for its ability to phosphorylate a recombinantly expressed fragment of clathrin, constituting the hub domain of the clathrin triskelion. This fragment, comprising the C-terminal third of the CHC (Liu et al., 1995), was known to contain the in vitro target site for CHC phosphorylation as described in further studies (see below). As a positive control for receptor kinase activity, a bacterially expressed protein containing the regulatory domain of EGFR (CT) fused to glutathione S-transferase (CT-GST) was tested for phosphorylation. When kinase activity was stimulated in the presence of γ-^{32}P-ATP, the CT-GST was phosphorylated but the recombinant hub fragment was not, indicating that clathrin is not a direct target of EGFR kinase (Figure 3A). The role of EGFR tyrosine kinase in CHC phosphorylation was investigated further using the EGFR-negative B82 cell line, transfected with either wild-type or mutant forms of EGFR (Chen et al., 1987, 1989) (Figure 3B). Only wild-type EGFR (K^+) was capable of tyrosine phosphorylation of CHC. EGF binding to EGFR with a kinase-inactivating mutation (K^-), truncated EGFR with active kinase but no regulatory domain (958), or truncated EGFR with a kinase-inactivating mutation also lacking the regulatory domain (M958) did not stimulate CHC phosphorylation. These findings demonstrate that EGFR kinase activity is necessary for CHC phosphorylation, but not sufficient, suggesting that downstream signaling is required to activate the kinase responsible for CHC modification.

Inhibition of SRC Family Kinases Affects Clathrin Phosphorylation, Recruitment, and EGF Uptake

SRC family kinases were candidates for mediating CHC phosphorylation because they can be activated upon EGF stimulation (Baass et al., 1995), pp60$^{v\text{-}src}$-transformed cells show increased clathrin phosphorylation (Martin-Perez et al., 1989), and SRC family kinases are observed in clathrin-coated vesicles in platelets (Stenberg et al., 1997). To determine whether SRC family kinases could be the effectors for CHC tyrosine phosphorylation in A431 cells, their activity was analyzed following EGF stimulation (Figure 4A). Three kinases, pp60$^{c\text{-}src}$, pp59^{fyn}, and pp62^{yes}, were immunoprecipitated

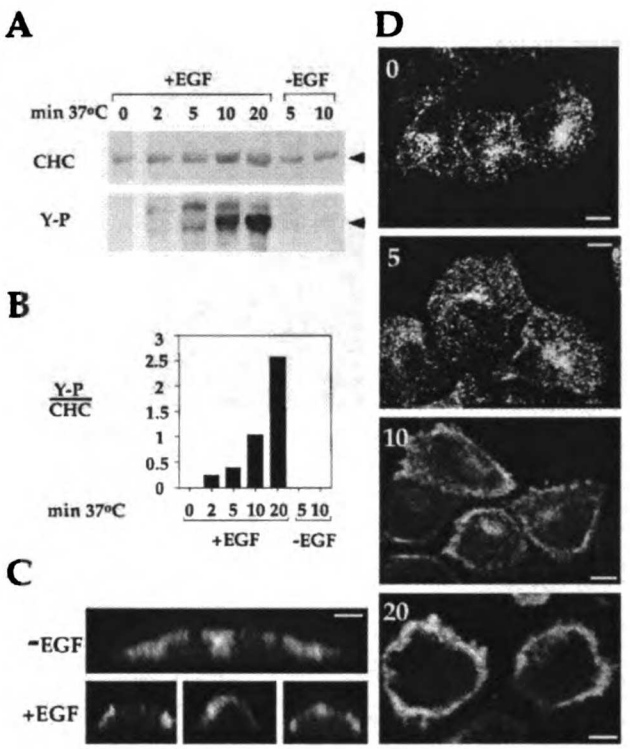

Figure 1. EGF Stimulation of A431 Cells Leads to CHC Tyrosine Phosphorylation and Peripheral Recruitment of Clathrin

A431 cells were serum starved, then incubated for 1 hr in the presence or absence of EGF at 4°C, followed by warming to 37°C for 0, 5, 10, or 20 min in the continued presence or absence of EGF.

(A) At the indicated time, after warming to induce EGF uptake, clathrin was immunoprecipitated from cell lysates and immunoblotted for clathrin heavy chain (CHC) and phosphotyrosine (Y-P), using the mAbs TD.1 and 4G10, respectively. Blots were stripped between exposure to different antibody probes. The arrowheads indicate the position of CHC.

(B) Immunoblot images in (A) were quantified, using the NIH Image software, and the ratio of the 4G10 to TD.1 signal is plotted to normalize the degree of tyrosine phosphorylation (Y-P) to the levels of CHC immunoprecipitated.

(C) A431 cells were treated with EGF or mock treated, as above, warmed for 20 min, and processed for immunofluorescent staining of clathrin using the anti-CHC mAb X22 and secondary antibody conjugated to fluorescein. Z section images were recorded by confocal microscopy. Bar is 10 μm and applies to all panels.

(D) A431 cells were treated with EGF as described above and were processed for immunofluorescent staining of clathrin, as in (C). Images were recorded by confocal microscopy after warming to induce EGF uptake for the indicated time. Bars, 10 μm.

from A431 cell lysate prepared 5 min after EGF internalization was induced. As assessed by their ability to phosphorylate the substrate enolase (Feder and Bishop, 1990), EGF-dependent activation of $pp60^{c\text{-}src}$ and $pp62^{yes}$ was observed, but $pp59^{fyn}$ was not activated, although it was present in A431 cells. PP1, an inhibitor of SRC family kinases (Hanke et al., 1996), was used to block activation of these kinases by EGF, and CHC tyrosine phosphorylation was significantly reduced (Figure 4B). To confirm that the PP1 inhibitor was, in this case, specific for SRC family kinases and did not simultaneously reduce EGFR tyrosine kinase activity, the EGF-induced autophosphorylation of EGFR was evaluated when cells were stimulated in the presence of PP1 or genistein (Figure 4C). After incubation with EGF, plus or minus inhibitor, EGFR was immunoprecipitated and its phosphorylation was assessed. The broad tyrosine kinase inhibitor genistein significantly reduced the amount of EGFR autophosphorylation in response to EGF, whereas treatment of cells with PP1, at concentrations blocking EGF-induced CHC phosphorylation, had no effect on EGFR autophosphorylation. Thus, the PP1 inhibitor affects CHC tyrosine phosphorylation directly by blocking SRC family kinase activity and not by blocking EGFR kinase activity. PP1 treatment also blocked EGF-induced clathrin recruitment to the cell periphery (Figure 4D) and delayed EGF uptake (Figure 4E). Interestingly, in the presence of PP1 a delay in EGF endocytosis was detected during the first 5 min of EGF uptake (Figure 4E) but was less pronounced after longer periods of EGF exposure (data not shown). This correlates with the inhibition of CHC phosphorylation, which is detectable as early as 2 min after EGF exposure (Figures 1A and 1B). However, the extensive redistribution of clathrin occurs with a longer time course (Figure 1D), so it may not be directly related to early endocytic events.

CHC Is a Substrate for $pp60^{c\text{-}src}$ In Vitro and In Vivo in the Assembly Control Domain

The effects of PP1, combined with analysis of activated SRC family kinases, implicate $pp60^{c\text{-}src}$ and/or $pp62^{yes}$ in EGF-dependent CHC phosphorylation and clathrin redistribution to the periphery of A431 cells. To assess the role of these kinases directly, cells with altered expression of SRC family kinases were tested for their steady-state levels of clathrin phosphorylation and their ability to phosphorylate clathrin in response to EGF treatment. In transfected 3T3 cells expressing high levels of $pp60^{c\text{-}src}$ (Lin et al., 1995), a 10-fold increase of steady-state CHC tyrosine phosphorylation was detected compared to wild-type 3T3 cells, suggesting that $pp60^{c\text{-}src}$ is a potential CHC kinase in vivo (Figure 5A). Fibroblast cell lines produced from mice lacking expression of various SRC family kinases were then tested for CHC phosphorylation upon EGF stimulation (Figure 5B). Cell lines from mice with a homozygous deletion of only

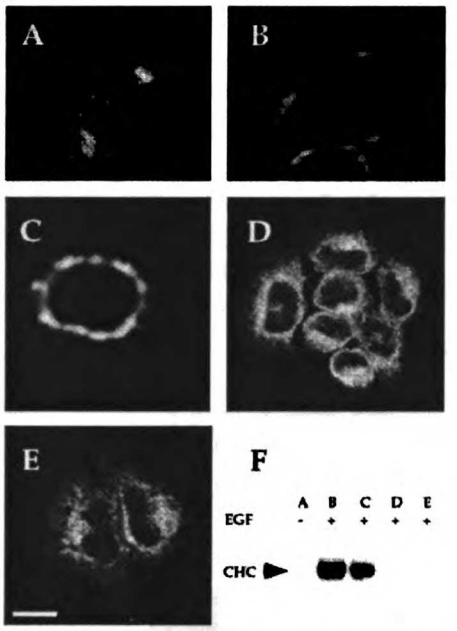

Figure 2. Tyrosine Kinase Inhibitors Prevent EGF-Dependent CHC Phosphorylation and Redistribution of Clathrin

(A–E) A431 cells were serum starved and treated with either 0.1% DMSO (A and B), 100 μM H7 (C), 1 μg/ml herbimycin A (D), or 50 nM staurosporin (E) for 3 hr prior to EGF treatment (B, C, D, and E) or mock treatment (A) at 4°C. After warming to 37°C for 20 min, in the presence of inhibitor or DMSO, cells were processed for immunofluorescent staining of clathrin using mAb X22 and a secondary goat anti-mouse antibody conjugated to fluorescein and visualized by confocal microscopy. Bar is 10 μm and applies to all panels.

(F) A431 cells were cultured with inhibitor and treated with EGF or mock treated, as in (A)–(E). Clathrin was immunoprecipitated from cell lysates, and tyrosine phosphorylation was analyzed by immunoblotting with mAb 4G10. CHC designates the position of the clathrin heavy chain.

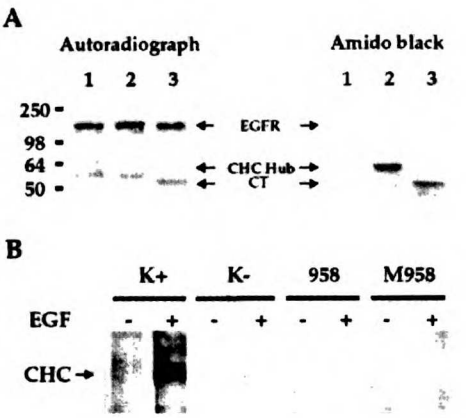

Figure 3. Full-Length, Kinase-Active EGFR Is Necessary but Not Sufficient for EGF-Dependent CHC Phosphorylation

(A) EGFR was immunoprecipitated from A431 cells and incubated with EGF and γ-^{32}P ATP alone (lane 1), with purified CHC hub fragment (lane 2), or with purifed GST fusion protein comprising the EGFR carboxy-terminal regulatory domain (CT) (lane 3). The kinase reaction was analyzed by SDS-PAGE, blotting onto nitrocellulose, and autoradiography (left). Protein fragments were detected on the blot by amido black staining (right). Migration positions of molecular weight marker proteins (in kilodaltons) are indicated at the left.

(B) B82 mouse L cells expressing different forms of EGFR (wild-type and mutant) were serum starved and incubated in the presence or absence of EGF at 4°C. After warming 20 min, cell lysates were prepared and clathrin immunoprecipitated using the mAb X22. CHC tyrosine phosphorylation was analyzed by immunoblotting with mAb 4G10. The EGFR transfectants are designated as follows: K^+, full-length wild-type EGFR; K^-, full-length kinase-inactivated EGFR; 958, EGFR truncated at residue 958 lacking the C-terminal regulatory domain; M958, the same as 958 but has a point mutation rendering the kinase domain inactive.

pp60$^{c\text{-}src}$ (1S and 1T) (Thomas et al., 1991) or lacking both pp60$^{c\text{-}src}$ and pp62^{yes} (Stein et al., 1994), but not lines lacking both pp62^{yes} and pp59^{fyn}, showed a significant reduction in CHC phosphorylation in response to EGF, identifying pp60$^{c\text{-}src}$ as the kinase responsible.

The target site for CHC phosphorylation by pp60$^{c\text{-}src}$ was then mapped in vitro and in vivo (Figure 6). Purified recombinant pp60$^{c\text{-}src}$ (Morgan et al., 1991) phosphorylated the CHC of purified clathrin (residues 1–1675) and bacterially expressed recombinant CHC hub domain (residues 1074–1675), to the same level, based on stoichiometry of ^{32}P modification (data not shown). These observations indicate that the target for CHC tyrosine phosphorylation is in the CHC hub domain. Accordingly, pp60$^{c\text{-}src}$ did not phosphorylate the N-terminal domain of CHC (residues 1–545) when tested against bacterially expressed recombinant fragments of bovine CHC (Liu et al., 1995) (Figure 6A). The pattern of phosphorylation of subfragments of the hub made it possible to identify a single pp60$^{c\text{-}src}$ target site. A CHC hub fragment encoding the amino acids 1074–1483 was a substrate for pp60$^{c\text{-}src}$, but a fragment encoding the amino acids 1074–1460 was not. Between amino acids 1460 and 1483, there is a single tyrosine residue at position 1477, with acidic amino acids to the N-terminal side of it and a leucine residue three positions C-terminal to it (Figure 6B). This is compatible with a SRC family kinase consensus sequence previously described (Songyang et al., 1993). The region of the CHC in which tyrosine 1477 is located is predicted to interact with clathrin light chains and is generally thought to be an assembly control region (Näthke et al., 1992).

To determine whether in vivo phosphorylation of CHC, induced by EGF binding, also mapped to tyrosine 1477, a site-specific mutation to phenylalanine (Y1477F) was engineered in a construct encoding the full-length human CHC (Nomura et al., 1994). An epitope tag, from T7 phage (Lutz-Freyermuth et al., 1990), was added for expression at the N terminus of the mutant. As a control, the wild-type human CHC was similarly epitope tagged, so that the fate of wild-type and mutant transfected clathrin could be analyzed. Both constructs were independently transfected into A431 cells, and stable clones,

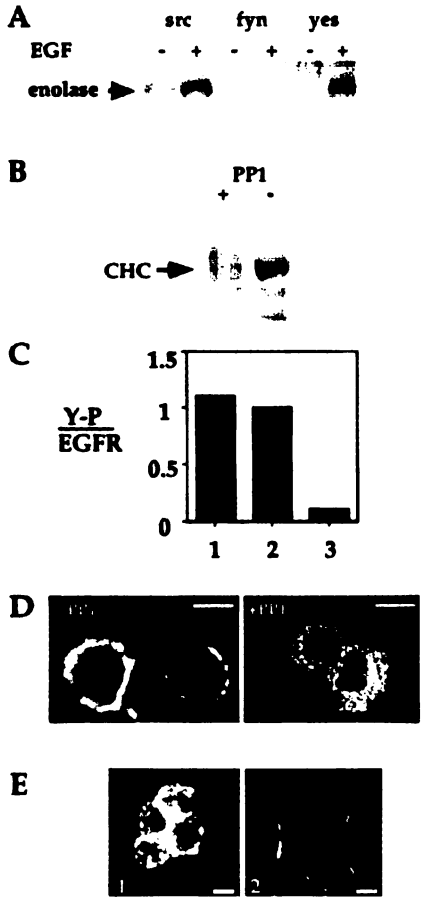

Figure 4. SRC Family Kinases Are Activated following EGF Stimulation, and Inhibition Affects CHC Phosphorylation, Clathrin Redistribution, and EGF Uptake

(A) A431 cells were serum starved and incubated with EGF or mock treated at 4°C. After warming to 37°C for either 0 or 5 min, the SRC family kinases pp59^{fyn} (fyn), pp60$^{c\text{-}src}$ (src), and pp62^{yes} (yes) were immunoprecipitated from cell lysates. Immunoprecipitates were incubated with γ-^{32}P ATP and acid-denatured enolase, a substrate for kinase activity. Enolase phosphorylation was detected following SDS-PAGE and autoradiography.

(B) A431 cells were cultured and stimulated with EGF for 5 min at 37°C, as described in (A). Prior to EGF stimulation cells were incubated in presence or absence of 1 μM PP1 for 15 min. Lysates were prepared and clathrin immunoprecipitated using the mAb X22, and phosphorylation was detected by immunoblotting with the mAb 4G10.

(C) A431 cells were cultured and stimulated with EGF for 5 min at 37°C, as described in (A), and lysates prepared. Prior to EGF stimulation, cells were incubated (1) in the absence of inhibitor, (2) with 1 μM PP1 for 15 min, or (3) with 50 μM genistein, and inhibitors were present during stimulation. EGFR was immunoprecipitated using antibody 986 and immunoblotted to detect EGFR with antibody 986 or phosphotyrosine (Y-P) with antibody 4G10. The blotting signals were quantified using NIH Image software and the ratios plotted to determine the degree of receptor phosphorylation normalized to the amount of EGFR immunoprecipitated.

(D) A431 cells were serum starved and incubated in the presence or absence of 1 μM PP1 for 15 min, prior to treatment with EGF for 1 hr at 4°C. After warming to 37°C for 20 min, cells were processed for immunofluorescent staining with mAb X22 and visualized by confocal microscopy to determine the localization of clathrin. Bar, 10 μm.

(E) A431 cells were serum starved and incubated with (1) 0.1% DMSO or (2) 1 μM PP1 for 15 min prior to treatment with 20 ng/ml EGF conjugated to Texas red at 4°C. Cells were then warmed to 37°C for 5 min, after which the uninternalized cell surface ligand was stripped by an acid wash, and cells were fixed in 4% paraformaldehyde. The distribution of Texas red–labeled EGF was visualized by fluorescence microscopy. Bar, 10 μm.

expressing the constructs at a low level, were isolated. Low-level expression was favored intentionally by our transfection strategy, so that expression of the mutant CHC would not result in dominant-negative inhibition of clathrin function. Morphological analysis of transfectants expressing the wild-type or mutant CHC, by staining with anti-T7 mAb, revealed a very weak but normal punctate clathrin staining pattern for the transfected CHCs (data not shown), indicating that they were incorporated into endogenous clathrin-coated vesicles. Transfectants were stimulated with EGF, and the epitope-tagged Y1477F CHC and wild-type CHC were immunoprecipitated with anti-T7 mAb. Y1477F CHC was not detectably tyrosine phosphorylated compared to transfected wild-type CHC in response to EGF stimulation (Figure 6C). In some experiments, a background level of tyrosine phosphorylation of Y1477F CHC was detectable, at a very low level, which might be due to infrequent trimerization of the mutant CHC with endogenous CHC. In our experience with expression of transfected clathrin hub molecules, transfected CHCs do not seem to trimerize at significant levels with endogenous CHCs (Liu et al., 1998). We therefore conclude from the mutant data that the major CHC site phosphorylated during ligand-induced endocytosis of EGF is tyrosine 1477, the target of pp60$^{c\text{-}src}$ kinase.

Loss of pp60$^{c\text{-}src}$ Activity Prevents Clathrin Redistribution and Delays EGF Endocytosis

To determine whether pp60$^{c\text{-}src}$ kinase phosphorylation of CHC, in response to EGF, is related to peripheral recruitment of clathrin, we analyzed EGF-mediated clathrin redistribution in mouse cell lines lacking expression of pp60$^{c\text{-}src}$ kinase (Figure 7A). Recruitment was measured biochemically in these cells. Levels of clathrin associated with the plasma membrane fraction, after EGF stimulation, were determined by quantitative immunoblotting. In the cell line 1T, produced by SV40T transformation of fibroblasts from an embryo lacking pp60$^{c\text{-}src}$, there was no significant clathrin recruitment in response to EGF, compared to the 8T line transformed by SV40 T antigen from wild-type embryo fibroblasts. Interestingly, 3T3-like wild-type mouse fibroblast lines, produced without SV40 transformation, did not display measurable clathrin recruitment in response to EGF (data not shown), even though they can phosphorylate clathrin upon EGF treatment. This indicates that CHC

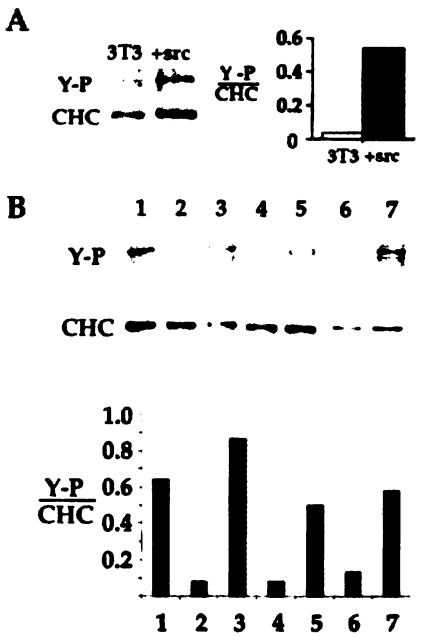

Figure 5. CHC Is Phosphorylated by pp60$^{c\text{-}src}$ In Vivo

(A) Clathrin was immunoprecipitated from 3T3 murine fibroblasts expressing normal and elevated (+src) levels of pp60$^{c\text{-}src}$ (Lin et al., 1995). Immunoprecipitates were immunoblotted for clathrin heavy chain (CHC) and tyrosine phosphorylation (Y-P) using the mAbs TD.1 and 4G10, respectively (stripping the blot between using different antibody probes) (left). The blotting signals were quantified using NIH Image software and the ratios plotted to determine the degree of CHC phosphorylation normalized to the amount of CHC immunoprecipitated (right).

(B) Cell lines produced from mice lacking expression of different SRC family kinases were cultured and stimulated with EGF for 20 min at 37°C, as described for A431 cells. Cell lysates were prepared and clathrin immunoprecipitated using mAb X22. Immunoprecipitates were immunoblotted for CHC and Y-P and the ratio of the signals quantified, as in (A). Cell lines tested were (1) +src 3T3 transfectant, shown in (A); (2) SV40T-transformed fibroblasts from mice lacking both pp60$^{c\text{-}src}$ and pp62^{yes} (SY1T); (3) 3T3-like fibroblasts from mice lacking both pp62^{yes} and pp59^{fyn} (FY1S); (4) 3T3-like fibroblasts from mice lacking pp60$^{c\text{-}src}$ (1S); (5) 3T3-like fibroblasts from wild-type mice (8S); (6) SV40T-transformed fibroblasts from mice lacking pp60$^{c\text{-}src}$ (1T); and (7) SV40T-transformed fibroblasts from wild-type mice (8T).

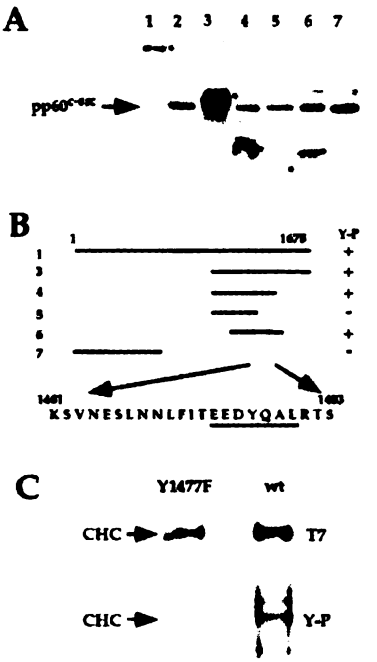

Figure 6. Tyrosine 1477 of CHC Is a Substrate for pp60$^{c\text{-}src}$ In Vitro and In Vivo

(A) Clathrin purified from bovine brains or bacterially expressed fragments of bovine clathrin were incubated with purified recombinant pp60$^{c\text{-}src}$ and γ-^{32}P ATP. Phosphorylation was analyzed by SDS-PAGE and autoradiography. Samples are as follows: purified bovine clathrin (lane 1), pp60$^{c\text{-}src}$ alone (lane 2), bovine CHC amino acids 1074–1675 (lane 3), bovine CHC amino acids 1074–1483 (lane 4), bovine CHC amino acids 1074–1460 (lane 5), bovine CHC amino acids 1213–1522 (lane 6), and bovine CHC amino acids 1–545 (lane 7). Note that pp60$^{c\text{-}src}$ was present in all samples, and its degree of autophosphorylation was variable. The asterisk to the right of the relevant lane denotes the migration position of CHC and bacterially expressed clathrin fragments, as determined by amido black staining (data not shown) of the nitrocellulose. Note that only phosphorylated clathrin and fragments and phosphorylated pp60$^{c\text{-}src}$ are visible.

(B) A diagrammatic representation of CHC and the fragments tested and their ability to become phosphorylated by pp60$^{c\text{-}src}$. The underlined sequence denotes the CHC sequence homologous to the SRC consensus sequence.

(C) Stably transfected A431 cells expressing either T7 epitope-tagged wild-type (wt) CHC or T7 epitope-tagged CHC containing a single point mutation (Y1477F) were serum starved and incubated for 1 hr with EGF at 4°C. After warming to 37°C for 20 min, lysates were prepared and the T7 epitope-tagged CHCs immunoprecipitated using a mAb recognizing the T7 epitope. Immunoprecipitates were immunoblotted for the T7 epitope (T7) to detect the CHC (top panel) and for phosphotyrosine (Y-P) (bottom panel). Blots were stripped between exposure to the different antibody probes.

phosphorylation is necessary but not sufficient for EGF-mediated clathrin recruitment and that other factors are involved.

The lack of clathrin recruitment in the pp60$^{c\text{-}src}$-minus 1T cells relative to the wild-type 8T cells reproduces the effect of PP1 inhibitor on A431 cells, relating pp60$^{c\text{-}src}$-mediated phosphorylation to clathrin redistribution. To determine whether the lack of pp60$^{c\text{-}src}$ also caused a delay in EGF endocytosis, as seen with PP1 treatment of A431 cells, the 1T and 8T cells were exposed to either ^{125}I-EGF or Oregon green–labeled EGF, and uptake was assessed. Kinetic analysis of internalization of ^{125}I-EGF showed that the rate of uptake by the pp60$^{c\text{-}src}$-minus 1T cells was slowed relative to the rate for 8T cells, with the rates equalizing after 1 min of EGF exposure (Figure 7B). Internalization of the Oregon green EGF showed little detectable endocytosis up to 3 min (Figure 7C) in

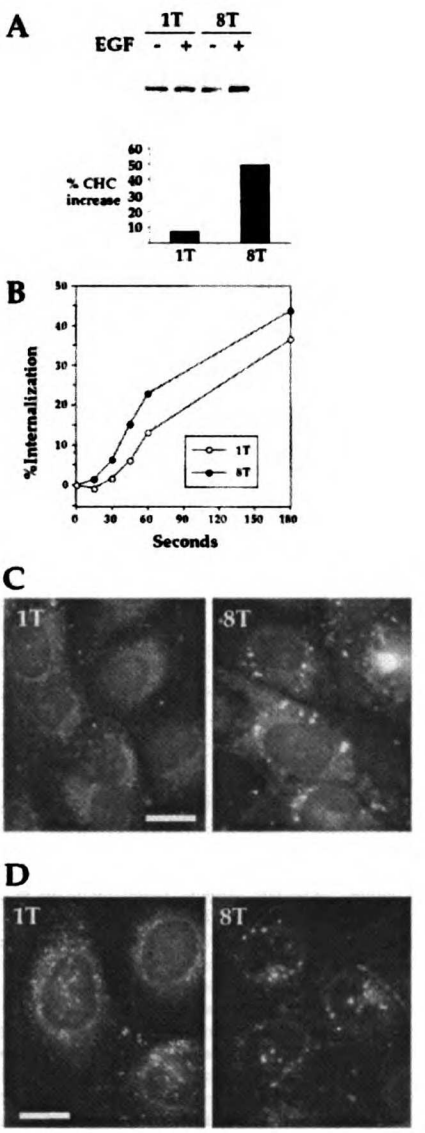

Figure 7. Genetic Deletion of pp60$^{c\text{-}src}$ Affects EGF-Induced Clathrin Redistribution and Delays Uptake

(A) SV40T-transformed fibroblasts from mice lacking pp60$^{c\text{-}src}$ (1T) and from wild-type mice (8T) were serum starved, followed by EGF treatment or mock treatment at 4°C. After warming for 20 min, cells were homogenized and the plasma membrane fraction isolated by differential centrifugation. This fraction was then assayed for total protein, and equivalent samples from each culture were analyzed for the presence of clathrin by immunoblotting with mAb TD.1 (top). Blotting signals were quantified using NIH image software, and the percent increase of CHC detected in the plasma membrane fraction in the presence of EGF (bottom) was calculated for each cell line as follows (CHC with EGF)−(CHC without EGF)/(CHC without EGF).

(B) SV40T-transformed fibroblasts from mice lacking pp60$^{c\text{-}src}$ (1T) and from wild-type mice (8T) were serum starved and exposed to ^{125}I-EGF at 4°C. Cells were warmed for the indicated time, then chilled and the percent of internalized ^{125}I-EGF determined. The data shown are typical of four independent experiments and are generated from duplicate samples for which the error bars were too small to plot.

(C and D) SV40T-transformed fibroblasts from mice lacking pp60$^{c\text{-}src}$ (1T) and from wild-type mice (8T) were serum starved and exposed to EGF conjugated to Oregon green at 4°C. Cells were warmed for 3 min (C) or 20 min (D), then chilled, acid stripped to remove surface-bound EGF, and viewed for fluorescence. Bars are 10 μm and apply to all panels.

1T cells, while internalization was readily visible over the same period for 8T cells. Oregon green EGF uptake was detectable in 1T cells from 5–20 min, but EGF accumulated more peripherally in the 1T cells than the 8T cells, suggesting a delay in intracellular targeting as well as in endocytosis (Figure 7D). This delay in the early stages of EGF-induced endocytosis for cells lacking pp60$^{c\text{-}src}$ corresponded to the same time course of the delay observed for EGF-induced endocytosis by PP1-treated A431 cells (Figure 4E).

Discussion

We report that EGFR signaling, in response to EGF binding, stimulates SRC kinase activity which is required for CHC phosphorylation and clathrin redistribution to the cell periphery, indicating that downstream receptor signaling has a direct effect upon the endocytic machinery. Specific inhibition or genetic deletion of SRC family kinase activity delays endocytosis of EGF. These results suggest that EGFR signaling can regulate clathrin-mediated membrane traffic and thereby defines a novel pathway in ligand-induced endocytosis for this receptor.

Regulation of Endocytosis by CHC Modification and Clathrin Recruitment

Ligand-induced endocytosis represents the extreme situation in which clathrin-mediated endocytosis is regulated, since receptor uptake occurs only when ligand has bound. This process is characteristic of some signaling receptors and although each receptor has unique aspects to its uptake, there seem to be some shared regulatory features, such as exposure of adaptor-binding motifs by receptor signaling (Schmid, 1997). A second one, established here, is a signaling-dependent effect on clathrin. This has already been described for endocytosis of the β2-adrenergic G protein–coupled receptor, which, when ligand-activated, binds β-arrestin, a protein that interacts directly with clathrin (Ferguson et al., 1996; Freedman and Lefkowitz, 1996; Goodman et al., 1996). Here we demonstrate that ligand activation of EGFR, a receptor tyrosine kinase, has a related mechanism, since it influences clathrin recruitment and causes direct modification of clathrin itself. Inhibition of EGF-induced clathrin phosphorylation has several effects, suggesting that this modification may influence EGF endocytosis at more than one step. Early stages of ligand-gated EGF uptake are delayed in the absence of CHC phosphorylation, due to an initial slowed rate of

uptake. In addition, EGF is not as efficiently concentrated in perinuclear vesicles after 20 min of uptake by pp60$^{c\text{-}src}$-minus cells unable to phosphorylate clathrin. Furthermore, the dramatic peripheral clathrin recruitment observed after 10 min of sustained EGF treatment is inhibited when CHC phosphorylation is inhibited. These observations indicate that clathrin phosphorylation has an immediate effect on enhancing EGF endocytosis and a subsequent effect on clathrin accumulation in the periphery and on intracellular targeting of EGF. The slowed intracellular targeting could reflect initial delays in endocytosis, but it could also reflect an alteration in endosomal sorting of EGF. In an earlier study (Felder et al., 1990), EGF receptors mutant in signaling were observed to have a short-term slowed rate of endocytosis, similar to what we observe in pp60$^{c\text{-}src}$-minus cells, and a defect in sorting from multivesicular bodies. Both of these effects could be explained by lack of pp60$^{c\text{-}src}$ phosphorylation of CHC, based on the findings reported here. Clathrin phosphorylation is in a region of the molecule that controls assembly, so immediate phosphorylation of local pools of clathrin upon EGF signaling could influence local coated pit formation. In addition, sustained treatment with EGF causes accumulation of clathrin in cell periphery dependent on CHC phosphorylation, suggesting a sustained effect on clathrin dynamics, which could have an effect on receptor traffic in the endosome.

Controlling clathrin phosphorylation and recruitment could possibly play a role in other instances of ligand-induced endocytosis and may, under certain circumstances, influence constitutive endocytosis. For example, tyrosine kinase inhibitors have been shown to reduce uptake of the asialoglycoprotein receptor (Fallon et al., 1994). Some signaling receptors, like FcεR1, do not induce clathrin recruitment and therefore must rely on other regulatory pathways (Santini and Keen, 1996). However, clathrin recruitment to the plasma membrane has been observed following insulin, nerve growth factor (NGF), and carbachol treatment of cells (Connolly et al., 1981; Gelsow and Childs, 1985; Corvera, 1990). In addition, expression of the Nef protein of human immunodeficiency virus, which causes increased internalization of CD4 and which binds the SRC family kinase pp56^{lck} (Baur et al., 1997), results in an increase in the number of coated pits at the plasma membrane (Foti et al., 1997). These observations suggest these instances of ligand-induced clathrin recruitment may also be linked to CHC phosphorylation. In fact, NGF activation of its receptor causes tyrosine phosphorylation of CHC and redistribution of clathrin to the cell periphery, similar to EGF treatment (E. C. B. et al., unpublished observations).

Regulation of Clathrin Assembly and Endocytosis by SRC Family Kinases

We have identified tyrosine 1477 as the site of pp60$^{c\text{-}src}$-mediated CHC phosphorylation during ligand-induced endocytosis of EGFR. Tyrosine 1477 is conserved in the three mammalian CHC sequences determined and in the CHC of *D. melanogaster*, *D. discoidum*, and *S. cerevisiae* (Liu et al., 1995). Our structural analysis of the light chain–binding region of CHC, which is in progress (J. A. Ybe et al., unpublished data), confirms that tyrosine 1477 is solvent exposed and located near the predicted light chain–binding site. The clathrin light chain subunits negatively regulate spontaneous clathrin assembly, so that cellular clathrin assembly is adaptor dependent (Ungewickell and Ungewickell, 1991; Ybe et al., 1998). It is possible that tyrosine phosphorylation of residue 1477 causes an increase in clathrin assembly by directly affecting CHC interactions or that it affects assembly indirectly by negating the inhibitory effects that light chains have on assembly. Alternatively, tyrosine phosphorylation of CHC could recruit a protein that might enhance assembly or enhance transport of clathrin to the cell periphery. Whether clathrin recruitment directly influences EGF uptake by increasing the local concentration of clathrin and promoting coated pit formation or whether the regulatory mechanism is more complex, possibly relating to changing the intracellular dynamics of clathrin, will be the focus of future studies. It should be pointed out that the phosphorylation and recruitment of clathrin represent only a subset of the molecular requirements for EGF endocytosis. In our analysis of mouse fibroblasts, CHC phosphorylation was found to be necessary and sufficient for clathrin recruitment in some cell lines (SV40 transformed) but not sufficient in others (3T3-like), implicating additional factors.

The work reported in this study suggests that pp60$^{c\text{-}src}$ is the kinase responsible for CHC tyrosine phosphorylation, at least in murine fibroblasts. A role for pp60$^{c\text{-}src}$ in EGFR endocytosis was previously indicated by the effect of its overexpression, which increased the internalization rate of EGFR (Ware et al., 1997). Our findings suggest the mechanism by which the overexpressed pp60$^{c\text{-}src}$ regulates enhanced endocytosis of EGFR could be its phosphorylation of CHC. In other situations, different SRC family kinase members may be responsible for modification of clathrin. Different tissues express different SRC family kinases, and clathrin-coated vesicles contain subsets of those kinases. Electron microscopy studies of platelets have shown that the SRC family kinases pp59^{fyn}, pp56^{lyn}, pp56^{fyn}, and pp56^{lck}, but not pp60^{src}, colocalize with clathrin to intracellular vesicles delivering material to the platelet granule (Stenberg et al., 1997). We have observed enrichment of pp62^{yes} in bovine brain coated vesicles (A. W. and F. M. B., unpublished observations). In the case of a pathway as important as regulated endocytosis, it would not be surprising if, in different tissues, different SRC family kinases could mediate clathrin phosphorylation. In fact, this is likely because the phenotype of mice lacking pp60$^{c\text{-}src}$ would be more dramatic if ligand-induced uptake of tyrosine kinase receptors were globally impaired. As with other pp60$^{c\text{-}src}$ functions in these mice, it is presumed that other SRC family kinases can compensate for pp60$^{c\text{-}src}$ defects in this receptor signaling pathway (Lowell and Soriano, 1996).

Receptor tyrosine kinases are still able to signal when they are internalized into intracellular organelles (Di Guglielmo et al., 1994; Baass et al., 1995; Grimes et al., 1996; Riccio et al., 1997). The purpose of a receptor tyrosine kinase regulating endocytosis, upon ligand stimulation, may therefore be to direct it to an intracellular location

from where it initiates additional signaling pathways. Our finding that ligand-induced endocytosis of EGFR results in induction of SRC family kinase phosphorylation of clathrin and clathrin redistribution suggests that EGFR and other receptor tyrosine kinases actively determine the subcellular location from which they carry out their physiological functions by regulating clathrin-mediated membrane traffic.

Experimental Procedures

Antibodies and Inhibitors

Antibodies to clathrin, used in this study, were mAb X22 (Brodsky, 1985) and mAb TD.1 (Näthke et al., 1992). Antibodies used that recognize SRC family kinases were 327, anti-pp60^{src} from J. M. Bishop, University of California, San Francisco; 217, anti-pp62^{yes} from J. Brugge, Ariad Pharmaceuticals; FYN-3, anti-pp59^{fyn} (Santa Cruz Biotechnology); and 4G10 anti-phosphotyrosine (Upstate Biotechnology Incorporated). Antibody 986 that recognizes EGFR was obtained from A. Sorkin (University of Colorado). For immunoblotting, secondary antibodies conjugated to horseradish peroxidase were from BioRad, and for immunofluorescence, secondary antibodies conjugated to either fluorescein or rhodamine were from Jackson Laboratories. Kinase inhibitors herbimycin A, staurosporin, genistein, H7 (Calbiochem), and PP1 (Biomol) were dissolved in DMSO and diluted into culture medium at the time of experimentation such that the final concentration of DMSO did not exceed 0.1%.

Cell Lines, EGF Treatment, and Immunoprecipitation

A431 cells (American Type Culture Collection) were cultured in Dulbecco's modified Eagle's medium (DMEM) (GIBCO BRL) containing 10% fetal calf serum (FCS) (GIBCO BRL) and grown to approximately 80% confluency prior to experimentation. For EGF treatment, A431 cells were serum starved in DMEM containing 0.1% FCS for 16 hr, chilled to 4°C, and incubated with EGF at a final concentration of 250 ng/ml for 1 hr. EGFR endocytosis was initiated by warming the cells to 37°C by flotation on a 37°C water bath. Two minutes prior to warming, sodium orthovanadate was added to a final concentration of 10 μM. After warming, cells were transferred to ice for 2 min, then cell lysate was prepared and clathrin immunoprecipitated using mAb X22 prebound to protein G-Sepharose (Pharmacia), as described previously (Wilde and Brodsky, 1996). Immunoprecipitates were analyzed by sodium dodecyl sulfate polyacrylamide (10%) gel electrophoresis (SDS-PAGE) and immunoblotting (Wilde and Brodsky, 1996). Immunoblots were quantitated from appropriate exposures using the NIH image software.

B82 mouse L cells expressing EGFR mutants were a gift from G. N. Gill, University of California, San Diego, and were cultured in DMEM containing 10% dialyzed FCS and 500 nM methotrexate (Chen et al., 1987, 1989).

3T3 cells overexpressing pp60$^{c\text{-}src}$ (NIH[pM5Mcsrc/focR/EPJD4) were from D. Shalloway, Cornell University (Lin et al., 1995). Lines 1S and 1T were from a mouse embryo with a homozygous deletion of pp60$^{c\text{-}src}$, and 8S and 8T were produced from a wild-type embryo. Lines 1T, 8T (Thomas et al., 1991), and the line SY1T from mice lacking both pp60$^{c\text{-}src}$ and pp62^{yes} (Stein et al., 1994) were immortalized by transfection with SV40 large T antigen. 1S, 8S, and the line FY1S lacking both pp62^{yes} and pp59^{fyn} were 3T3-like fibroblast cultures.

Indirect Immunofluorescence

Cells were cultured on glass coverslips, stimulated as described above, and fixed with paraformaldehyde for antibody staining, as described (Wong and Brodsky, 1992). Cells were viewed using a Biorad MRC 1000 confocal microscope, and a single section 75% from the top of the cell is shown, except where specified otherwise. Images were processed using Adobe Photoshop software.

Kinase Assays

SRC family kinases were immunoprecipitated and assayed for their ability to phosphorylate acid-denatured enolase to measure activation (Feder and Bishop, 1990), as follows. A431 cells (approximately 80% confluency) were stimulated with EGF stimulation, as above, and lysed in 20 mM Tris (pH 7.4), 137 mM NaCl, 10% glycerol, 1% NP40, 2 mM EDTA, 1 mg/ml pepstatin A, aprotinin and leupeptin, and 0.1 mM PMSF. From this lysate, pp60$^{c\text{-}src}$, pp59^{fyn}, and pp62^{yes} were immunoprecipitated using the antibodies 327, fyn3, and 2.7, respectively. Immunoprecipitates were washed three times with lysis buffer and twice with the kinase reaction buffer, 20 mM HEPES (pH 7.0), 10 mM $MgCl_2$, 0.5% Triton X-100, with 10 mM $MnCl_2$ and 0.1 mM sodium pervanadate added immediately prior to use, followed by resuspension in 30 μl prepared substrate (denatured enolase) with the addition of unlabeled ATP to a final concentration of 1 μM and 0.5 μl of γ-^{32}P ATP (>3000 Ci/mmol, 10 mCi/ml) (NEN). The mixture was incubated at 30°C for 15 min and the reaction stopped by the addition of 10 μl of SDS-PAGE sample buffer and boiling for 5 min. Substrate was prepared by incubating 50 μl of 1 mg/ml enolase with 50 μl of 50 mM sodium acetate at 30°C for 10 min, followed by neutralization with 60 μl 1 M Tris (pH 8.8) and 840 μl of kinase buffer. Enolase phosphorylation was analyzed by SDS-PAGE and autoradiography using BioMax film (Kodak).

To assay for EGFR kinase activity, EGFR was immunoprecipitated from A431 cells using the antibody 986 prebound to protein G-Sepharose beads, then washed three times in immunoprecipitation buffer (20 mM Tris [pH 7.4], 137 mM NaCl, 10% glycerol, 1% NP40, 2 mM EDTA, 1 mg/ml pepstatin A, aprotinin and leupeptin, and 0.1 mM PMSF), followed by three washes in kinase assay buffer (20 mM HEPES [pH 7.0], 10 mM $MgCl_2$, 0.5% Triton X-100, with 10 mM $MnCl_2$ and 0.1 mM sodium pervanadate added immediately prior to use). The immunoprecipitate was then resuspended in 100 μl of kinase assay buffer containing 1 ng EGF and 5 μg of recombinant protein, either CHC hub domain (Liu et al., 1995) or CT-GST, a fusion protein between glutathione-S-transferase and the regulatory domain of EGFR (Nesterov et al., 1995).

In Vitro Phosphorylation of CHC

Recombinant pp60$^{c\text{-}src}$ was from D. O. Morgan (University of California, San Francisco) (Morgan et al., 1991). Thirty nanograms of pp60$^{c\text{-}src}$ was incubated with 5 μg of clathrin fragments (prepared as described by Liu et al. [1995]) in 10 mM $MgCl_2$ and 10 mM $MnCl_2$, 0.5% Triton X-100, and 20 mM Tris (pH 7.4) for 15 min, RT. The reaction was stopped by addition of EDTA (final concentration 2 mM) and SDS-PAGE sample buffer, then boiled for 5 min. The extent of tyrosine phosphorylation was analyzed by immunoblotting using mAb 4G10.

Construction of CHC Point Mutant

The cDNA encoding the human clathrin heavy chain (KIAA 0034) was from T. Nagase, Kazusa DNA Research Institute Foundation, Japan (Nomura et al., 1994). A single point mutation at position 4429 (T to A) in the human cDNA was made using the Stratagene QuikChange site-directed mutagenesis kit. Wild-type and mutant cDNAs were first ligated into the pET23a vector (Novagen), 3′ of the T7 epitope tag before being cloned into the eukaryotic expression vector pCINeo (Promega). Plasmids were transfected into A431 cells by using a calcium phosphate transfection protocol (Liu et al., 1996) and selected in 500 μg/ml Geneticin (GIBCO BRL). T7 epitope-tagged Y1477F and wild-type CHC were detected using a mAb against the T7 epitope (Novagen).

Plasma Membrane Isolation

The plasma membrane fraction of mouse fibroblasts was isolated by differential centrifugation following dounce homogenization of EGF-stimulated cells in 20 mM MES (pH 6.5), 1 mM EDTA, and 255 mM sucrose (Corvera, 1990). Membranes pelleted by 15 min centrifugation at 12,000 g, from the supernatant of a 10 min spin at 3000 g, were shown to contain all the cell surface biotinylated protein from a test sample to confirm the presence of plasma membrane. These membranes were solubilized in 0.5 M Tris (pH 8.0) 1% NP40 and analyzed for associated clathrin by immunoblotting.

EGF Internalization Assays

A431 cells cultured on glass coverslips were serum starved for 2 hr, then incubated with 1 μM PP1 for 15 min at 37°C. The cells were then chilled to 4°C and incubated with 20 ng/ml of Texas red–labeled

EGF (Molecular Probes) for 1 hr. Cells were warmed to 37°C for 5 min, transferred to ice, and stripped of cell surface–bound ligand by incubation in ice-cold 0.2 M acetic acid (pH 2.5) containing 0.5 M NaCl for 5 min. Cells were fixed in 4% paraformaldehyde and viewed using a Zeiss Axiophot microscope. The 1T and 8T cell lines were grown on coverslips coated with 20 μg/ml type IV collagen (Sigma) and 100 μg/ml poly-D-lysine and cultured for 16 hr in starvation medium (DMEM with 0.1% fetal calf serum, 20 mM HEPES). After chilling to 4°C, cells were exposed to mouse submaxillary gland EGF conjugated to Oregon green 514 (Molecular Probes) at a concentration of 1 ng/ml, still at 4°C in starvation medium, for 1 hr. Cells were then washed in starvation medium and fresh starvation medium added at 4°C. Cells were then transferred to a 37°C water bath and at designated time points put back on ice and acid stripped, as above. Cells were then fixed and viewed with a Zeiss Axiophot microscope. For ^{125}I-EGF uptake experiments, 1T and 8T cells were serum starved overnight, as above, and incubated at 4°C with ^{125}I-EGF (mouse submaxillary gland [ICN]) at 0.032 ng/ml. To establish background binding, unlabeled EGF (Boehinger Mannheim) was added at 1 μg/ml to two samples. Samples were then washed with cold starvation medium and transferred to a 37°C water bath for designated times of internalization, then the cells were immediately chilled, the supernatant removed, and cells were acid stripped. The cells were solubilized in 1% NP-40, 150 mM NaCl, 50 mM Tris (pH 7.4), and the cell lysate (X), the acid strip (Y), and the supernatant after binding (Z) were counted for ^{125}I-EGF. The percent internalization was calculated by X/(X+Y+Z). Background binding was not subtracted, as it was typically <2% of the total counts bound. However, stripping efficiency was taken into account by measuring the percent count bounds after 0 min of warming and stripping. This number, typically 10%–15% of the total counts bound, was subtracted from the percent internalized before plotting, so that internalization at time 0 was 0%.

Acknowledgments

We are grateful to D. O. Morgan for purified recombinant pp60$^{c\text{-}src}$, G. N. Gill for transfectants expressing wild-type and mutant EGFR and the plasmid encoding the recombinant fusion protein CT-GST, D. Shalloway for the 3T3 transfectant overexpressing pp60$^{c\text{-}src}$, and T. Nagase for the human CHC cDNA. We also thank A. Sorkin, J. M. Bishop, and J. Brugge for providing antibodies and A. Sorkin, C. Lowell, F. Luton, and D. Slowiejko for helpful discussion. This work was supported by National Institutes of Health grants GM38093 and GM57657 to F. M. B. and a postdoctoral fellowship from the American Heart Association, California affiliate to A. W. We thank M. Von Zastrow and the Carnegie Institution of Washington and Y. Zheng for facilitating completion of this work.

Received May 26, 1998; revised January 26, 1999.

References

Baass, P.C., Di Guglielmo, G.M., Authier, F., Posner, B.I., and Bergeron, J.J.M. (1995). Compartmentalized signal transduction by receptor tyrosine kinases. Trends Cell Biol. *5*, 465–470.

Baur, A.S., Sass, G., Laffert, B., Willbold, D., Cheng-Mayer, C., and Peterlin, B.M. (1997). The N terminus of Nef from HIV-1/SIV associates with a protein complex containing Lck and a serine kinase. Immunity *6*, 283–291.

Blank, G.S., and Brodsky, F.M. (1987). Clathrin assembly involves a light chain-binding region. J. Cell Biol. *105*, 2011–2019.

Brodsky, F.M. (1985). Clathrin structure characterized with monoclonal antibodies. I. analysis of multiple antigenic sites. J. Cell Biol. *101*, 2047–2054.

Brodsky, F.M. (1988). Living with clathrin: its role in intracellular membrane traffic. Science *242*, 1396–1402.

Cadena, D.L., Chan, C., and Gill, G.N. (1994). The intracellular tyrosine kinase domain of the epidermal growth factor receptor undergoes a conformational change upon autophosphorylation. J. Biol. Chem. *269*, 1–6.

Chen, W.S., Lazar, C.S., Poenie, M., Tsien, R.Y., Gill, G.N., and Rosenfeld, M.G. (1987). Requirement for intrinsic protein tyrosine kinase activity in the immediate and late actions of the EGF receptor. Nature *328*, 820–823.

Chen, W.S., Lazar, C.S., Lund, K.A., Welsh, J.B., Chang, C.-P., Walton, G.M., Der, C.J., Wiley, H.S., and Gill, G.N. (1989). Functional independence of the epidermal growth factor receptor from a domain required for ligand-induced internalization and calcium regulation. Cell *59*, 33–43.

Connolly, J.L., Green, S.A., and Greene, L.A. (1981). Pit formation and rapid changes in surface morphology of sympathetic neurons in response to nerve growth factor. J. Cell Biol. *90*, 176–180.

Connolly, J.L., Green, S.A., and Greene, L.A. (1984). Comparison of rapid changes in surface morphology and coated pit formation of PC12 cells in response to nerve growth factor, epidermal growth factor, and dibutyryl cyclic AMP. J. Cell Biol. *98*, 457–465.

Corvera, S. (1990). Insulin stimulates the assembly of cytosolic clathrin onto adipocyte plasma membranes. J. Biol. Chem. *265*, 2413–2416.

Di Guglielmo, G.M., Baass, P.C., Ou, W.-J., Posner, B.I., and Bergeron, J.J.M. (1994). Compartmentalizaton of SHC, GRB2 and mSOS, and hyperphosphorylaton of Raf-1 by EGF but not insulin in liver parenchyma. EMBO J. *13*, 4269–4277.

Fallon, R.J., Danaher, M., Saylors, R.L., and Saxena, A. (1994). Defective asialoglycoprotein receptor endocytosis mediated by tyrosine kinase inhibitors. J. Biol. Chem. *269*, 11011–11017.

Feder, D., and Bishop, J.M. (1990). Purification and enzymatic characterization of pp60$^{c\text{-}src}$ from human platelets. J. Biol. Chem. *265*, 8205–8211.

Felder, D., Miller, K., Moehren, G., Ullrich, A., Schelssinger, J., and Hopkins, C.R. (1990). Kinase activity controls the sorting of epidermal growth factor receptor with the multivesicular body. Cell *61*, 623–634.

Ferguson, S.S., Barak, L.S., Zhang, J., and Caron, M.G. (1996). G-protein-coupled receptor regulation: role of G-protein-coupled receptor kinases and arrestins. Can. J. Physiol. Pharmacol. *74*, 1095–1110.

Foti, M., Mangasarian, A., Piguet, V., Lew, D.P., Krause, K.-H., Trono, D., and Carpentier, J.-L. (1997). Nef-mediated clathrin-coated pit formation. J. Cell Biol. *139*, 37–47.

Freedman, N.J., and Lefkowitz, R.J. (1996). Desensitization of G protein-coupled receptors. Recent Prog. Horm. Res. *51*, 352–353.

Gelsow, M.J., and Childs, J. (1985). Cholinergic stimulation of chromaffin cells induces rapid coating of the plasma membrane. Eur. J. Cell Biol. *38*, 51–56.

Goodman, J., Oscar B., Krupnick, J.G., Santini, F., Gurevich, V.V., Penn, R.B., Gagnon, A.W., Keen, J.H., and Benovic, J.L. (1996). β-arrestin acts as a clathrin adaptor in endocytosis of the β2-adrenergic receptor. Nature *383*, 447–450.

Grimes, M.L., Zhou, J., Beattie, E.C., Yuen, E.C., Hall, D.E., Valletta, J.S., Topp, K.S., LaVail, J.H., Bunnett, N.W., and Mobley, W.C. (1996). Endocytosis of activated TrkA: evidence that nerve growth factor induces formation of signaling endosomes. J. Neurosci. *16*, 7950–7964.

Hanke, J.H., Gardner, J.P., Dow, R.L., Changelian, P.S., Brissette, W.H., Weringer, E.J., Pollok, B.A., and Connelly, P.A. (1996). Discovery of a novel, potent, and Src family-selective tyrosine kinase inhibitor. J. Biol. Chem. *271*, 695–701.

Holen, I., Gordon, P.B., Fengsrud, M., Berg, T.O., and Seglen, P.O. (1995). Inhibition of autophagy and multiple steps in asialoglycoprotein endocytosis by inhibitors of tyrosine kinases (tyrphostins). J. Biol. Chem. *270*, 12823–12831.

Lamaze, C., and Schmid, S.L. (1995). Recruitment of epidermal growth factor receptors into coated pits requires their activated tyrosine kinase. J. Cell Biol. *129*, 45–54.

Lin, P.-H., Shenoy, S., Galitski, T., and Shalloway, D. (1995). Transformation of mouse cells by wild-type mouse c-Src. Oncogene *10*, 401–405.

Liu, S.-H., Wong, M.L., Craik, C.S., and Brodsky, F.M. (1995). Regulation of clathrin assembly and trimerization defined using recombinant triskelion hubs. Cell *83*, 257–267.

Liu, S.-H., Marks, M.S., and Brodsky, F.M. (1998). A dominant negative clathrin mutant differentially affects trafficking of molecules with distinct sorting motifs in the class II MHC pathway. J. Cell Biol. *140*, 1023–1037.

Lowell, C.A., and Soriano, P. (1996). Knockouts of Src-family kinases: stiff bones, wimpy T cells, and bad memories. Genes Dev. *10*, 1845–1857.

Lutz-Freyermuth, C., Query, C.C., and Keene, J.D. (1990). Quantitative determination that one of two potential RNA-binding domains of the A protein component of the U1 small nuclear ribonucleoprotein complex binds with high affinity to stem-loop II of U1 RNA. Proc. Natl. Acad. Sci. USA *87*, 6393–6397.

Martin-Perez, J., Bar-Zvi, D., Branton, D., and Erikson, R.L. (1989). Transformation by Rous sarcoma virus induces clathrin heavy chain phosphorylation. J. Cell Biol. *109*, 577–584.

Morgan, D.O., Kaplan, J.M., Bishop, J.M., and Varmus, H.E. (1991). Production of $p60^{c\text{-}src}$ by baculovirus expression and immunoaffinity purification. Methods Enzymol. *200*, 645–660.

Náthke, I.S., Heuser, J., Lupas, A., Stock, J., Turck, C.W., and Brodsky, F.M. (1992). Folding and trimerization of clathrin subunits at the triskelion hub. Cell *68*, 899–910.

Nesterov, A., Kurten, R.C., and Gill, G.N. (1995). Association of epidermal growth factor receptors with coated pit adaptins via a tyrosine phosphorylation-regulated mechanism. J. Biol. Chem. *270*, 6320–6327.

Nomura, N., Miyajima, N., Sazuka, T., Tanaka, A., Kawarabayasi, Y., Sato, S., Nagase, T., Seki, N., Ishikawa, K., and Tabata, S. (1994). Prediction of the coding sequences of unidentified human genes. I. the coding sequences of 40 new genes (KIAA0001-KIAA0040) deduced by analysis of randomly sampled cDNA clones from human immature myeloid cell line KG-1. DNA Res. *1*, 27–35.

Pearse, B.M.F., and Robinson, M.S. (1990). Clathrin, adaptors and sorting. Annu. Rev. Cell Biol. *6*, 151–171.

Riccio, A., Pierchala, B.A., Ciarallo, C.L., and Ginty, D.D. (1997). An NGF-TrkA-mediated retrograde signal to transcription factor CREB in sympathetic neurons. Science *277*, 1097–1100.

Santini, F., and Keen, J.H. (1996). Endocytosis of activated receptors and clathrin-coated pit formation: deciphering the chicken or egg relationship. J. Cell Biol. *132*, 1025–1036.

Schlessinger, J., and Ullrich, A. (1992). Growth factor signaling by RTKs. Neuron *9*, 383–392.

Schmid, S.L. (1997). Clathrin-coated vesicle formation and protein sorting: an integrated process. Annu. Rev. Biochem. *66*, 511–548.

Slepnev, V.I., Ochoa, G.-C., Butler, M.H., Grabs, D., and De Camilli, P. (1998). Role of phosphorylation in regulation of the assembly of endocytic coat complexes. Science *281*, 821–824.

Songyang, Z., Shoelson, S.E., Chaudhuri, M., Gish, G., Pawson, T., Haser, W.G., King, F., Roberts, T., Ratnofsky, S., Lechleider, R.J., et al. (1993). SH2 domains recognize specific phosphopeptide sequences. Cell *72*, 767–778.

Stein, P.L., Vogel, H., and Soriano, P. (1994). Combined deficiencies of src, fyn, and yes tyrosine kinases in mutant mice. Genes Dev. *8*, 1999–2007.

Stenberg, P.E., Pestina, T.I., Barrie, R.J., and Jackson, C.W. (1997). The Src family kinases, Fgr, Fyn, Lck, and Lyn, colocalize with coated membranes in platelets. Blood *89*, 2384–2393.

Thomas, J.E., Soriano, P., and Brugge, J.S. (1991). Phosphorylation of c-Src on tyrosine 527 by another protein tyrosine kinase. Science *254*, 568–571.

Ungewickell, E., and Ungewickell, H. (1991). Bovine brain clathrin light chains impede heavy chain assembly in vitro. J. Biol. Chem. *266*, 12710–12714.

Ware, M.F., Tice, D.A., Parsons, S.J., and Lauffenburger, D.A. (1997). Overexpression of cellular Src in fibroblasts enhances endocytic internalization of epidermal growth factor receptor. J. Biol. Chem. *272*, 30185–30190.

Wilde, A., and Brodsky, F.M. (1996). *In vivo* phosphorylation of adaptors regulates their interaction with clathrin. J. Cell Biol. *135*, 635–645.

Wong, D.H., and Brodsky, F.M. (1992). 100-kD proteins of Golgi and *trans*-Golgi network-associated coated vesicles have related but distinct membrane binding properties. J. Cell Biol. *117*, 1171–1179.

Ybe, J.A., Greene, B., Liu, S.-H., Pley, U., Parham, P., and Brodsky, F.M. (1998). Clathrin self-assembly is regulated by three light chain residues controlling the formation of critical salt bridges. EMBO J. *17*, 1297–1303.